November 2015

A High-Resolution Paleoenvironmental and Paleoclimatic History of Extreme Events on the Laminated Sediment Record from Basin Pond, Fayette, Maine, U.S.A.

Daniel R. Miller
University of Massachusetts Amherst

A HIGH-RESOLUTION PALEOENVIRONMENTAL AND PALEOCLIMATIC HISTORY OF EXTREME EVENTS ON THE LAMINATED SEDIMENT RECORD FROM BASIN POND, FAYETTE, MAINE, U.S.A.

A Thesis Presented

by

DANIEL R. MILLER

Submitted to the Graduate School of the
University of Massachusetts Amherst in partial fulfillment
of the requirements for the degree of

MASTERS OF SCIENCE

September 2015

Department of Geosciences

A HIGH-RESOLUTION PALEOENVIRONMENTAL AND PALEOCLIMATIC HISTORY OF EXTREME EVENTS ON THE LAMINATED SEDIMENT RECORD FROM BASIN POND, FAYETTE, MAINE, U.S.A.

A Thesis Presented

by

DANIEL R. MILLER

Approved as to style and content by:

_____
Raymond S. Bradley, Chair

_____
Isla S. Castañeda, Member

_____
Jonathan Woodruff, Member

_____
Timothy Cook, Member

_____
Julie Brigham-Grette, Department Head
Department of Geosciences

ACKNOWLEDGMENTS

This thesis is the culmination of four semesters of hard but worthwhile work. While only one name may be on this thesis, this project could not have been done without the help of a multitude of people both at the University of Massachusetts – Amherst and back home. First and foremost, I would like to thank my advisor, Dr. Raymond Bradley, for his guidance and support. Despite being a world-renowned climate scientist and seemingly being in a different country every week, somehow Ray found time for a lowly grad student and was always there to answer all my questions, concerns, and thoughts. Ray always supported any endeavors or directions I was interested in pursuing, even if that was a 3 month stint in New Zealand. Thanks Ray, for introducing me to Paleolimnology and field work, and for letting me loose to play around with some really cool lake mud. I feel I have learned more in the past two years than I have at any other institution, and a large part of that is thanks to you. With your help and support, I'm excited to apply what I have learned going forward into my PhD.

I would also like to thank my committee, who have all given me valuable help throughout the entirety of this project. To Dr. Isla Castañeda, for your unending knowledge and enthusiasm for organic geochemistry and its applications. Thank you for all of the time and energy you put in to introducing me to the field of organic geochemistry, and for being there whenever I had a question or was confused. Your teaching methods and enthusiasm are unrivaled, and I can't wait to continue work in the biogeochem lab. To Dr. Jon Woodruff and Dr. Tim Cook, for helping with any questions I had about sedimentology or XRF data and for giving me additional crash courses in

field work. Field work was one of the highlights of my first two years at UMass, and was definitely made all the better by you both.

I'd also like to thank the Department of Interior's Northeast Climate Science Center and the United States Geological Survey (USGS) for providing funding for this research project. Special thanks to Dr. Debra Willard, coordinator of the Climate and Land Use Change Research and Development Program at the USGS, for providing funding for radiocarbon analysis. Thank you to the NECSC staff, fellows and the people that make everything operate smoothly on a daily basis. Special thanks to Toni Lyn and Addie Rose for making the experience of being a fellow so enjoyable and worthwhile. Last but certainly not least, to:

My family, for supporting me no matter what and always pushing me to be better;

My friends back home, for reminding me that no matter where you end up, once a Buckeye, always a Buckeye. O-H!

My friends here at school, who somehow put up with my insanity and still like to spend time with me;

Petie, for the unwavering adoration only a trusty canine sidekick can give.

"Spitter-spatter, let's get at her, bring me back some mud, honey!"

ABSTRACT

A HIGH-RESOLUTION PALEOENVIRONMENTAL AND PALEOCLIMATIC HISTORY OF EXTREME EVENTS ON THE LAMINATED SEDIMENT RECORD FROM BASIN POND, FAYETTE, MAINE, U.S.A.

SEPTEMBER 2015

DANIEL R. MILLER, B.S., THE OHIO STATE UNIVERSITY

M.S., UNIVERSITY OF MASSACHUSETTS AMHERST

Directed by: Distinguished Professor Raymond S. Bradley

Future impacts from climate change can be better understood by placing modern climate trends into perspective through extension of the short instrumental records of climate variability. This is especially true for extreme climatic events (such as hurricanes, floods, fires and droughts), as the period of instrumental records provides only a few examples and these have likely have been influenced by anthropogenic warming. Multi-parameter records showing the past range of climate variability can be obtained from lakes. Lakes are particularly good recorders of climate variability because sediment from the surrounding environment accumulates in lakes, making them sensitive recorders of climate variability and providing high-resolution histories of local environmental conditions in the past. Furthermore, algae and other microorganisms produced within the lake (and its surrounding catchment area) can also be used as sensitive recorders of past environmental conditions of the lake, such as lake temperature and lake productivity. In some cases, such as at Basin Pond, Fayette, Maine, sediment is preserved efficiently enough to produce distinguishable annual laminations (varves) in the sedimentary record. The varved record at Basin Pond was used to construct an accurate, highly-resolved age-to-depth model over the past 300 years.

Using a multi-proxy analysis, including organic biomarker analysis of molecular compounds and sedimentological features preserved in the sediment record, a history of environmental change at Basin Pond was constructed. Basin Pond and its surrounding catchment area has been affected by human activity throughout the 20th century, as seen through the fluctuations in lake productivity levels mid-century. The most significant change, seen as a drop in dinoflagellate algae activity in the lake in the mid-20th century, is most likely an effect of the chemical treatment of Basin Pond to remove "unwanted species" from the lake environment.

These sedimentary analyses were compared with the record of known extreme events (from instrumental measurements and historical documents), including 129 years of high-resolution (daily) precipitation and temperature meteorological data, 19 tropical systems over the past 145 years, and two known wildfire events over the past 190 years. While only the largest storms show a possible signal in the sedimentary record, longer-term trends in precipitation, including the increase in precipitation seen throughout the last half of the 20th century and the decreased precipitation of the mid-20th century, are thought to be captured in the analysis of long-chain *n*-alkane distributions. Furthermore, Polycyclic Aromatic Hydrocarbons (PAHs), a class of organic compounds that can be used to trace combustion activity, were found in abundance in the Basin Pond sedimentary record. Peaks in the abundances of two PAHs (retene and chrysene) and the ratio retene/(retene + chrysene) were found to be highly correlated with the known wildfire events occurring in the historical period, demonstrating the potential for using these compounds and ratio as a robust proxy for regional wildfire events in northeastern U.S lacustrine sediment records.

TABLE OF CONTENTS

Page

ACKNOWLEDGMENTS iv

ABSTRACT vi

LIST OF TABLES xii

LIST OF FIGURES xiii

CHAPTER

1: INTRODUCTION AND PROJECT BACKGROUND 1

1.1 Introduction 1

1.2 Overview of Geologic and Environmental History of the Northeastern U.S. 3

1.3 Laminated Sediment Records in the NE US 5

1.4 The Record of Extreme Events in the Northeastern U.S. 9

1.4.1 Extreme events in the Historical Period 9

1.4.1.1 Modern Records (1944 – present) 10

1.4.1.2 Pre-Modern Records (1851-1944) 11

1.4.1.3 Early Historical Period (1500-1850) 13

1.4.2 Extreme Events in Paleoclimate and Paleoenvironmental Studies 14

1.4.2.1 Paleotempestology 15

1.4.2.2 Flood Events in Paleoclimatic Studies 20

1.4.2.3 Droughts in Paleoclimate Studies 21

1.4.2.4 Extreme Event Reconstructions in Biogeochemical Studies 22

1.4.2.4.1 Precipitation History using Biogeochemistry 22

1.4.2.4.2 Wildfire History using Biogeochemistry 25

1.5 Summary 29

2: SITE INFORMATION AND FIELD WORK AT BASIN POND, FAYETTE, MAINE 31

2.1 Site Information 31

2.1.1 – Past Studies at Basin Pond 33

2.1.1.1 Age Models of Past Studies 34

2.1.2 Basin Pond during the Historical Period 35

2.2 Field Work 36

3: DATA COLLECTION AND METHODS 42

3.1 Climatic and Meteorological Data during the Historical Period 42

3.2 – Analyses Performed 43

3.2.1 – Age Model 43

3.2.2 – Nondestructive Analysis 45

3.2.2.1 - Geotek Multi-Sensor Core Logger (MSCL) 45

3.2.2.2 Itrax X-Ray Fluorescence (XRF) Core Scanner 45

3.2.3 - Discrete Sample Analysis 45

3.2.3.1 Biogeochemical Analysis 46

3.2.3.1.1 *n*-alkane Analysis 48

3.2.3.1.2 Analysis of Polycyclic Aromatic Hydrocarbons (PAH) 48

3.2.3.1.3 Analysis of Polar Fractions 50

3.2.3.2 Bulk Geochemical Analysis 50

4: RESULTS 53

4.1 Basin Pond Climatic History 53

4.2 Basin Pond Age Model 54

4.3 Non-destructive Analysis 56

4.3.1 Geotek Core Scanner Data 56

4.3.2 Elemental XRF Scanning Data 57

4.4 Biogeochemical Data 58

4.4.1 *n*-alkanes 58

4.4.2 Polycyclic Aromatic Hydrocarbons 58

4.4.3 Algal Lipids and *n*-alkanols 59

4.5 Bulk Geochemical Data 59

5: DISCUSSION 67

5.1 Human Disturbance and Catchment History 67

5.1.1 Lake Primary Productivity Fluctuations from Lipid Biomarkers 68

5.2 Extreme Events in the Sedimentary Record 72

5.2.1 Paleo-storm Records at Basin Pond 72

5.3.2 Precipitation History and Hydrological Interpretations 74

5.2.3 Wildfire Record 77

5.3 Conclusions 79

5.4 Future Work 81

5.4.1 Extension of Paleoclimate Records into the Pre-historic Era 81

5.4.2 Comparison of PAH Fire Record and Other Fire Proxies 81

5.4.3 Age Model Fine-Tuning and Compound-Specific Radiocarbon Dating……...82

5.4.4 Temperature Reconstructions from the Basin Pond Sedimentary Record……...82

APPENDIX

SUPPLEMENTARY DATA TABLES AND MASS SPECTRA 94

REFERENCES 109

LIST OF TABLES

Table		Page
1.1	Summary of storm records by time period, found by Ludlum (1963)……	14
1.2	Summary of the proxies used in Sun et al. (2013)……..	24
2.1	Varve count ages and radiocarbon age estimates from the Basin Pond sedimentary sequence from the Frost (2005) study……..…….	35
3.1	Meteorological Stations used in the creation of a met data stack for Basin Pond, Fayette, Maine……	42
3.2	Description of radiocarbon samples……...	44
3.3	Radiograph and XRF settings used for all core scans on the Itrax XRF Core Scanner at UMass – Amherst……	46
3.4	Instrument method information, including carrier gas, fractions analyzed, temperature ramps for each method, and duration the maximum temperature was held……..…….....	49
3.5	PAH compounds identified on the GC-MS and retention times……	50
4.1	Summary of lead-210 (Pb-210) and cesium-137 (Cs-137) radioisotopic dating results. Activity are measured in Bq/g……	54
4.2	Summary of radiocarbon dating results. C14 Lab indicates where samples were processed and analyzed: U.S. Geological Survey Eastern Geology and Paleoclimate Science Center Radiocarbon Laboratory (USGS), or the Woods Hole Oceanographic Institute AMS Radiocarbon Facilities (WHOI)…..……..…	56
4.3	Average Sedimentation Rates of the Basin Pond sediment record from various dating techniques (varve count chronology, radioisotopic dating, radiocarbon dating)…….	56

LIST OF FIGURES

Figure Page

1.1 Deglaciation History of Maine, Borns et al. (2004)…….....5

1.2 Hurricane Tracks from 1859 – present within 150 miles of Boston, MA, USA. (National Hurricane Center, NOAA)……..13

1.3 Formation of Overwash records in lacustrine and marsh settings, from Donnelly et al. 2001……...16

1.4 XRF Radiograph images from Boldt et al. (2010), with identified storm deposits correlated across cores…….18

1.5 Varve Thickness and Hurricane History from Boston, MA, USA (Besonen 2006)……..19

1.6 Correlation of *n*-alkane proxies with the Pacific Decadal Oscillation (PDO) and precipitation in Northeast China. A) The compound-specific $\delta^{13}C$ values of long-chain *n*-alkanes and the PDO index, B) The Paq index and the PDO index. (Sun et al 2013)……25

1.7 PAH abundances through time compared with charcoal, fire, and precipitation histories at Yosemite National Park, USA. PAH fluxes are shown as the Sum of Low Molecular Weight (LMW) PAH and the sum of High Molecular Weight (HMW) PAH. Denis et al (2012)……...28

2.1 Google Earth Map of Basin Pond, located in south central Maine……38

2.2 Basin Pond Bathymetric Profile, completed by the USGS (2015)…….38

2.3 Pollen Assemblages based on Pollen Accumulation Rates of the Basin Pond sedimentary record over the last 1,600 years. (from Gajewski 1987)……...39

2.4 Charcoal counts plotted with various pollen assemblages taken from the Gajewski 1987 study. (Clark and Royall 1996)…….39

2.5 Fall-Winter water column profiles from Frost (2005). Profiles depicted were taken over a year on Sept 17, 2003, Sept 20, 2004, and Oct 31, 2004……40

2.6 Images from March 2014 Basin Pond Field Campaign. A) Subsampling Core BP2014-3D for radioisotopic dating, B) Basin Pond at sunset, and C) Researchers with Core BP2014-5D……...41

3.1 Map of all meteorological (met) stations used in the compilation of the met records used in this study……...52

3.2 Map of historical storm tracks within 50 miles of Basin Pond, Fayette, Maine (NOAA)……...52

4.1 Annual precipitation totals (in mm) and average annual temperatures (in degrees C) ……60

4.2 Average temperature (and associated error) for the state of Maine, U.S.A, over the past 250 years. Data compiled by the Berkeley Earth Surface Temperature Project from 97 current stations and 74 former stations……..…60

4.3 A) Core BP2014-5D ½ X-Ray Radiographic Image, showing high – resolution (100μm) fluctuations in density, detailing the fine-scale laminations throughout the Basin Pond sedimentary record. B) Zoomed-in view of core 5D ½ radiographic image, with associated radiograph greyscale values plotted in blue and overlayed onto the image……..61

4.4 A) Basin Pond Age Model, based upon radiocarbon ages, varve chronology, and Pb-210 radioisotopic dates. B) Age Model for the historic period of the Basin Pond sediment record, based on varve counts and Pb-210 dates…….62

4.5 A) Image of the Basin Pond sediment core, B) bulk density values, C) magnetic susceptibility, and D) L* spectral values, as measured from the geotek core scanner…….63

4.6 Correlation plots with linear regression analysis of X-Ray Radiographic Greyscale Values versus iron (top left, green), potassium (top right, light blue), titanium (bottom left, red), and silicon (bottom right, dark blue). All elemental data have been normalized to titanium. Correlation coefficients can be seen in the upper right corner of each plot. Note statistically significant ($p<0.00001$) correlation of Si/Ti and Ti with radiographic values, but little correlation is seen with Fe/Ti or K/Ti……..……..64

4.7 A) Titanium abundance, Si/Ti abundances, and radiographic greyscale values plotted over the past ~230 years. B) Highlighted interval from 1815 – 1827 seen in figure 5.5a. This section was chosen based on distinguished laminations in the radiographic record……...……..65

4.8 Bulk Geochemical Data from discrete samples of the Basin Pond sedimentary record, including A) total organic carbon content (TOC), B) total nitrogen content, C) the ratio of total carbon to total nitrogen (C/N), and D) dry bulk density, measured in grams per cubic centimeter……...66

5.1 Mass Accumulation Rates (MAR), measured in μg/yr/cm^2, of all algal lipids found in Basin Pond sediment samples……..……..84

5.2 Relative abundances and distribution of selected algal lipids……85

5.3 Elemental Titanium Counts smoothed to 1mm resolution, long-chain *n*-alkane abundances (C27+C29+C31+C33, measured in ug/g sediment), magnetic susceptibility measurements, bulk sediment total organic carbon to total nitrogen (C/N) ratio, and algal lipid relative abundances. Yellow highlighted area indicates the major shift in algal lipids distributions at Basin Pond, while the black dashed line indicates the chemical treatment of Basin Pond in July of 1955……86

5.4 Varve thickness anomalies (in mm), measured by subtracting varve thickness from the 7-year running average thickness. Titanium (dark red) and Fe/Ti (orange) abundances are also plotted. Extreme precipitation events (occurring from May – October) greater than 3.61cm in the Basin Pond region dating 130 years are plotted in the bottom bar graph. Note the highlighted (yellow) precipitation events occurring in 1932 and 1998, and the corresponding peaks in each of the proxy records shown……....87

5.5 Total Growing Season Precipitation record (in mm) and varve thickness measurements. Bolded lines indicate running averages (7-year running average). Arrows show potential areas of correlation between the two records, indicating a slight lead of the varve thickness data……..……88

5.6 *n* -alkane distribution throughout the Basin Pond sediment record. Histogram bars indicate mean values of each *n*-alkane (measured in μg/g sediment) throughout the record……89

5.7 Image of Basin Pond catchment area, showing C3 forest as the dominant vegetation type……...…89

5.8 *n* - alkane proxies compared to average growing season (April – September) precipitation and temperature at Basin Pond. Bolded lines in the precipitation and temperature plots indicate the 7-yr averages, replicating the 7-year window of each sample used in biogeochemical analysis…….90

5.9 Mass Accumulation Rates (measured in μg/yr/cm^2) of retene and chrysene, as well as the retene / (retene + chrysene) ratio. Vertical red lines indicate known wildfire events in the region…….……..91

5.10 Comparison of precipitation records and the retene / (retene + chrysene) ratio from the Basin Pond sediment record. Top plot is the annual precip totals, while the middle plot is the August – September – October (ASO) seasonal precipitation totals. Vertical red line indicates the 1947 wildfire……..92

CHAPTER 1

INTRODUCTION AND PROJECT BACKGROUND

1.1 Introduction

Climate change is one of the most complex and challenging issues facing the world today. A changing climate will affect humankind economically and alter our physical environment, presenting ethical challenges in how we respond. Future impacts from climate change can be better understood by placing modern climate trends into perspective through extension of the short instrumental records of climate variability. This is especially true for extreme climatic events (such as hurricanes, floods, fires and droughts), as the period of instrumental records provides only a few examples and these have likely have been influenced by anthropogenic warming.

The northeastern United States (NE US) is one of the most heavily-populated and developed regions of the world. The region is comprised of complex, sprawling urban centers and rural regions, both of which are vital to the economic and cultural character of the region. Furthermore, both urban and rural regions in the NE US contain communities that have been historically susceptible to extreme climatic events and climate change (Horton et al., 2014). Over the past 120 years, average temperatures in the NE US have increased by 2ºF, precipitation has increased by more than 10%, and sea levels have also risen (Kunkel, 2013). Despite our knowledge of the long-term trends in the region's climate, little is known about how extreme events have been affected by climate change. A future increase in the frequency of climate extremes due to climate change would have major social and economic impacts in the NE US (Horton et al., 2014). However, *the natural frequencies at which extreme events occur in the NE US are*

presently unknown.

In order to better understand how extreme events are evolving with climate change in the NE US, this thesis project aims to (1) determine how known extreme events are documented by instrumental measurements and historical records, (2) to identify how human activities and rapid environmental change in lakes and lake catchment areas are expressed in the sedimentary record, and (3) to distinguish and evaluate how climatic events are expressed in the physical and geochemical properties of a lacustrine sedimentary sequence. Using this information, analysis and interpretation of the sedimentary record can be used to extend the record of known extreme events beyond the brief period of instrumental measurements into pre-historic times, providing a better understanding of the background frequencies of extreme events in the region before anthropogenic forcing.

To address these questions, a suite of sedimentary, organic geochemical, and inorganic geochemical techniques have been used to examine the record of hurricanes, floods, droughts, and fires from a single site. Such a study has not yet been conducted at a lake in the NE US. The sedimentary record of Basin Pond, Fayette, Maine, presents a unique archive of paleoenvironmental information in the region. Basin Pond is unique in that the sedimentary record provides an excellent archive of paleoenvironmental conditions due to the discrete nature of sediment deposition. While many lakes are diamictic and experience turnovers of the water column, helping to transport oxygen to all depths, Basin Pond's water column is meromictic, or is sufficiently stratified to prevent any late turnovers (Wetzel, 1983; Frost 2005). As a result, the sediments are preserved with minimal mixing, and likely form annual layers ("varves") because the

bottom waters are continuously devoid of oxygen (O'Sullivan, 1983), making this lake an ideal target for a high-resolution paleoclimate analysis.

1.2 Overview of Geologic and Environmental History of the Northeastern U.S.

The modern landscape of the NE US – particularly New England – was largely shaped into today's environment during the last glaciation of the Northern Hemisphere and the subsequent deglaciation leading from the Pleistocene Epoch into the Holocene Epoch. Near the end of the Pleistocene epoch, the Laurentide Ice Sheet covered most of northern North America, including almost all of New England, extending to the Ronkonkoma Moraine on Long Island, NY and Georges Bank in the Gulf of Maine (Stone and Borns, 1986). Throughout the transition from the Pleistocene into the Holocene epoch, deglaciation occurred across the region in a south – to – north progression.

Extensive work has been performed over the past century on documenting the glacial melt progression across New England. In the early 1920's, geologist Ernst Antevs began constructing the New England Varve Chronology (NEVC) from glacial deposits preserved in the annually laminated sediment sequences of glacial lake Hitchcock (Antevs, 1922; Ridge et al., 2012). Since then, more work has been performed to update the original sequence using radiocarbon dating techniques as well as additional varve chronologies, helping to form the new North American Varve Chronology (NAVC), a continuous sequence spanning most of the last deglaciation (18,200-12,500 yr BP) (Ridge et al., 2012).

A slightly different story unfolds when addressing the timing of the deglaciation of Maine and eastern New England. Glacial geology of Maine also records the northward

recession of the Laurentide Ice Sheet as seen in the NAVC, but on differing time scales than Western New England. The pattern of deglaciation across southern Maine has been reconstructed from various end moraines, fans, and deltas, using radiocarbon dating to constrain the chronology more accurately (Borns Jr. et al., 2004; Weddle and Retelle, 2001). These chronologies show that Maine was deglaciated in a northward progression between 14,500-10,000 yr BP, with rapid recession occurring between 13,000-11,000 yr BP during the Bolling/Allerod time period (Borns Jr. et al., 2004). In south-central Maine, deglaciation can be constrained even more through a radiocarbon age taken from a Portlandia Arctica mollusk shell in Lewiston, Maine, dating to 12,300 yrs BP (Borns Jr. et al., 2004; Weddle and Retelle, 2001). The deglaciation of Maine is illustrated in Figure 1.1 (Borns Jr. et al., 2004).

Through this deglaciation process, the landscape was drastically altered. As glaciers moved, they scoured the landscape and bedrock, producing rock basins and damming river valleys. In the NE US, as the ice receded, these basins and dammed valleys became lakes and ponds. One other particular feature formed by deglaciation are the numerous kettle holes and kettle ponds found throughout the NE US (Bennett and Glasser, 2011). As a glacier recedes, large ice blocks calve from the front terminus of the glacier and can become partially or entirely buried by glacial outwash. As the large blocks of ice melt, kettle holes are left in place of the ice, which fill with water and form kettle ponds (Bennett and Glasser, 2011). While most kettle ponds are less than ten meters deep, some kettle ponds, such as Basin Pond, can be much deeper.

Following deglaciation of Maine and the NE US, vegetation migrated northward, slowly shifting from tundra to a heavily forested landscape over a 1,000-4,000 year

period (Davis and Jacobson Jr., 1985; Frost, 2005). In the region of south-central Maine, high-resolution postglacial pollen records show that a tundra landscape dominated the area from deglaciation to 10,800 ^{14}C years BP, when an abrupt increase in arboreal pollen concentrations occurred, indicating a transition to woodland, and then to forest by 7,300 ^{14}C years BP (Anderson et al., 1992; Frost, 2005). The landscape has undergone little change since then, apart from anthropogenic disturbances over the past 200 years (Anderson et al., 1992; Frost, 2005).

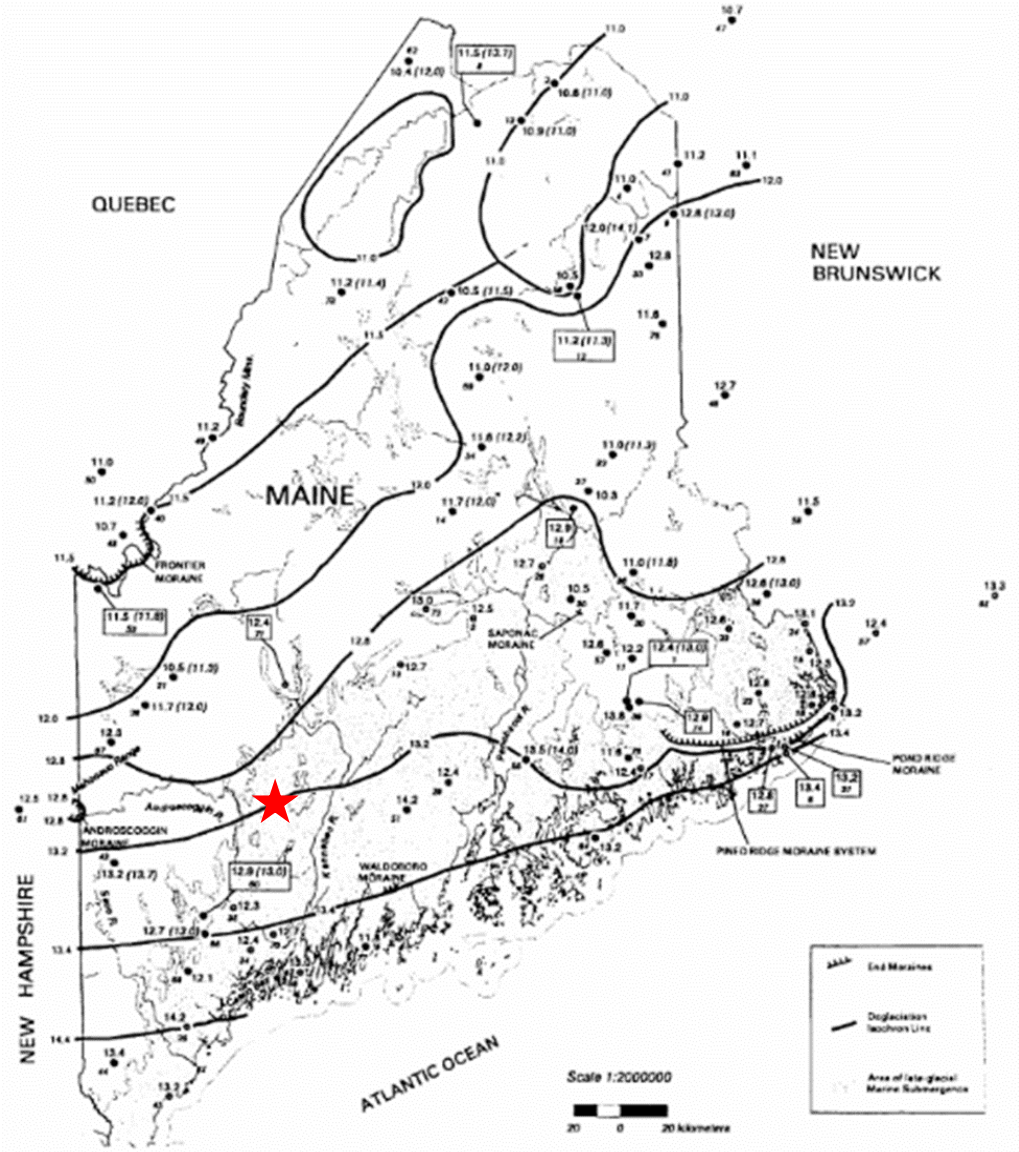

Figure 1.1: Deglaciation History of Maine, Borns et al. (2004). Red Star indicates location of Basin Pond. Favette. Maine.

1.3 Laminated Sediment Records in the NE US

Multi-parameter records showing the past range of climate variability can be obtained from lakes. Lakes are particularly good recorders of climate variability because sediment from the surrounding environment accumulates in lakes at relatively high rates, providing high-resolution histories of local environmental conditions in the characteristics of their sediments (Bradley, 2014; Ellis et al., 2004). Therefore, sediment cores can potentially provide detailed climate and paleoenvironmental records in their stratigraphies.

One caveat of using lake sediment cores for paleoenvironmental and paleoclimate reconstructions is that these records are usually dependent on radioisotopic dating methods to create accurate age-to-sediment depth models, in order to look at these sediment records with respect to time. Accurate dating is of critical importance in paleoclimatic studies, as without them it is impossible to make inferences as to when certain climatic shifts or events occurred (Bradley, 2014). Therefore, having a precise age model for a sedimentary record is a fundamental component of paleoclimatic studies.

In certain cases, lacustrine systems can record the annual climatic cycle extremely well through the deposition and preservation of annually resolved laminated sediment (Anderson and Dean, 1988; Bradley, 2014; Zolitschka et al., 2015). These laminations, known as “varves”, can be immensely useful in paleoclimatic and paleoenvironmental studies, as they allow for a sub-annual analysis of the sedimentary sequence and can bridge the divide between long, poorly-resolved sediment records and short, detailed climatic monitoring records (Zolitschka et al., 2014). However, varves are rarely preserved in lacustrine and marine settings due to multiple processes that can mix,

disturb, or alter the preservation of these annual laminations (Bradley, 2014).

One of the main characteristics of lakes with varved sedimentary sequences is maintaining continuous stratification of the water column, known as meromixis (Frost, 2005; O'Sullivan, 1983). In order to sustain a strongly stratified water column, meromictic lakes are usually deep enough to prevent any seasonal overturning or mixing of the water column throughout the year from surficial processes (e.g. wind-driven mixing of the water column, etc…). Due to this stratification, bottom waters are devoid of any oxygen, known as anoxia (O'Sullivan, 1983; Wetzel, 1983). Anoxic conditions at the sediment-water interface may also be separated from the upper water column by a salinity gradient, or a chemocline, that makes the bottom waters of meromictic lakes an unfavorable place for aerobic organisms to live (Bradley, 2014; Frost, 2005; Wetzel, 1983). As a result, there is a lack of organisms to cause bioturbation of the sediment, aiding in the preservation of the laminated sediments (Zolitschka et al., 2015).

Varved sediments have been classified into four types based on their composition (O'Sullivan, 1983). Ferrogenic and calcareous laminae are formed by seasonal changes in the chemical precipitation at a site (O'Sullivan, 1983). Clastic varves occur mainly in polar regions and are caused by a large influx of allochthonous sediment washing into a lake for a portion of the year. Each clastic laminae is comprised of a coarse bottom caused by the allochthonous material being washed in during the spring and summer seasons from fluvial input, with a clay-rich cap that is formed during the winter season (Frost, 2005; O'Sullivan, 1983). Finally, biogenic laminae are formed by seasonal deposition of organic material, usually caused by blooms of microalgae in certain seasons of the year. Biogenic varves are composed of a light-colored, diatom-rich layer deposited

from a spring or summer bloom, with a darker, humous-rich layer deposited during the iced-over winter season (O'Sullivan, 1983).

In the central and northeastern United States, varved sediment sequences from several lakes have been utilized in paleoenvironmental studies. At Elk Lake, Minnesota, studies led by Walter Dean and J. Platt Bradbury have been conducted looking at the continuous varved sediment record that spans the entire Holocene epoch (Bradbury and Dean, 1993). Extensive analyses of this sediment record have included varve thickness, gray-scale density, various inorganic geochemical and stable isotope measurements, all aimed at reconstructing past climatic changes in the central US throughout the Holocene (Bradbury and Dean, 1993; Bradbury et al., 2002; Dean, 2002, 1997; Dean et al., 2002). The varved sediment record at Fayetteville Green Lake, New York, has been studied looking at late glacial-Holocene atmospheric circulation and precipitation across the region (M. Kirby et al., 2002; Kirby et al., 2001; M. E. Kirby et al., 2002). Pollen records have been reconstructed at several sites with laminated sediment records (e.g. Pout Pond, New Hampshire: Allison et al., 1986; Laurel Lake and Stockbridge Bowl, Berkshires, Massachusetts: Ludlam, 1976; Soukup, 1975). Finally, a laminated sediment record from Lower Mystic Lake, Boston, Massachusetts, was used to reconstruct a hurricane record from varve thickness (Besonen, 2006; Besonen et al., 2008). This record will be discussed in more detail later in this chapter.

It is important to note that the laminated sediment record at Basin Pond, Fayette, Maine, has also been the center of several studies over the past three decades (Clark et al., 1996; Clark and Royall, 1996, 1994; Doner, 1990; Frost, 2005; Gajewski, 1988; Gajewski et al., 1987; Perkins, 1985). The focus and results of these studies will be

discussed in detail in chapter two.

1.4 The Record of Extreme Events in the Northeastern U.S.

The NE US is historically susceptible to extreme climatic events, such as tropical storms, wildfires, extreme flooding events and severe droughts. Landfalling tropical storms in the region were some of the deadliest and costliest natural disasters on Earth (e.g. Hurricane Sandy, 2012) (Murnane and Liu, 2004; National Oceanic and Atmospheric Administration (NOAA), 2014a). The NE US has also been home to some of the deadliest and largest wildfires in North America during the historical period (e.g. Miramichi Fire, 1825) (Fahey and Reiners, 1981; Fobes, 1948). Furthermore, with sixty-four million people living in the Northeastern United States, the Northeast Megalopolis is home to several of the largest cities in the US, the nation's capital, and several of the world's largest companies, businesses, and financial centers (Horton et al., 2014).

Despite the fact that the NE US is prone to extreme climatic events, little is known about the long-term frequency of these events, as accurate meteorological records and observational data only extend back roughly 100 years across the region. To address this issue, extensive work has been conducted on reconstructing longer records of extreme events in the NE US. The work thus far has been focused in two main areas: compilations and assessments of historical records from recent centuries, and paleoclimate reconstructions of extreme events – particularly of hurricane strikes, wildfires, and droughts and flooding – on multi-centennial to millennial time scales.

1.4.1 Extreme events in the Historical Period

Historical records of extreme events in the NE US exist from present day and extend back into the late 15th Century. In 1494, Christopher Columbus encountered and

documented the first known European record of a “true West Indian storm”, or a hurricane, while on his second voyage to the Americas (Ludlum, 1963). This was the first European record of extreme events in the region, and over the next four centuries, documents, journal entries, and news archives were the primary source of information on extreme events. In the middle to late 19th century, meteorological observations began in many areas of the NE US, allowing for the tracking and impact of events to be recorded more accurately than ever before. Another large step forward in tracking extreme events occurred in the middle 20th century, with the beginning of satellite era and aircraft storm reconnaissance.

1.4.1.1 Modern Records (1944 – present)

The modern era, or the time period from 1944 to present day, is defined by a couple of major developments in technology and in the field of meteorology. In storm tracking, the establishment of the modern storm monitoring and detection system can be dated to 1944, when routine aircraft reconnaissance missions of North Atlantic Basin storms began (Goldenberg et al., 2001). This aided in producing reliable and accurate data on the positioning, movement, and strength of the storm, whereas prior to this, records were taken from surface observations and historical accounts. The second primary development in tracking most climatic events came in the early 1960’s with the development and use of satellites. TIROS III (Television Infrared Observational Satellite), launched in July of 1961, was the first satellite to ever photograph a hurricane from above the atmosphere. While Hurricane Esther was the first hurricane to be discovered by satellite, four other hurricanes during the 1961 hurricane season were also photographed: Anna, Betsy, Carla, and Debbie (Cortright, 1968). Furthermore, it became

evident through the images that there was a correlation between hurricane intensity and the degree of organization seen in the satellite images of the storms. Outside of tracking hurricanes, satellites have also been used to identify and track wildfire expansion, as smoke plumes and burn scars can be identified in satellite imagery. These major developments brought in a new era of wildfire management and storm tracking, making it possible to remotely track the lifespan of an extreme event.

Statistical studies have been able to utilize the vast amount of data from this time period by looking at storm tracks and their impacts on the NE US. Work has also been done on the influence of tropical storm precipitation on annual extreme precipitation amounts. Barlow et al. (2011) performed an analysis of daily observational data from 1975-1999 over North America and found that the majority of extreme precipitation events along the east coast (especially in the northeastern US) are associated with hurricane-related activity

1.4.1.2 Pre-Modern Records (1851-1944)

Prior to 1944, high-resolution climate and meteorological data regarding extreme events becomes more scattered but still exists. Daily meteorological data, including precipitation and temperature measurements, exist for a handful of stations across the NE US, some of which extend back to the 1880's. This is extremely useful in identifying extreme events such as droughts, storms, and fires in the region.

Although reliable data on hurricane tracks and intensities are scarce prior to 1944, much work has been done over the past several decades on compiling a North Atlantic Hurricane Database back through 1851. Some of the first efforts to construct a hurricane database were done in the 1960's to help provide information on tropical storm

forecasting (Murnane and Liu, 2004). From this, a historical data set of all tropical storm activity (including hurricanes and tropical storms) in the North Atlantic Basin from 1851 through present day – known as HURDAT – was created. This database has been used as the primary source of information in studies pertaining to hurricane activity in the Atlantic (Jarvinen et al., 1984; Murnane and Liu, 2004). HURDAT is based upon the "best tracks" information of storms from 1851 to present, using synoptic times for best track times (00, 06, 12, and 18z).

Recently, a second generation of the database, known as HURDAT2, expanded upon the original format, adding "best tracks" available from the Automated Tropical Cyclone Forecast system database. HURDAT2 includes non-synoptic best track times to track maximum rainfall and intensity, tropical depressions (the original HURDAT only included tropical storms and hurricanes), and best track wind radii (Landsea et al., 2012). Storm tracks and intensities from 1851 through the present day can been seen in Figure 1.2, based upon data from the HURDAT2 database (National Oceanic and Atmospheric Administration (NOAA), 2014a). Apart from the National Hurricane Center databases and meteorological observation archives, the other primary source of information on extreme events are news archives. A handful of extreme events have been well documented by local newspapers and news stations throughout the NE US, including floods and wildfires. For example, in October of 1947, newspapers across New England documented a week-long spread of wildfires throughout many towns in southern Maine, dubbing the event "The Week Maine Burned" (Fahey and Reiners, 1981; Fobes, 1948). This wildfire event caused an estimated $25 - $30 million in 1947 dollars ($230 - $280 million in 2006 dollars), burned 2,655 structures, killed 16, and injured over 10,000

people, making it one of the costliest natural disasters in Maine history (Butler, 2014; Fahey and Reiners, 1981; Fobes, 1948).

1.4.1.3 Early Historical Period (1500-1850)

Prior to 1850, there is very little information about extreme events in the NE US. As there are no (or extremely limited) observational data prior to this time period, the main source of data come from news articles, personal diaries, or ship logs about the impact of these events, mainly landfalling hurricanes. Several compilations of certain storms or time intervals have been made. An example of this is the work of Noves

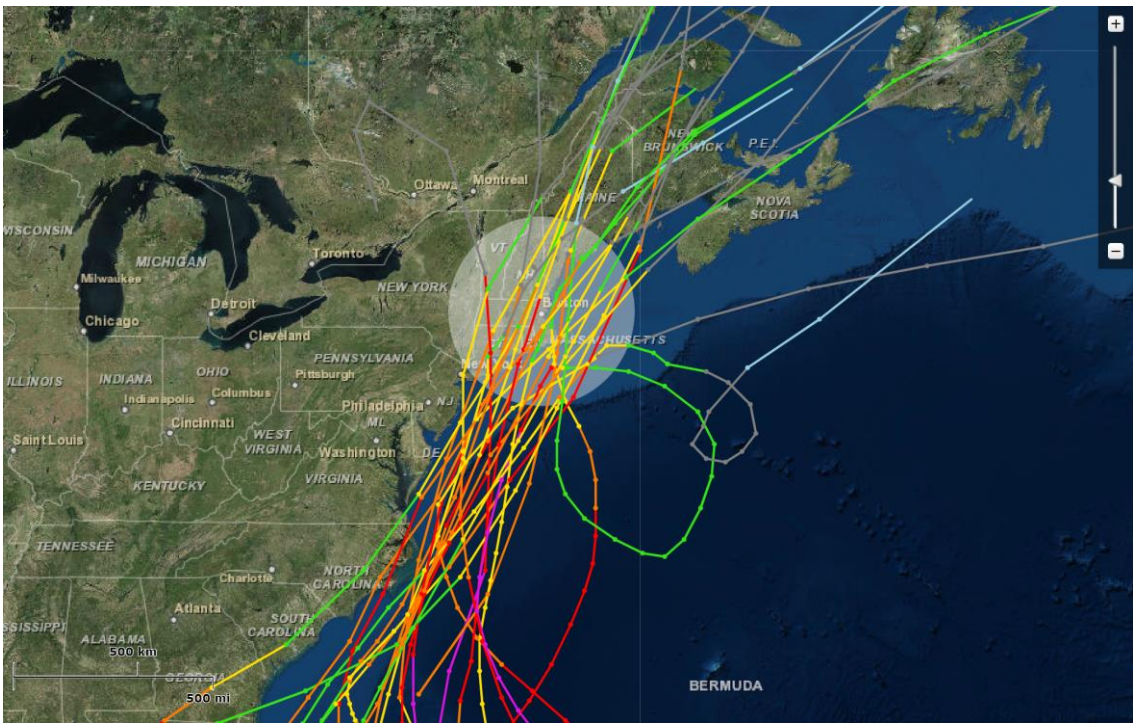

Figure 1.2 – Hurricane Tracks from 1859 – present within 150 miles of Boston, MA, USA. (National Hurricane Center, NOAA)

Darling, Esq. in 1842, where Darling compiled all the historical accounts of a hurricane passing over New England in September 1815, including 28 accounts from sea and over 25 accounts from land (Darling, 1842). Accounts of wildfires in the region are extremely limited; only a small handful of accounts record past wildfire activity prior to the 20th

century. One such event occurred in 1825, when the Great Miramichi Fire burned an estimated three million acres of land across Maine and New Brunswick, killing over 160 people (Fobes, 1948).

Perhaps the most influential compilation of all records during this time-period of American history comes from David Ludlum. In 1963, Ludlum published a compilation of hurricanes from 1494 - 1870. The first account of a hurricane in the Americas came from Christopher Columbus's second voyage in 1494, where he described a "true West Indian storm" (Ludlum, 1963). Over the next several centuries, progressively more records of hurricanes (especially landfalling hurricanes) were kept as the Americas become more populated. Ludlum's 1963 work has been the main source of historical hurricane information for studies over the past 50 years from the period prior to 1850. A summary of all storm records found by Ludlum can be seen in Table 1.1.

Time Period	Hatteras North	Hatteras South	Gulf Coast	Total
1501-1700	7	5	5	17
1701-1814	29	40	23	92
1815-1870	29	56	51	136

T able 1.1: Summary of storm records by time period, found by Ludlum (1963).

1.4.2 Extreme Events in Paleoclimate and Paleoenvironmental Studies

One of the fundamental issues when looking at the natural variability of extreme events in the Northeastern U.S. is that our records from the historical period are inadequate when attempting to determine variation in frequencies on centennial or longer timescales. Reliable records, as discussed previously, only extend back roughly 100-150 years in the US, as records prior to this are sparse and potentially have large error.

Therefore, accurately reconstructing extreme events from pre-historic times is essential for looking at the natural variability and frequencies of storms, droughts, floods, and wildfires in the NE US. Fortunately, a growing amount of paleoclimate research in recent years has focused on reconstructing records of hurricane frequencies, precipitation trends, and wildfire histories.

1.4.2.1 Paleotempestology

Paleotempestology, or the study of prehistoric tropical cyclones, is a growing field of research that has attempted to extend our records of hurricane activity in the Atlantic Basin thousands of years into the past (Murnane and Liu, 2004; Nott, 2004). While multiple types of records have been studied (tree rings, corals, speleothems, and sediment records), sedimentary records have dominated this field of study, particularly in the NE US. Nevertheless, tree ring studies (e.g. Miller et al., 2006; Reams and Van Deusen, 1996), coral studies (e.g. Hetzinger et al., 2006, 2008), and speleothem records (e.g. Frappier et al., 2007) have given valuable insight into hurricane activity across the eastern US and North Atlantic Basin, in some cases on sub-annual time scales.

The majority of work over the past two to three decades in the field of paleotempestology has been through the use of geological sediment records from coastal lakes, marshes, and lagoons (Murnane and Liu, 2004). These coastal lakes, marshes, and lagoons have a barrier, usually a narrow strip of sandy land, blocking it from the ocean. However, during intense storms such as severe hurricanes, these barriers can be overwashed due to high surf and storm surge flooding, and sand layers from the storm are deposited in the protected lake, marsh, or lagoon. These sand layers deposited during an overwash storm event can be easily identified in sediment cores from these areas (Figure

1.3), making them a potential proxy for past hurricane strikes on much longer time scales than any of the other proxy records previously discussed (Donnelly et al., 2001; Murnane and Liu, 2004; Nott, 2004). It is important to note that this while this work originated largely in the Gulf Coast region of the U.S., it has been applied to a handful of sites in the Northeastern U.S. in recent years.

The first overwash records for the NE US were obtained by Dr. Jeffrey Donnelly and colleagues at Brown University. In Donnelly et al. (2001), a 700 year record from Succotash Salt Marsh, East Matunuck, Rhode Island, included six overwash deposits. The top four fans were correlated with known hurricane strikes in the historical period (1954, 1938, 1815, and 1635/1638). The remaining fans were estimated to have been deposited between 1411-1446 AD and 1295-1407 AD through radiocarbon dating (Donnelly et al., 2001). A similar study was done by Donnelly and colleagues in 2001 on a salt marsh in Whale Beach, New Jersey. This study found two major storm strikes over the past 700 years, including one seemingly correlated with the hurricane of 1821, and another prehistoric storm dated between 1278-1438 AD. Interestingly, the Ash Wednesday "Nor'easter" of 1962 also was recorded as an overwash event, indicating that at this site both Nor'easters and hurricanes can produce sufficient surge to create an overwash event in the sediment record.

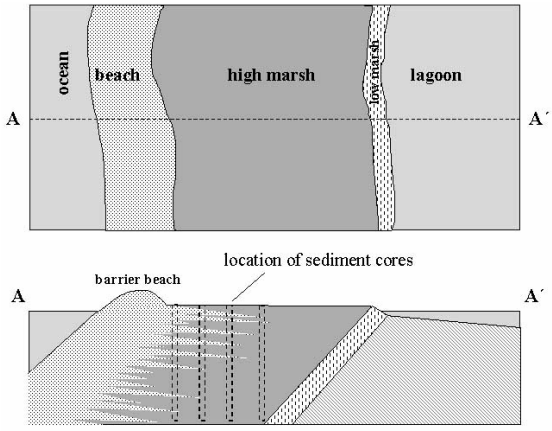

Figure 1.3: Donnelly et al., 2001

Other records from New England have been obtained over the past decade producing similar hurricane reconstructions. A record from Brigantine Marsh, New

Jersey, indicated several fans relating to both Nor'easters and hurricanes, including two prehistoric storms dating between 550 – 1400 AD (Donnelly et al., 2004). Several salt marshes on western Long Island were studied and produced a record of hurricane activity over the past 3,500 years, including storm deposits that likely correspond to events in 1893, 1821, 1788, and 1693 (Scileppi and Donnelly, 2007). These records showed little evidence of intense hurricane strikes over several hundred years prior to the 18th century, with multiple overwash deposits during the time period from ~2,200 – 900 years before present. More recently, advances in technology have allowed for new techniques to be utilized in core analysis. In a study by Boldt et al. (2010), X-Ray Fluorescence (XRF) scanning was performed on sediment cores from Mattapoisett Marsh, Cape Cod, in southeastern New England. Radiographs from each core were used to find overwash deposits at a high resolution (200 microns) as seen in Figure 1.4. This study found that 23 prehistoric (pre-1630) storm layers were deposited, or an average of 1.5 events per century. Interestingly, this record produced a relatively constant hurricane frequency over the past two millennia, with the 15th-16th centuries being the most active time period of the past 2,000 years. Due to the high resolution of this record, this is to date the longest and most complete reconstruction of hurricane-induced overwash in the northeastern U.S. (Boldt et al., 2010).

Despite the fact that the majority of work done in paleotempestology has focused on sediment overwash studies in the NE US, there are several limitations that influence the results seen in these studies. One of the most apparent limitations pertains to the age models used in these studies, and more specifically the dating of the overwash deposits. Almost all of these studies rely on a small number of radiocarbon dates occurring near an

overwash deposit in the sediment core. The errors associated with radiocarbon dating can be substantial, as seen in Donnelly et al. (2004), where a prehistoric overwash record had an age range of roughly 850 years (550AD – 1400 AD).

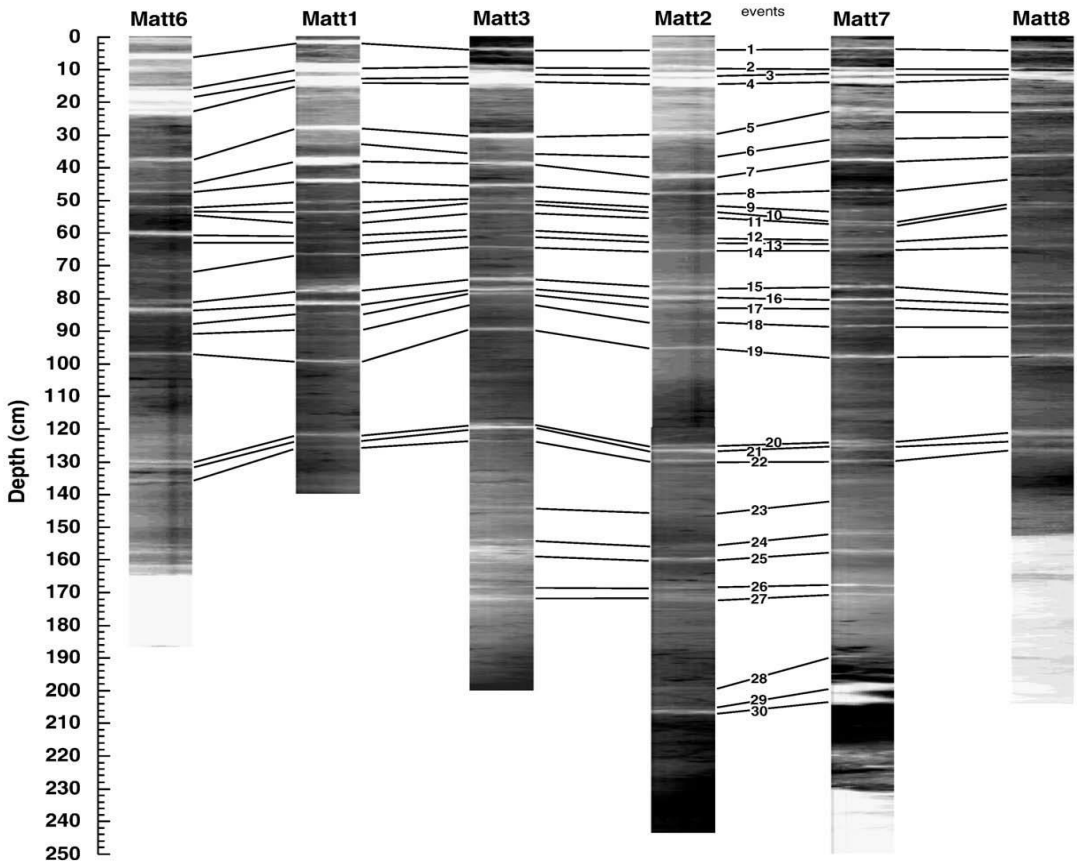

Figure 1.4: XRF Radiograph images from Boldt et al. (2010), with identified storm deposits correlated across cores.

While overwash studies provide invaluable information about landfalling storms in a region, more work is needed to independently confirm the results seen in these studies. In addressing the issue of the low resolution of these studies, highly-resolved records of hurricane activity extending back into prehistoric times are needed to be able to make accurate statements on the variability and frequencies of hurricanes. One such study has been done by Mark Besonen and colleagues at Lower Mystic Lake outside of Boston, Massachusetts. This record is particularly significant due to the annual

laminations ("varves") that are present throughout the recent sediment. The varves in this sediment record are caused by the chemical stratification of the lake water due to mixing of salt water into the lake during periods of high tide or low outflow, which aided in making the water anoxic at depth, protecting the sediment from bioturbation and allowing fine laminations to occur over the last millennium (Besonen, 2006). These varves allowed an annually-resolved hurricane record to be reconstructed for the Boston area by analyzing the thickness of graded beds throughout the sediment record. Results from this study, seen in Figure 1.5, show that almost all of the prominent graded beds in the historical period correspond to years in which category 2 to 3 hurricanes are known to have made landfall in the region (Besonen et al., 2008). Looking at prehistoric times, it was found that hurricane activity was high from the 12th – 16th centuries, and was low from the 17th – 19th centuries. While these results are different from the overwash study results from this region, they are consistent with other paleoclimate indicators for the North Atlantic such as sea surface temperature (Besonen et al., 2008). Therefore, this study shows the most complete and accurate record of hurricane activity for the greater Boston area. However, this is a single record, so in order

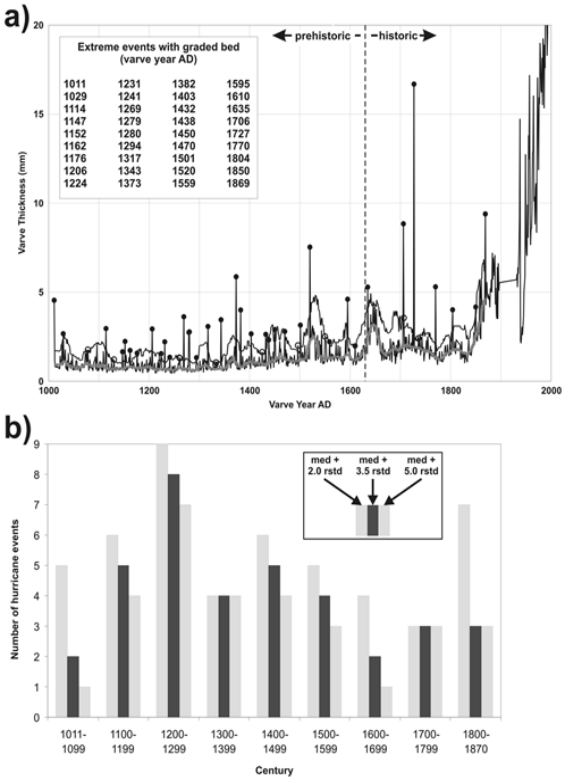

Figure 1.5: Varve Thickness and Hurricane History from Boston, MA, USA (Besonen 2006)

to make accurate statements about landfalling hurricane frequencies over larger areas and regions (such as the entire NE US), more study sites are needed to validate these findings and to aid in further constraining results seen in overwash studies.

1.4.2.2 Flood Events in Paleoclimatic Studies

While hurricanes can cause widespread flooding and catastrophic damage across a region, other types of extreme precipitation events, such as non-hurricane related flooding and severe droughts, can have severe consequences in the NE US. Some of the earliest work regarding flood frequencies throughout the Holocene found that even slight changes in climate can cause significant changes in flood frequency in a short period of time (Ely, 1997; Knox, 2000, 1993). Recently, increased interest and attention has been directed into flood records, as understanding how climate effects changing flood variability has "low to medium confidence" (IPCC, 2012). Studies have begun to reconstruct precipitation regimes in regions throughout the world using a multi-proxy approach, combining multiple analyses and proxies in a single study. This approach can be particularly advantageous for determining laminations linked to past floods (Schillereff et al., 2014).

Recent work on lacustrine sediment records from Europe have used analyses such as bulk density, magnetic susceptibility, elemental composition through X-Ray Fluorescence, grain size, and carbon and nitrogen isotope analysis to identify flood layers and to determine flood frequencies across the continent. These studies have been performed in the Swiss and North Italian Alps (Glur et al., 2013; Wirth et al., 2013), and southern Scandinavia (Støren et al., 2012; Støren and Paasche, 2014), resulting in records that extend back thousands of years. In the United States, paleoflood studies have been

completed using similar approaches in the western U.S. (Ely, 1997), in the Upper Mississippi River Valley and Midwestern U.S. (Knox, 2000, 1993), and the Northeastern U.S. (Noren et al., 2002; Parris et al., 2010).

1.4.2.3 Droughts in Paleoclimate Studies

Long term fluctuations in the precipitation balance, including precipitation extremes such as droughts, have also been studied across the United States in recent years. Some work looking at drought frequency has been done using tree-ring chronologies. For example, in a study by Pederson et al., thirty-two tree ring chronologies were used to reconstruct a precipitation history for New York, a city that has suffered from several water warnings and emergencies in the past three decades despite an increase in precipitation and no severe droughts. Research found that droughts similar to the last severe drought, occurring from 1962-1966, were more frequent and longer in duration throughout the 16^{th} and 17^{th} centuries (Pederson et al., 2012).

Over the past decade, lake level reconstructions extending throughout the Holocene have been performed in the Midwestern and NE US using a multi-proxy analysis of transects of cores from kettle ponds. For example, Shuman and Donnelly reconstructed past fluctuations in lake level in two small closed kettle ponds in southeastern Massachusetts using ground-penetrating radar (GPR). GPR was used to identify unconformities located near shore in lacustrine sediments, which provide the approximate magnitude of past lake level declines (Shuman and Donnelly, 2006). Since then, more proxies have been used in combination with GPR, including pollen assemblages, stable isotope analysis, Loss-on-Ignition (LOI) analysis, and X-Ray Fluorescence (XRF) analysis (Newby et al., 2014; Shuman et al., 2009; Valero-Garcés et

al., 1997).

1.4.2.4 Extreme Event Reconstructions in Biogeochemical Studies

Another area of research that can be used to examine a precipitation regime in sedimentary records is through studying the biogeochemistry of the sediment records. Organic geochemical proxies have been increasingly used in studies to reconstruct paleoenvironmental and paleoclimatic variability in lacustrine sediment records (Castañeda and Schouten, 2011). Organic matter preserved in lacustrine sediment can record signals of past environmental conditions at the time of deposition, making them an advantageous and effective tool in environmental reconstructions. In particular, compounds preserved in sediments that can be traced to a particular organism or process, known as biomarkers, can be analyzed to monitor lake conditions throughout time (Castañeda and Schouten, 2011). Biomarker work can be particularly useful when a lake efficiently preserves organic matter in its sedimentary sequence.

1.4.2.4.1 Precipitation History using Biogeochemistry

One such biomarker class that has been used extensively in paleoenvironmental studies is straight-chained *n*-alkanes. Due to their stable molecular structure and lack of functional groups, *n*-alkanes are long-lived molecules that can survive in the fossil record for millions of years (Eglinton et al., 1991; Peters et al., 2005). *n*-alkanes are produced by numerous organisms, and the dominant chain lengths, carbon number distributions, and isotopic compositions can vary depending on their source (Bush and McInerney, 2013; Castañeda and Schouten, 2011). Long-chain *n*-alkanes ($C_{27} - C_{35}$) have been found to be produced mainly in the epicuticular waxes of higher terrestrial plants (Bush and McInerney, 2013; Castañeda and Schouten, 2011; Eglinton and Hamilton, 1967). Short-

chain (C_{17} - C_{21}) *n*-alkanes are mainly produced by aquatic algae (Cranwell et al., 1987; Giger et al., 1980), while mid-chain (C_{23} - C_{25}) *n*-alkanes are a dominant component of aquatic plants, or macrophytes (Ficken et al., 2000).

Due to particular *n*-alkane distributions that are produced by certain source organisms, biogeochemical studies of sedimentary *n*-alkanes have focused on the application of ratios of particular chain lengths in an effort to reconstruct past environmental conditions (Bush and McInerney, 2013). Long-chain (C_{27}+C_{29}+C_{31}) to short-chain (C_{15}+C_{17}+C_{19}) ratios have been used to assess the relative input of terrestrial versus aquatic sources of organic matter in lacustrine settings (Castañeda and Schouten, 2011; Meyers, 1997; Sun et al., 2013). The Average Chain Length (ACL) ratio of *n*-alkane distributions in sediment can be used in some lakes to look at aridity and temperature fluctuations over time (Peltzer and Gagosian, 1989; Rommerskirchen et al., 2003; Zhang et al., 2006). The "Paq ratio" describes the abundance of mid-chain *n*-alkanes over the sum of mid-chain and long-chain *n*-alkanes, and has been used to estimate moisture-dependent variations in lake sediments (Ficken et al., 2000; Sun et al., 2013; Zhou et al., 2010).

Other measurements commonly utilized include compound-specific carbon and hydrogen isotope measurements ($\delta^{13}C$ and δD, respectively). $\delta^{13}C$ values of long-chain *n*-alkanes provide information on the carbon fixation pathway used during photosynthesis, thus giving a way to distinguish the plant types (C_3 or C_4 plants) from which the *n*-alkanes are sourced (Freeman et al., 1990; Schefuß et al., 2003). Furthermore, water-use efficiency (WUE) has been found to be a significant factor that affects carbon isotope composition in plants, and studies have shown a significant negative correlation between

$\delta^{13}C$ values and effective precipitation in a region (Sun et al., 2013). The hydrogen isotopic composition (δD) of *n*-alkanes can also be correlated with precipitation. While in some locations δD tracks moisture sources, δD of *n*-alkanes can potentially be used as a hydrology and temperature proxy when processes regarding isotope fractionation are understood (Pautler et al., 2014). When utilized in combination with other proxies, these two measurements of isotopic composition of *n*-alkanes can be useful indicators of effective precipitation or drought stress in a region (Sun et al., 2013; Yamamoto et al., 2010; Zhou et al., 2010).

One study that utilizes a majority of the proxies described above in reconstructing fluctuations in precipitation was performed by Sun et al, 2013 in northeast China. This study was performed on a varved sediment record from Lake Xiaolongwan, and correlated several *n*-alkane proxies (ACL, Paq, grass-to-tree values, and $\delta^{13}C$ values) with historical precipitation, flood, and drought records from the region over the past 1,600 years (Table 1.2). This study found that these proxies, particularly the Paq ratio and $\delta^{13}C_{wax}$ values, show distinct decadal variations that correlate well with the precipitation history for the region. Furthermore, they found that these proxies also correspond to warm and cold phases of the Pacific Decadal Oscillation (PDO), which regulates summer monsoon rainfall on decadal timescales in the region, as seen in Figure 1.6 (Sun et al., 2013). This study is a good example of how research on *n*-alkane distributions in lake sediment can be used to look at long-term precipitation trends and extremes, such as severe droughts.

Proxy	**Calculation**
ACL	$\Sigma(C_{23}$ to $C_{33})$
Paq Ratio	$(C_{23}+C_{25})/(C_{23}+C_{25}+C_{29}+C_{31})$
Grass to Tree Ratio	C_{31} / C_{27}

Table 1.2: Summary of the proxies used in Sun et al. (2013).

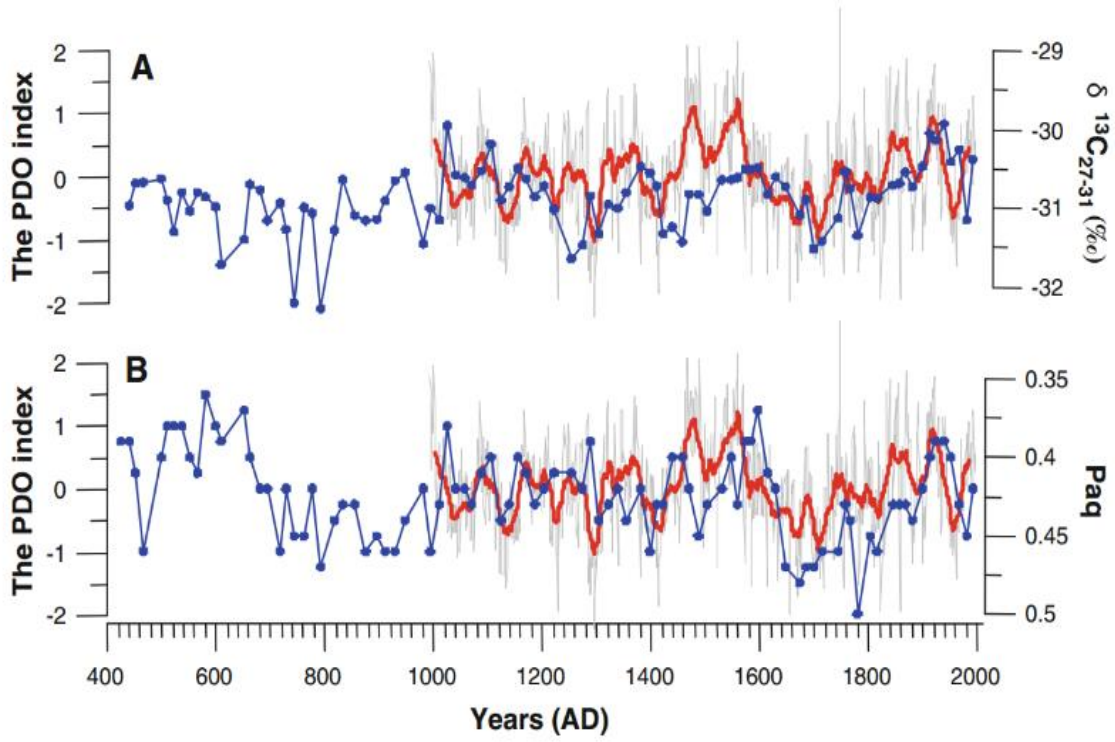

Figure 1.6 – Correlation of *n*-alkane proxies with the Pacific Decadal Oscillation (PDO) and precipitation in Northeast China. A) $\delta^{13}C$ values of long-chain *n*-alkanes (blue) and the PDO index (red, B) Paq index (blue) and the PDO index (red). (Sun et al 2013)

1.4.2.4.2 Wildfire History using Biogeochemistry

Wildfire reconstructions have become a major topic in climate change research over the past several decades. Understanding wildfires, including fire frequency and anthropogenic impacts on wildfires, is critical in the context of global climate change because wildfires have direct impacts on carbon storage, atmospheric composition, ecosystem diversity, and land management practices (Clark and Royall, 1995; Denis et al., 2012; Gill and Bradstock, 1995; Kirchgeorg et al., 2014; Werf et al., 2004). Fire frequency is expected to increase in most global warming scenarios, and costs relating to wildfire management and damage have already been shown to be increasing in recent years (Denis et al., 2012). Furthermore, there is still uncertainty about how human

disturbance, particularly in the NE US, affects the natural, pre-settlement burning regime due to our lack of continuous records of fire history for pre-settlement times (Clark and Royall, 1995). Therefore, reconstructions of wildfire history are a major factor in understanding climate-wildfire feedbacks and how climate influences natural wildfire regimes (Denis et al., 2012).

Reconstructions of wildfire history have been performed across the NE US and Eastern Canada for several decades (e.g. Swain, 1973). Until recently, the most common methods used for wildfire reconstructions were the analysis of sedimentary charcoal and tree-ring fire scars. In the NE US, tree-ring studies looking at fire history are extremely limited due to human disturbance on forest ecosystems in the region (Barton et al., 2012; Lorimer, 1977; Parshall et al., 2003). Because of this, most wildfire studies have focused on charcoal fossil counts in the lacustrine sediment record (e.g. Devil's Bathtub, NY (Clark et al., 1996); Crawford Lake, Ontario (Clark and Royall, 1995); Maine and New Hampshire (Fahey and Reiners, 1981); Cape Cod, Massachusetts (Parshall et al., 2003); Piermont Marsh, lower Hudson River Valley, New York (Pederson et al., 2005); Swain, 1973).

While this method has greatly increased our understanding of past wildfire activity, there are some limitations. Charcoal analysis is a time intensive procedure and can require large volumes of sediment per sample (up to 5 cc of sediment) depending on sediment composition and charcoal abundance (Denis et al., 2012; Whitlock and Larsen, 2001). Other factors, such as the physical processes of charcoal deposition and decomposition, as well as remobilization and re-deposition, can also affect fire history reconstructions and interpretation of results (Whitlock and Anderson, 2003).

Recent developments in instrumentation and in the field of biogeochemistry have facilitated the study of compound classes that can also be used as a wildfire proxy. One such compound class that has been increasingly studied is polycyclic aromatic hydrocarbons (PAHs). PAHs are a group of hydrocarbons (organic compounds that consist of the elements carbon and hydrogen) that can be produced through natural and anthropogenic processes (Bianchi and Canuel, 2011). PAHs were first found in soils by Blumer in 1961, and have since been studied across various ecosystems and environments, including lakes. There are three major types of PAHs: petrogenic PAHs (related to petroleum processes), biogenic PAHs (generated by biologic processes such as early diagenesis), and pyrogenic PAHs (predominantly unbranched, mostly 3-6 ring hydrocarbons, made through the partial combustion of organic material) (Page et al., 1999).

Due to the fact that pyrogenic PAHs are mainly created during combustion, these compounds can be used to trace combustion processes, such as fossil fuel burning or forest fire activity (Denis et al., 2012; Page et al., 1999; M.B. Yunker et al., 2002). Therefore, the historical record of PAHs in sediment cores can be used in pre-industrial periods as proxies for the frequency and size of wildfires (Musa Bandowe et al., 2014). One study that reconstructed wildfire history using PAHs was carried out at Swamp Lake in Yosemite National Park, U.S.A. Researchers found that PAHs produced during wildfires record local fire events and intensity, and that low molecular weight (LMW) PAHs (e.g., fluoranthene, pyrene, and benz[a]anthracene) are the best recorders of fire at this location, whereas high molecular weight (HMW) PAHs likely record fire intensity (see Figure 1.7) (Denis et al., 2012). Other studies have created ratios of different PAHs,

such as Retene/(Retene + Chrysene), and Anthracene/(Anthracene + Phenanthrene), which have been utilized as proxies for varying sources of the PAHs, such as fossil fuels or modern biomass burning (Denis et al., 2012; Kuo et al., 2011; Yan et al., 2005; Mark B Yunker et al., 2002).

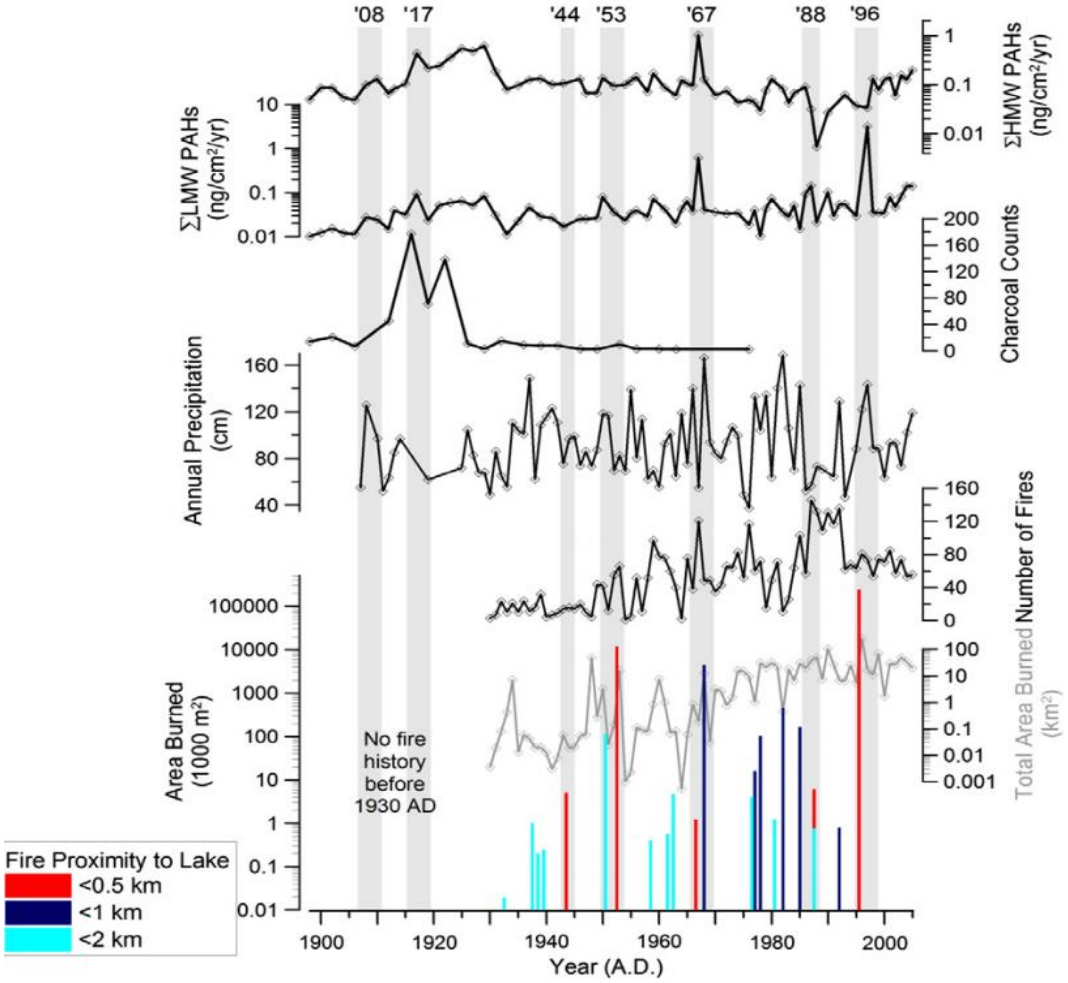

Figure 1.7 – PAH abundances through time compared with charcoal, fire, and precipitation histories at Yosemite National Park, USA. PAH fluxes are shown as the Sum of Low Molecular Weight (LMW) PAH and the sum of High Molecular Weight (HMW) PAH. Denis et al (2012)

Due to their usefulness as a proxy for wildfire detection in relation to climatic and anthropogenic forcing, PAHs have been used in reconstructions prior to the historical period (pre-1800AD), with several studies across the world looking at pre-historic fire history using PAHs. One such study created a 2,600 year-long record of PAH deposition

in sediment cores at Holzmaar, Germany, and used it as an indicator of variability in climate and human activity in the region (Musa Bandowe et al., 2014). Another study, performed on sediment cores from Lake Lille Lungegardsvannet, Bergen, Norway, looked at PAH concentrations during the last 5,400 years. This study found several significant concentration increases in pre-industrial times, corresponding to urban fires in the city of Bergen, Norway, as well as human factors in recent times (i.e. heating, traffic pollution, etc..) (Andersson et al., 2014). While more work is needed to constrain PAHs as a proxy for fire activity, they have been shown to correlate well with fire history, and provide a promising method to reconstruct proxy for wildfire activity to supplement more traditional methods of measurement, such as charcoal analysis. New techniques for measuring PAHs in low abundances due to analytical improvements have been developed, allowing for more studies to use PAHs as proxies for fire history.

1.5 Summary

The Northeastern United States is one of the most heavily populated regions in the world that is susceptible to multiple types of extreme climatic events such as hurricanes, flooding events, severe droughts, and wildfires. Furthermore, this region has experienced anthropogenic climate change over the past century. Despite our knowledge of how anthropogenic climate change is affecting the region's climate, little is known about how the frequencies of extreme events in the northeast have been affected by climate change. In order to address this issue, this thesis project aims to (1) determine how known extreme events are documented by instrumental measurements and historical records, (2) to identify how human activities and rapid environmental change in the catchment area are expressed in the sedimentary record, and (3) to distinguish and

evaluate how climatic events are expressed in the physical and geochemical properties of a lacustrine sedimentary sequence. This information can then be used to extend the record of known extreme events beyond the brief period of instrumental measurements into pre-historic times.

To address these questions, the following hypotheses will be tested:

(1) There has been human disturbance in the catchment area during the past 200 years, and is seen in the sedimentary record of Basin Pond

(2) Extreme events (hurricanes, floods, droughts, and wildfires) can be identified in the Basin Pond sedimentary record throughout the historic period using a suite of sedimentary, organic geochemical, and inorganic geochemical analyses.

While the NE US has a rich history in paleolimnological studies looking at the region's environmental history, most studies that have been performed focus on pollen analysis and Loss-on-Ignition to reconstruct vegetation changes and organic matter input throughout the Holocene (Allison et al., 1986; R. Brugam, 1978; R. B. Brugam, 1978; Davis, 1969; Davis and Ford, 1982; Gonzales and Grimm, 2009; Leopold, 1956; Oswald et al., 2007; Shuman, 2003; Shuman et al., 2001; Spear et al., 1994; Thorson and Webb, 1991; Wellner and Dwyer, 1996; Whitehead, 1979; Winkler, 1985; Winkler and Sanford, 1995). Furthermore, as described previously in this chapter, most studies reconstructing extreme events in the Northeast have primarily focused on one type of event (e.g. hurricane records or wildfire reconstructions). This creates a unique opportunity for this research, as looking at multiple extreme events in this annually-resolved sediment record in the NE US has not been carried out before.

CHAPTER 2

SITE INFORMATION AND FIELD WORK AT BASIN POND, FAYETTE, MAINE

2.1 Site Information

Basin Pond is a small (13.8 hectares (ha) lake area) and deep (32.6 m max depth) lake located in Fayette, Kennebec County, Maine at 44º28'N, 70 º03'W at an elevation of 124 meters above sea level (Frost, 2005; Gajewski et al., 1987; Perkins, 1985) (see Figure 2.1). At 53.0 Ha, the Basin Pond watershed is roughly 3.5 times larger than the lake size (Frost, 2005). The pond has no inlets, with the main source of water input into the lake coming from groundwater and precipitation. The only outlet from Basin Pond is a small, dammed stream running westward into the adjacent David Pond (Frost, 2005; Perkins, 1985). The catchment area of the pond contains one residential building, with the remaining majority of the area being located within the "Basin Pond Conservation Area" (Frost, 2005). Basin Pond is managed and maintained by the Basin-Tilton-Davis Pond Association and is annually stocked with splake by the Maine Department of Inland Fisheries and Wildlife (starting in 1981), with conservative regulations in place to protect the fishery in Basin Pond (United States Geological Survey (USGS), 1996).

The surficial deposits of Basin Pond and its watershed are comprised almost entirely of glacial till over bedrock, with the catchment area situated on an intrusive Devonian granite pluton (Baker, 1999; Frost, 2005). The granite consists of quartz, plagioclase, microcline, muscovite, biotite, and chlorite (Baker, 1999). The western and southern shorelines of the lake are steep banks, whereas the northern and eastern shorelines are gentle-sloping banks with large boulders present. The catchment area is

dominated by a well-developed forest, comprised of deciduous hardwoods and evergreen trees, with hemlock being the most abundant species (Perkins, 1985).

Basin Pond has been surveyed multiple times throughout the past 60 years by the United States Geological Survey (USGS),the Maine Department of Inland Fisheries and Wildlife, and the Department of Environmental Protection, with the first survey occurring in 1955 and revisions in 1970, 1987, and 1996. With the first surveying, the pond was "chemically reclaimed" to remove undesired species that were in competition with the trout population of the pond, using the chemical piscicide rotenone (United States Geological Survey (USGS), 1996; personal communication, Department of Environmental Protection). Since this chemical reclamation, three unwanted fish species have become re-established in the pond. In each survey, as well as in a couple of the studies performed at Basin Pond (discussed in the next section), water profiles were taken, consisting of water quality, temperature, pH, salinity, and other profiles (Frost, 2005; Perkins, 1985; United States Geological Survey (USGS), 1996). In modern times, pH values of Basin Pond waters range between 6.53-6.76 (Doner, 1985). Average air temperatures at Basin Pond range from roughly 21ºC in the summer to -5.5ºC in the winter, and average total annual precipitation is roughly 112 cm (Baker, 1999). Water column temperature profiles have found that the surface waters fluctuate with the air temperature, peaking near 25.5ºC in the summer, while bottom waters stay near 4 ºC throughout the entire year (United States Geological Survey (USGS), 1996). Basin Pond ice-in occurs from late November – early December, while ice break usually occurs from mid-March – mid April. A more in-depth discussion of the modern climate of the region is given in the next chapter.

2.1.1 – Past Studies at Basin Pond

A handful of past studies have taken place on the sediments of Basin Pond, each focusing on different aspects of the region's environmental history. Beginning in 1984, a study by Joanne S. Perkins was conducted on investigating the Basin Pond catchment area's response to a major shift in the forest structure of the region, known as the Hemlock Decline, occurring at roughly 4,800 years before present. In this study, Perkins proposed to reconstruct the environmental history from this time period using Loss-on-Ignition, pollen, and grain-size analyses, using varve-counts as the chronology for the sedimentary archive (Perkins, 1985). However, little information could be found on the results of this study. This study was further investigated by Dr. Lisa Doner in 1990 at the University of Maine - Orono, who studied the Basin Pond sediment record of the Younger Dryas stadial and the early Holocene using LOI and grain size analyses (Doner, 1990).

Through the 1980's and 1990's, studies reconstructing past environmental changes in the Basin Pond catchment area were conducted focusing on pollen and charcoal records. In a study by Konrad Gajewski and colleagues, pollen records indicated various shifts in the dominant type of tree species at the pond over the past 1600 years. High levels of *Tsuga* and *Fagus* were found early in the record, shifting to mainly non-arboreal pollen in the last 150 years, indicating human disturbance (see figure 2.3) (Gajewski et al., 1987). Further work by Gajewski reconstructed past annual precipitation and summertime temperatures for Basin Pond over the past 1600 years from this pollen record, which was marked by a steady decrease in temperature throughout the record and a relatively stable precipitation regime until recent years, when precipitation decreased

(Gajewski, 1988). In the 1990's, J.S. Clark and P.D. Royall investigated the fire history at Basin Pond throughout the past 1600 years using sedimentary charcoal analysis (see figure 2.4), and found that there was very low fire frequency or even a lack of a fire signal seen at Basin Pond (Clark and Royall, 1996, 1994).

The most recent work conducted on the Basin Pond sedimentary record prior to this study was done by Daniel Frost as part of an undergraduate thesis at Bates College, Lewiston, Maine, in 2005. Frost's thesis focused on using proxy data based on physical sedimentology (lithology, varve thickness, Loss-on-Ignition) and bulk organic matter biogeochemistry (organic matter carbon/nitrogen ratios, $\delta^{13}C$), based upon varve chronologies and radiocarbon ages, to reconstruct climate variability throughout the past 12,000 years (Frost, 2005). Several valuable results came from this study, such as water column profiles taken at different times throughout the year, indicating anoxia and a persistent chemocline at depth (see figure 2.5). This thermal and chemo-stratification of the water column at times when overturning usually occurs (spring and fall), was found to be sufficient to prevent turnover at any point in the year in the Basin Pond water column. While these water column profiles suggest that Basin Pond loses thermal stratification directly before "ice-in", the rapid development of ice prevents any significant mixing and wind-driven circulation of the water column, making the diffusion of dissolved oxygen into the bottom waters minimal (Frost, 2005).

2.1.1.1 Age Models of Past Studies

While numerous studies have been performed on the Basin Pond sedimentary record, a concise, independently dated age model has been difficult to produce in all of the studies carried out so far. In nearly every past study, varve chronologies were the only

dating method used on the sedimentary record. While this gives a reasonably accurate method of dating on yearly timescales, this method is based on the assumption that the Basin Pond sedimentary record is truly varved, which to date has not been proven. Thus, other dating methods independent of varve counts, are needed to help confirm the annual nature of these laminations. It is important to note that many of the early studies that used age models based on varve counts had vastly differing age chronologies (on the scale of several hundred years), indicating the error that can exist when conducting varve counts.

The only study completed at Basin Pond that utilized another method of dating was the study by Frost (2005). In this study, several radiocarbon dates were obtained from plant macrofossils preserved in the sediment record, and ages were found with varying error margins. When comparing the ages from varve counts to the ages from radiocarbon dating, the discrepancies were significant, as can be seen in table 2.1. This was interpreted as errors in both dating methods due to several unconformities in the sediment record, but brings light to the necessity of further work constraining the age model from the Basin Pond sedimentary record.

Depth (cm):	**119 - 120 cm**	**179 - 180 cm**	**254.5 cm**
Radiocarbon Ages:	3600 +- 50	6290 +- 60	10960 +- 60
Varve Ages:	2306	4338	--
Age Difference:	**1,294 yrs**	**1,952 yrs**	

Table 2.1: Varve count ages and radiocarbon age estimates from the Basin Pond sedimentary sequence from the Frost (2005) study.

2.1.2 Basin Pond during the Historical Period

Based on the past studies performed on the lake, as well as work completed by the USGS and Maine Department of Inland Fisheries and Wildlife, a rough view of the catchment history over the past century can be formed. This is particularly important, as

most past studies performed at Basin Pond acknowledge a signal of human disturbance in the catchment area, but discuss it in little detail, leaving this time period a gray area in the catchment history. The best example of this involves deforestation of the catchment area: to the best of my knowledge, no historical records exist on the timing of the logging of this area. However, most studies indicate varying time periods where catchment deforestation is assumed, based on proxy data.

One major event in Basin Pond was the chemical reclamation of the pond, occurring in 1955, by the Department of Inland Fisheries and Wildlife. This consisted of chemically altering the water column with rotenone to remove unwanted fish and algal species that are competitors with trout or inhibit trout growth. Rotenone is a highly active photosensitizer used as an insecticide and piscicide, and works by inhibiting the cellular respiration of animals (Robertson and Smith-Vaniz, 2008). Apart from this event, little altering of the water column has been performed, apart from an experimental introduction of blueback trout in 1969 and an experimental stocking program of splake in 1981 (United States Geological Survey (USGS), 1996). A house was built in the 1980's in the catchment area, but to the best of our knowledge, no other major construction project was completed.

2.2 Field Work

Primary field work at Basin Pond was completed on March 8, 2014, by Dr. Raymond Bradley and graduate student Daniel Miller of the Department of Geosciences at the University of Massachusetts – Amherst, with colleagues Dr. Mike Retelle, Daniel Frost, and undergraduate student Julie Savage from Bates College in Lewiston, Maine. Sediment coring was performed from the ice surface in the deepest part of the lake at a

depth of 32 meters (44º27.456' N, 70º 03.149' W). A total of five sediment cores were taken over the course of the day using UWITEC gravity coring system. The first two cores, BP2014-1D (65cm length) and BP2014-2D (72cm length), were taken in hopes of capturing the sediment-water interface for Lead-210 and Cesium-137 dating. However, the interface was overshot, so these cores were capped and saved for analysis. The third core, BP2014-3D (37cm length after subsampling), captured the sediment-water interface, and was then subsampled in the field at 0.5 cm resolution. Samples were stored in whirl-pak™ bags, while the remainder of the core was capped and saved for analysis. Cores BP2014-4D and BP2014-5D (1.5 m and 1.75 m, respectively) were taken and capped with zorbitol and florofoam.

Cores were transferred to the Department of Geosciences at UMass – Amherst and stored vertically in a walk-in freezer in the Department of Geosciences facilities until analysis. Core splitting occurred March 11, 2014, using a geotek core splitter. Because of the length of core BP2014-5D, it was cut into two sections for analysis prior to splitting. Each section was then renamed BP2014-5D.A (100 cm in length) and BP2014-5D.B (roughly 75 cm in length). It is important to note that approximately 2cm of sediment was lost at the bottom of core 5D.A during the splitting of 5D. Upon splitting, cores were preserved in several layers of plastic wrap and returned to the freezer until analysis.

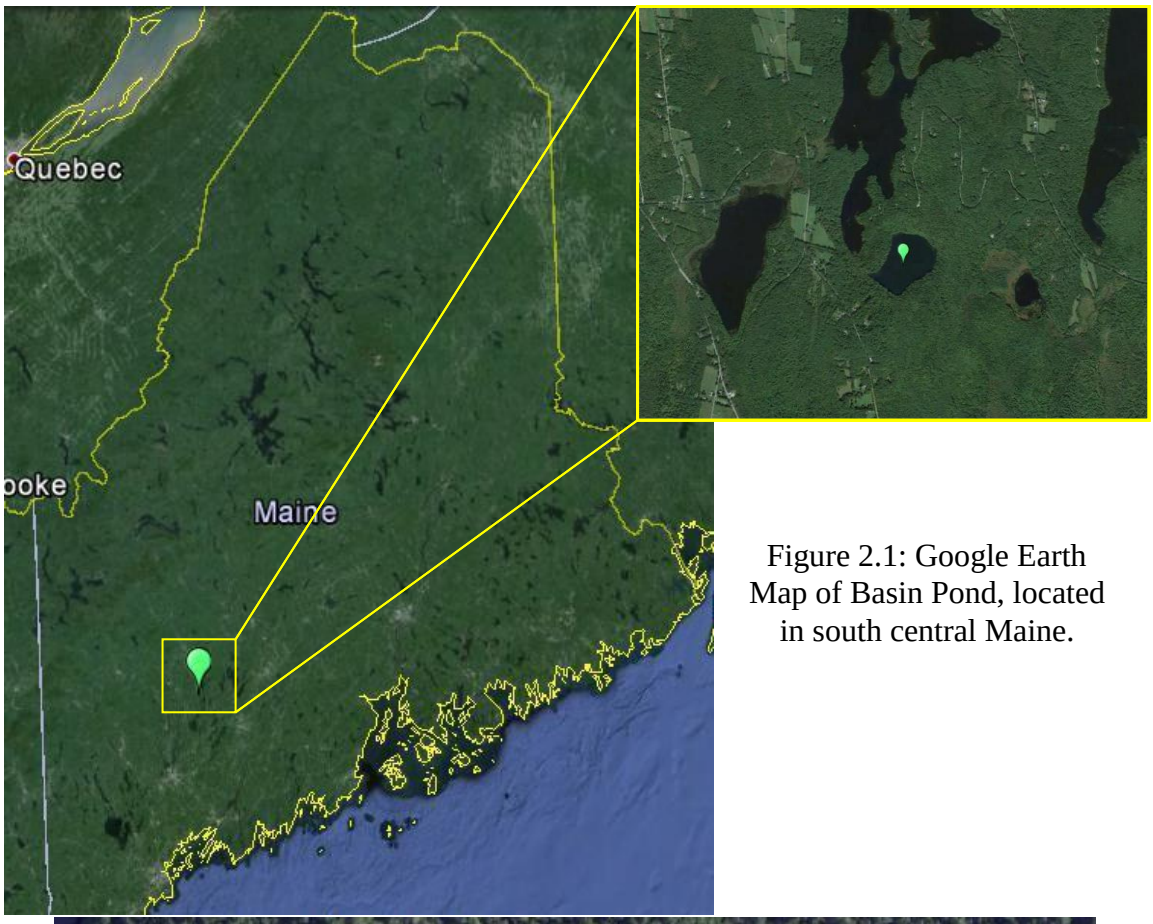

Figure 2.1: Google Earth Map of Basin Pond, located in south central Maine.

Figure 2.2: Basin Pond Bathymetric Profile, completed by the USGS (2015)

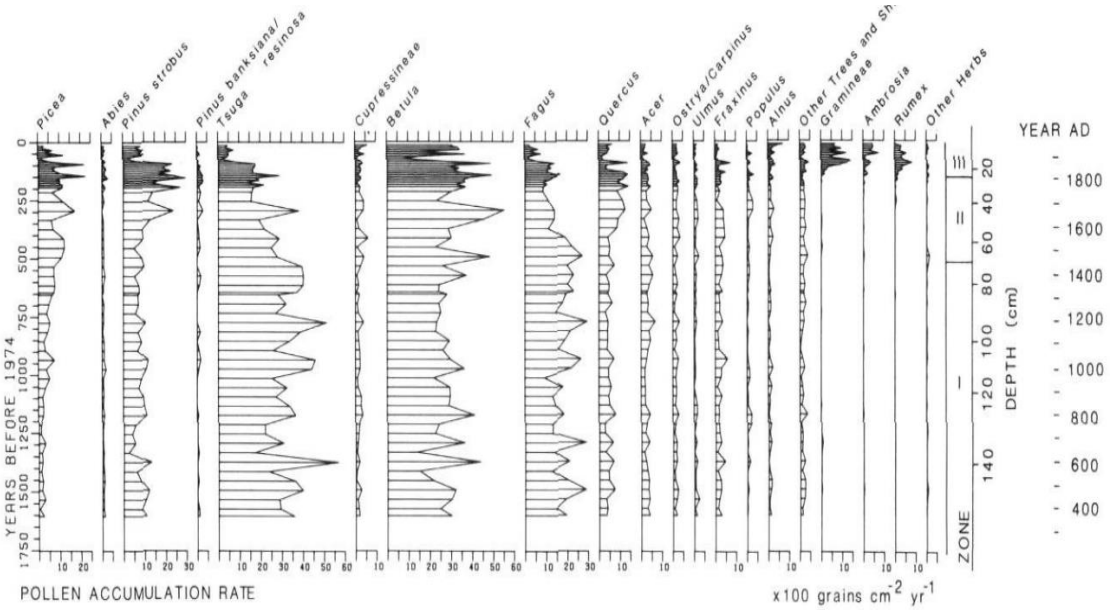

Figure 2.3: Pollen Assemblages based on Pollen Accumulation Rates (PAR) of the Basin Pond sedimentary record over the last 1,600 years. (from Gajewski 1987)

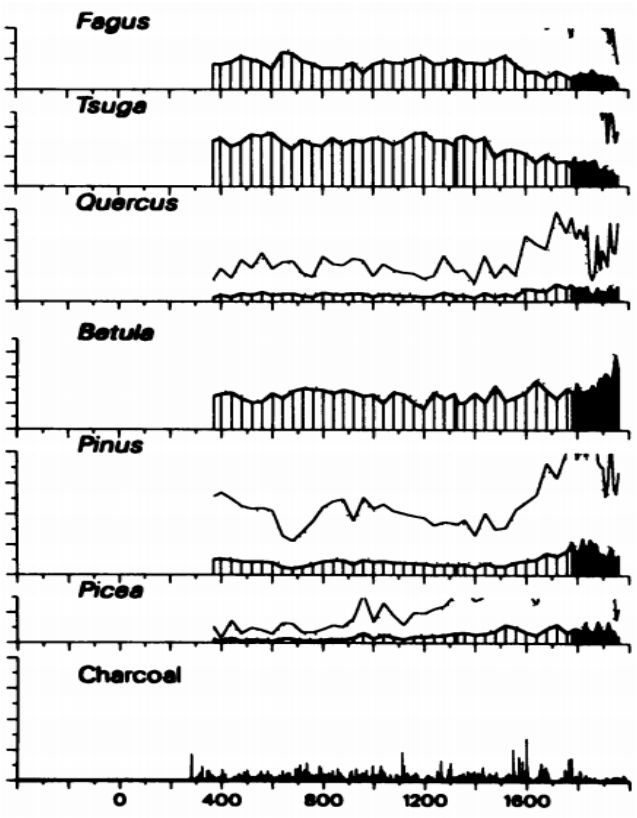

Figure 2.4: Charcoal counts plotted with various pollen assemblages taken from the Gajewski 1987 study. (Clark and Royall 1996)

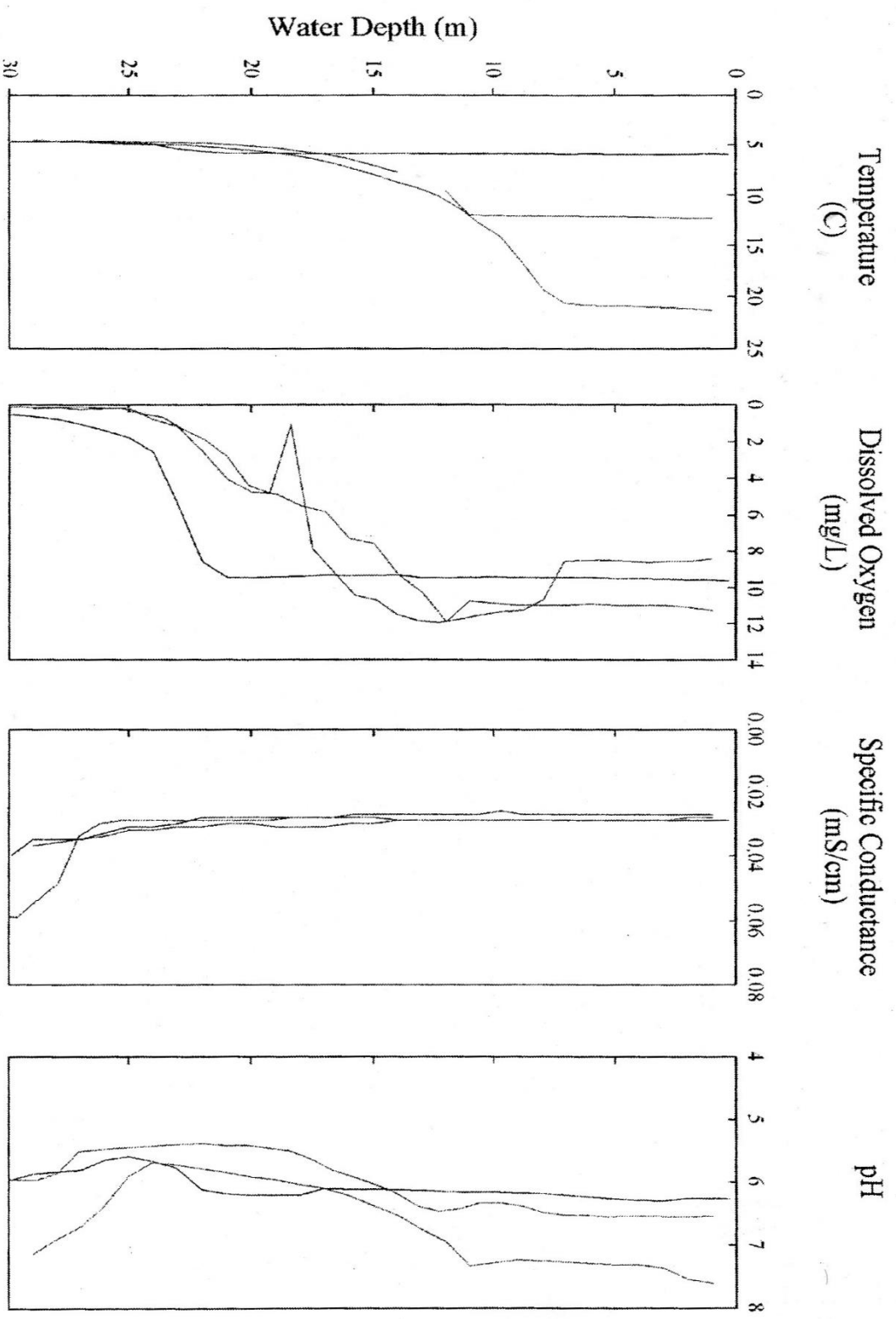

Figure 2.5: Fall-Winter water column profiles from Frost (2005). Profiles depicted were taken over a year on Sept 17, 2003, Sept 20, 2004, and Oct 31, 2004. Note a persistent chemocline and anoxia at depth in all profiles.

Figure 2.6: Images from March 2014 Basin Pond Field Campaign. A)Top left: subsampling Core BP2014-3D for radioisotopic dating. B)Top Right: Basin Pond at sunset. C)Bottom, from Right to Left: Dr. Raymond Bradley, Daniel Frost, Julie Savage, and Daniel Miller with Core BP2014-5D.

CHAPTER 3

DATA COLLECTION AND METHODS

3.1 Climatic and Meteorological Data during the Historical Period

Historical records for Basin Pond, Fayette, Maine, have been compiled and are comprised of meteorological observations and of local archives of information such as newspapers or news stations. The vast majority of these are meteorological daily observational data (including precipitation amounts, temperature, cloud cover, snowfall amounts, humidity) from meteorological observational stations (MET stations) located within 20 miles of Basin Pond. Daily records were maintained and accessed through the National Climatic Data Center (part of the National Oceanic and Atmospheric Administration). In order to ensure maximum temporal coverage, daily records from the three closest stations – Kents Hill, Farmington, and Livermore Falls – were compiled, as shown in table 3.1 (Figure 3.1). Fortunately, these data formed a nearly continuous and complete 129 year record of observational data fromOctober of 1885 to the present day (National Oceanic and Atmospheric Administration (NOAA), 2014b). Analysis included obtaining the yearly monthly, seasonal, and yearly averages of both local precipitation and temperature.

Station Name	Elevation (m)	Start Date	End Date
Kents Hill	152.4	10/1/1885	5/31/1893
Farmington	128	6/1/1893	07/31/2002
Livermore Falls	115.8	08/01/2002	10/14/2014

Table 3.1 – Meteorological Stations used in the creation of a met data stack for Basin Pond, Fayette, Maine

A record of historical storm tracks was compiled from the archives of the National Oceanic and Atmospheric Administration (NOAA) Coastal Services Center and the National Hurricane Center. A search for any storm (hurricane, tropical storm, tropical

depression, or extratropical) was conducted within a 50 mile radius of Basin Pond, Fayette, ME as a search filter (Figure 3.2). Results from the search included 25 total storms from 1869 to present, or the last 145 years. The results of this search, including details on the type and strength of the storms, can be seen in Appendix A. Precipitation amounts for storms post-1885 were taken from the MET stations records described previously. Lastly, extreme events were found, as described through Maine news archives. This was particularly important for events such as wildfires.

3.2 – Analyses Performed

Shortly after coring, all sediment cores were split, extruded, and logged at the University of Massachusetts – Amherst, Joseph Hartshorn Quaternary Laboratory. Examination and laboratory analysis on the physical and biogeochemical properties of the Basin Pond sedimentary record began in March of 2014. Details on the completed analyses are described below.

3.2.1 – Age Model

Age estimates for the Basin Pond sediment record are based on radioisotopic dating, radiocarbon dating, and varve counts. For radioisotopic analysis, core BP2014-3D was subsampled at 0.5cm resolution slices in the field. Each slice was stored in a 4 ounce WhirlPak™ bag and brought back to UMass for radioisotopic dating analysis. Samples were then freeze dried, homogenized, and transferred to plastic containers for analysis. Heavy metal counts of lead-210, lead-214, and Cesium-137, were conducted on a Gamma Counter in the UMass sedimentology lab.

Radiocarbon dating was also carried out on discrete samples from the sediment record. Four macrofossils of plant material were taken from the BP2014-5D core at

varying depths, and were sent to the U.S. Geological Survey Eastern Geology and Paleoclimate Science Center Radiocarbon Laboratory in Reston, Virginia, for radiocarbon analysis in June of 2014. An additional six samples were sent to The Woods Hole Oceanographic Institute AMS radiocarbon facilities for radiocarbon analysis in February of 2015. Radiocarbon age estimates of terrestrial macrofossils were calibrated to years before present (1950) and then compared with the Pb-210 and Cs-137 horizons using the 'R' program 'BChron'. No corrections for 'old' carbon were made to these dates since they came from terrestrial macrofossils. A summary of radiocarbon samples can be seen in Table 3.2, including depths in the sedimentary record at which each sample was found, dry weight (in mg), and type of sample.

Sample Name	Core	Depth (cm)	Type	Dry weight (mg)
BPR-DRM-001	5D 1/2	29 – 31	plant	11.0**
BPR-DRM-002	5D 1/2	75 – 76	plant	11.1**
BPR-DRM-003	5D 2/2	135.5 - 136.5	plant	35.5**
BPR-DRM-004	5D 2/2	165 - 167	plant	10.1**
BPR_WHOI_004	5D 1/2	20 – 21	plant/seed	2.7
BPR_WHOI_008	5D 1/2	26 – 27	plant	7.4
BPR_WHOI_009	5D 1/2	33 – 35	plant	4.0
BPR_WHOI_012	5D 1/2	36 – 39	plant	3.3
BPR_WHOI_022	5D 1/2	82 – 84	plant	1.7
BPR_WHOI_026	5D 1/2	54 – 56	plant	2.7

Table 3.2: Description of radiocarbon samples. **Denotes wet macrofossil weight in mg, not dried.

Finally, varve counts were completed using X-Ray radiograph images from cores BP2014-1D and BP2014-5D. Scans were completed on the ITRAX X-Ray Fluorescence analyzer at the University of Massachusetts. Each radiograph was completed at 100 micron resolution, allowing for the density fluctuations between laminations to be seen throughout both cores. Raw grayscale values were then extracted from the radiographic

images. Each lamination in the upper 16cm of the sediment record was then counted and compared to the age-depth models compiled from the radioisotopic and radiocarbon dating techniques described above.

3.2.2 – Nondestructive Analysis

3.2.2.1 - Geotek Multi-Sensor Core Logger (MSCL)

All split sediment cores were imaged and logged on the Geotek MSCL at the University of Massachusetts – Amherst for gamma ray attenuation density, magnetic susceptibility (MS), and spectral properties. Core images were taken using a Nikon AF Nikkor 50mm f/1.8 D lens equipped with a Tiffen circular polarizer. Magnetic susceptibility was measured using a Bartington Point Sensor, while the color spectrophotometry was measured using a Konica Minolta Spectrophotometer CM-2600d. All geotek measurements were made at 0.3cm resolution.

3.2.2.2 Itrax X-Ray Fluorescence (XRF) Core Scanner

Split core sections were also scanned at 1mm resolution on an ITRAX X-Ray Fluorescence (XRF) core scanner (Cox Analytical Systems) located at the University of Massachusetts – Amherst using a Molybdenum (Mo) tube. Due to the lack of resolution between core laminations in the X-Ray radiographs as well as the elemental data, BP2014-1D and BP2014-5D were rescanned at a higher (100 micron) resolution. XRF core scanning allows for the high-resolution identification of changes in elemental composition throughout a sedimentary record, as well as producing X-Radiograph images (Shanahan et al. 2008; Rothwell & Rack, 2006). X-radiograph and XRF settings for all runs are shown below in Table 3.3.

3.2.3 - Discrete Sample Analysis

Core	Rad Voltage	Rad Current	Rad Exposure Time	Step size	XRF exposure time	XRF voltage	XRF current
BP2014-1D	60 kV	50 mA	1200 ms	1 mm	10 s	30 kV	55 mA
BP2014-2D	60 kV	50 mA	1200 ms	1 mm	10 s	30 kV	55 mA
BP2014-3D	60 kV	50 mA	1200 ms	1 mm	10 s	30 kV	55 mA
BP2014-4D	60 kV	50 mA	1200 ms	1 mm	10 s	30 kV	55 mA
BP2014-5Da	60 kV	50 mA	1200 ms	1 mm	10 s	30 kV	55 mA
BP2014-5Db	60 kV	50 mA	1200 ms	1 mm	10 s	30 kV	55 mA
BP2014-1D	40 kV	45 mA	1000 ms	100 μm	10 s	30 kV	55mA
BP2014-5Da	40 kV	45 mA	1000 ms	100 μm	10 s	30 kV	55mA

Table 3.3 – Radiograph and XRF settings used for all core scans on the Itrax XRF Core Scanner at UMass – Amherst. Radiograph is abbreviated "Rad" in the table.

3.2.3.1 Biogeochemical Analysis

Thirty discrete samples were extruded from core BP2014-5D 1/2 at 0.5cm resolution, starting at the sediment water interface and extending down to 15cm depth. An additional twenty-seven samples (0.5cm width) were taken every 2cm down to 68cm depth. All samples were placed in Whirl-Pak™ sample bags and were subsequently freeze-dried for 36 hours. Samples were homogenized in sample bags after freeze drying, and then were weighed in preparation for lipid extraction. Sample descriptions, including depth in core, dry sediment weight, and lipid extract weight, can be found in Appendix A.

Each sample was subjected to Accelerated Solvent Extraction (ASE) to obtain the total lipid extract of each sediment sample. Due to the organic-rich nature of each sample, relatively small amounts of sediment were needed for lipid extraction. Samples weighing between 0.10 and 0.30 grams were mixed with equal amounts of pre-extracted

diatomaceous earth. Samples were then extracted using a Dionex accelerated solvent extractor (ASE 200) with 60ml Ichem vials at a temperature of 100ºC with a dichloromethane/methanol (9:1, v/v) mixture. The resulting Total Lipid Extract (TLE) was dried under a steady stream of N_2 gas using a TurboVAP sample drier. Once dried, vials containing the TLE were again weighed, so that the weight of each TLE could be obtained. TLEs were then transferred to 4ml combusted glass vials using a small amount of 2:1 DCM:MeOH, rinsing each vial 4 times to ensure maximum transfer of TLE's.

TLEs were then separated into apolar (9:1 Hexane:DCM v/v), ketone (1:1 DCM:Hexane v/v), and polar (1:1 DCM:MeOH v/v) fractions using alumina oxide column chromatography. Columns were made using 5¾-inch glass Pasteur pipettes with a small amount of packed quartz wool placed in the bottom of each column. Columns were then filled approximately 2/3 full with activated alumina oxide, heated at 150ºC for two hours and cooled for 1.5 hours to activate the alumina oxide. Just prior to use, columns were rinsed with 3-4ml of 9:1 hexane:DCM (v/v). Samples were then run through the columns using ~1ml of each solvent mix listed above per rinse. This process was repeated 4 times with each mix, so that roughly 4ml of each solvent mix, loaded with the TLE, was run through the column. Each fraction was collected in new, combusted 4ml glass vials, and was dried under a constant stream of N_2.

Apolar and ketone fractions were dried down under a constant stream of N_2 and then transferred to 2ml vials using 2 hexane rinses and 2 DCM rinses. Samples in 2ml vials were then dried and brought up in 100 µl of hexanes for analysis. Polar fractions were split in half so that a portion could be filtered for analysis on a high-performance liquid chromatograph (HPLC). The other half was derivatized using 25µl of acetonitrile

and 25µl of bistrimethylsiyltrifluoroacetamide (BSTFA) at 60 ºC for 30 minutes. Derivatized polar fractions were then dried and brought up in 100 µl EtOAc for analysis.

3.2.3.1.1 *n*-alkane Analysis

Analysis of *n*-alkanes was done by analyzing the apolar fractions of each sample. These compounds were identified in the apolar fractions using a Hewlett Packard 6890 series gas chromatograph coupled to an Agilent 5973 Mass spectrometer (GC-MS) using a Restek Rtx-5ms column (60m x 250 µm x 0.25 µm). For details on the programming of the GC-MS for apolar analysis, see table 3.4. Mass spectra were measured from 50 to 600 *m/z*, and compounds were subsequently identified based on their characteristic fragmentation patterns in each mass spectra and also by their retention times throughout the run.

n-alkanes were quantified using an Agilent 7890A dual gas chromatograph-flame ionization detector (GC-FID) equipped with two Agilent 7693 autosamplers and two identical columns (Agilent 19091J-416: 325°C: 60m x 320µm x 0.25 µm, HP-5 5% Phenyl Methyl Siloxan). The GC-FID method for sample apolar sample analysis was similar to that on the GC-MS, and can be found in table 3.4. *n*-alkanes concentrations were quantified through the comparison of integrated peak areas to an external calibration curve of peak areas where squalene was injected and run using the same method at multiple concentrations on both GC-FID injectors.

3.2.3.1.2 Analysis of Polycyclic Aromatic Hydrocarbons (PAH)

Polycyclic aromatic hydrocarbons (PAH) were identified and quantified on the GC-MS system described above. PAH compounds were first found in the ketone fractions and were thus analyzed in this fraction. However, after finding significant PAH

abundances in the apolar fractions, the ketone and apolar fractions were combined and analyzed on the GC-MS and GC-FID. Only methods and results from the combined fractions will be discussed from this point forward.

Instrument	Carrier Gas	Fraction Analyzed	Temperature Ramp	Max Temp Duration (mins)
GC-MS	He	Apolar	70ºC - 130ºC @ 20ºC min-1 130ºC - 320ºC @ 4ºC min-1	20
GC-FID	He	Apolar	70ºC - 130ºC @ 10ºC min-1 130ºC - 320ºC @ 4ºC min-1	10
GC-MS	He	Apolar/Ketone	50ºC - 130ºC @ 10ºC min-1 130ºC - 320ºC @ 4ºC min-1	15
GC-MS	He	Polar	60ºC - 130ºC @ 20ºC min-1 130ºC - 320ºC @ 4ºC min-1	15
GC-FID	He	Polar	60ºC - 130ºC @ 20ºC min-1 130ºC - 320ºC @ 4ºC min-1	15

Table 3.4 - Instrument method information, including carrier gas, fractions analyzed, temperature ramps for each method, and duration the maximum temperature was held.

Due to the low abundances of PAH compounds in each sample, peaks could not be identified and quantified on the GC-FID runs. PAH were identified and also quantified on the GC-MS running in Selected Ion Monitoring (SIM) Mode. Running in SIM mode, as opposed to full-scan mode, allows for a pre-determined set of major ion masses to be counted, allowing certain compounds with those characteristic major ions to be more readily identified. The SIM method used on the GC-MS to identify PAH samples is described in table 3.4. In this SIM mode, 12 ion masses were targeted, and 17 common PAH compounds were identified. 16 of these PAH were identified from a RESTEK SV Calibration Mix PAH Standard, while retene was identified from a CHIRON AS standard. Both standards were diluted to 100µg/2mL vial and run on the GC-MS. PAH peak retention times and mass spectra were then compared to sample runs, allowing for

PAH peaks to be identified in all samples. PAH abundances were quantified on the GC-MS after creating calibration curves for each of the 17 PAH compounds, based on varying injection amounts on GC-MS runs.

Retention Order	PAH Compound	Major Ion	Average Retention Time	Standard
1	naphthalene	128	12.989	Restek
2	acenaphthylene	152	19.617	Restek
3	acenaphthene	153	20.55	Restek
4	fluorene	166	23.176	Restek
5	phenanthrene	178	28.465	Restek
6	anthracene	178	28.731	Restek
7	fluoranthene	202	35.414	Restek
8	pyrene	202	36.704	Restek
9	retene	219	38.641	Chiron
10	benzo(a)anthracene	228	43.829	Restek
11	chrysene	228	44.094	Restek
12	benzo(b)fluoranthene	252	49.857	Restek
13	benzo(k)fluoranthene	252	50.012	Restek
14	benzo(a)pyrene	252	51.495	Restek
15	indeno(1,2,3,cd)pyrene	276	56.754	Restek
17	dibenz(a,h)anthracene	278	56.831	Restek
16	benzo[g,h,i]perylene	276	57.97	Restek

Table 3.5 – PAH compounds identified on the GC-MS and retention times.

3.2.3.1.3 Analysis of Polar Fractions

A handful of compounds, including algal lipids, *n*-alkanols, sterols, and stanols, were identified and quantified using the same GC-MS and GC-FID systems described previously. Method information on both GC-MS and GC-FID runs can be found in table 3.4.

3.2.3.2 Bulk Geochemical Analysis

Discrete sediment samples were taken from core BP2014-5D 1/2 at 0.5cm resolution from 0cm – 15cm depth for bulk geochemical analysis. Samples were then

freeze-dried for 24 hours and stored in a dessicator until analysis. Between 2.5-3.5 mg of dried sediment per sample was weighed using an analytical mass balance and transferred to combusted silver capsules for bulk geochemical analyses, including total organic carbon (TOC) content and total nitrogen (TN) content. Samples were analyzed by a Costech ECS 4010 Elemental Analyzer.

Dry bulk density was measured at 0.5cm resolution from Core BP2014-5D from 0cm to 15cm depth. Wet sediment samples of a known volume (1cc) were taken using combusted glass pipettes and were weighed. Samples were then placed in a 100ºC oven for 24 hours to dry. Once samples were dried, they were stored in a dessicator to cool to room temperature, and then weighed again. Dry bulk density was calculated by taking the dry sediment weight over the known sediment volume.

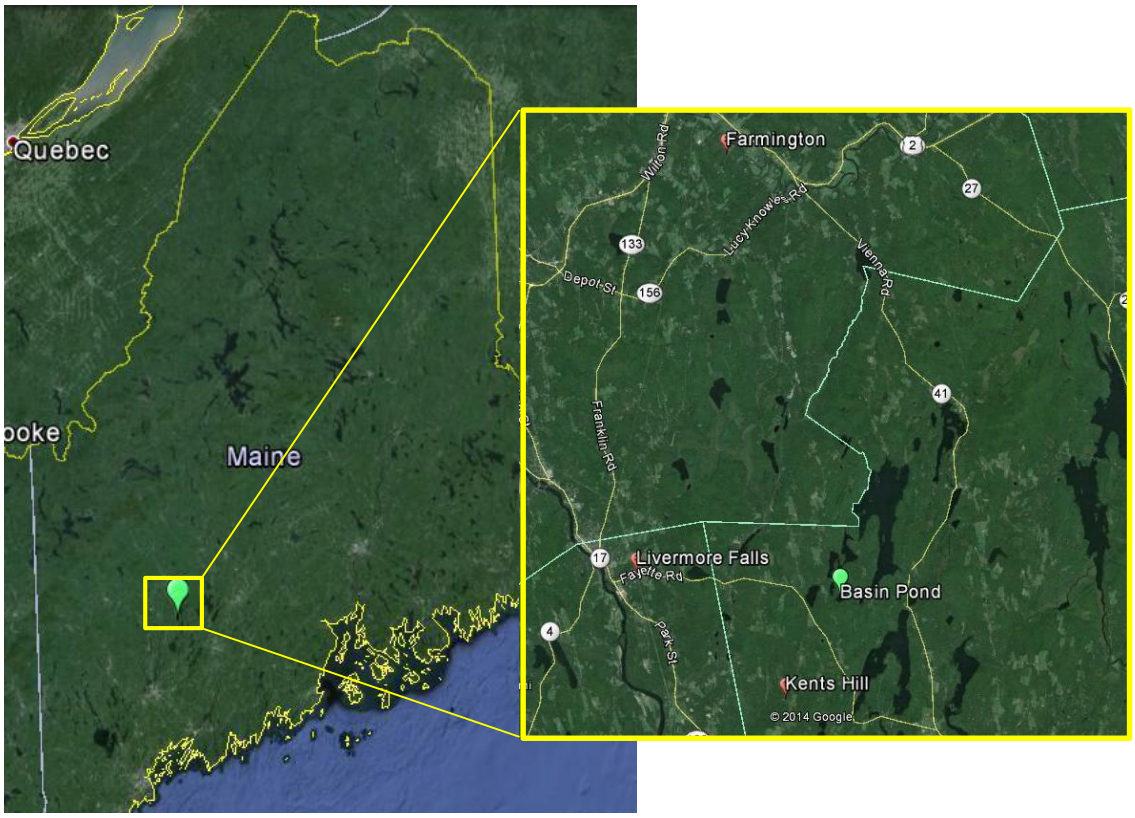

Figure 3.1 – Map of all meteorological (met) stations used in the compilation of the met records used in this study.

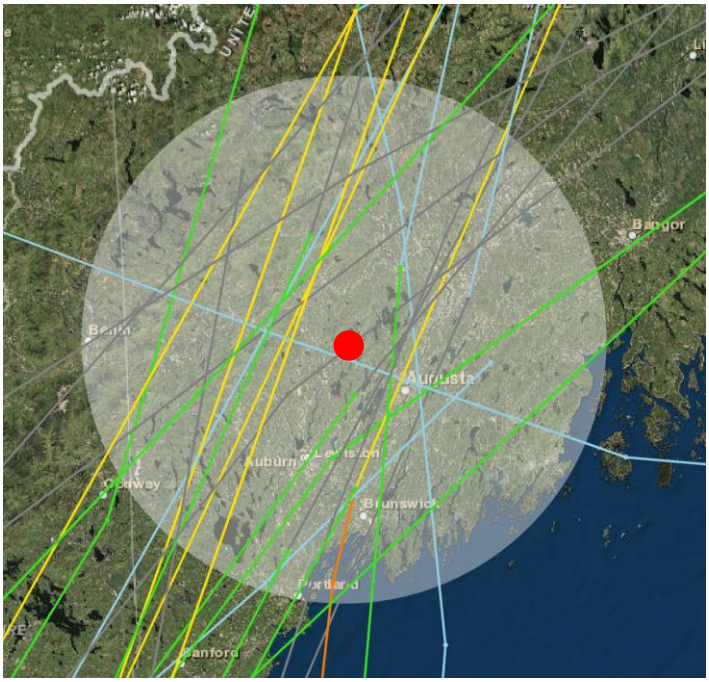

Figure 3.2 – Map of historical storm tracks within 50 miles of Basin Pond, Fayette, Maine (red circle). (NOAA).

CHAPTER 4

RESULTS

4.1 Basin Pond Climatic History

Daily meteorological station data was compiled for the period October 1885 to September 2014. Analysis was performed on the precipitation and temperature records to obtain monthly, seasonal, and yearly averages for the Basin Pond region. Records throughout this 129 year period were 98.71% complete. From 1886-1897, coverage was slightly less than the remaining data stack (1897-present), with 13 of the total 144 months with incomplete data sets (90.97% coverage). Thus, any interpretations of proxy data in relation to the meteorological data prior to 1897 will be done with caution. After addressing the early years of station data collection, records are essentially continuous from 1898 – 2014 (99.6% coverage), with the only missing data occurring from August – December 1909.

Average precipitation over the 129 year time period varied greatly from 80 cm/year to over 160 cm/year. Upon smoothing the data set, a strong cyclicity is evident on a 15-20 year period, with a gradual, steady increase in precipitation occurring over the past 60 years. Average yearly temperatures fluctuate from 4°C to 10°C. Again, upon smoothing the data set, temperatures are steady or increasing slightly in the early record until the 1950's, when they rapidly decrease. This occurs until the late 1970's, after which they begin to increase to present-day levels. Yearly precipitation and temperature trends can be seen in Figure 4.1. These trends correlate well with other data stacks for the larger region, such as temperature averages for the state of Maine (Figure 4.2), and will therefore be assumed to be an accurate representation of local climate of the micro-region

of Basin Pond (Berkeley Earth Surface Temperature).

4.2 Basin Pond Age Model

Lead-210 and Cesium-137 counts were measured and results can be seen in Table 4.1. Typically, the onset and peak in Cs-137 activity correlate well with the onset of global atmospheric nuclear testing (1954) and the peak in nuclear testing (1963), while the Pb-210 decay curve correlates with the onset of industrialization in a region. At Basin Pond, however, due to the detection of Cs-137 for several centimeters down-core of the peak and onset of atmospheric nuclear testing, it is likely that Cs-137 is migrating throughout the sediment after deposition, causing the failure in the Cs-137 dating method. This has been observed in other lakes throughout the Northeastern U.S., and has been hypothesized to be caused by the molecular diffusion and re-adsorption of Cs-137 in sediments (Davis, 1984). For Pb-210 calibration to ages, supported Pb-210 activity was described as the background state, or the measured activity of the deepest sediment sample at 14.75cm and were then converted to ages before present (before 2013).

Depth (cm)	Pb-210 Activity	Pb-210 unsupported	Pb-210 Yrs	Cs-137 Activity	Cs-137 yrs
1.00	4.5124	4.4283	-	0.2340	-
2.25	2.6172	2.5330	1995.0383	0.3553	1963
3.00	1.8558	1.7717	1983.5439	0.0445	1954
3.75	1.1202	1.0360	1966.2912	0.0394	-
4.25	0.9909	0.9067	1962.0053	0.0303	-
4.75	0.7258	0.6417	1950.8879	0.0344	-
5.25	0.5141	0.4299	1938.0122	0.0252	-
5.75	0.4387	0.3546	1931.8130	0.0186	-
6.50	0.4022	0.3181	1928.3220	0.0248	-
14.75	0.0842	0.0000	1819.6411	0.0000	-

Table 4.1- Summary of lead-210 (Pb-210) and cesium-137 (Cs-137) radioisotopic dating results. Activity are measured in Bq/g.

Varve counts were performed using inverted X-Ray radiographic images from the Itrax Core Scanner (Figure 4.3a,b). Grayscale values were extracted from radiographs, and peaks were counted with respect to depth. Apart from 0 – 0.58cm depth, varves were clearly visible in the radiograph values allowing for relatively simple detection throughout the top 16cm. An age model was created for the varve chronology by performing a linear regression on the data, producing a strong correlation ($R^2 = 0.995$) (Figure 4.4b).

Results from the ten AMS radiocarbon dated samples can be seen below in Table 4.2. Three of the four radiocarbon ages from USGS (BPR-DRM-001, BPR-DRM-002, and BPR-DRM-004) were excluded from this analysis as they were incorrectly weighed when sampling, and were too small to likely produce accurate ages with traditional dating techniques at the USGS radiocarbon facilities. The remaining samples were analyzed using small sample techniques at WHOI NOSAMS facilities. One of the six samples came back as post-modern (occurring after the calendar year 1950), and has been excluded from the age model. This exclusion is not due to an anomalous age, but rather due to higher-resolution, more detailed dating techniques for the post-modern time period mentioned above. The remaining radiocarbon ages were calibrated to years before present (1950) using the northern hemisphere IntCal13 ^{14}C calibration curve. This was done using the 'R' package BChron, which calibrates ages and calculates and plots the probability of each age along with the standard deviation (Figure 4.4a).

Average sedimentation rates in the Basin Pond sediment record from Pb-210 dating is roughly 0.057cm per year, while the average sedimentation rate from the varve chronology is slightly higher at 0.070cm per year. While there is a slight difference in

Sample Name	C14 Lab	Depth (cm)	Age (yrs BP(1950))	Error (+- yrs)
BPR-DRM-001	USGS	14 - 16	530	35
BPR-DRM-002	USGS	60 - 61	350	60
BPR-DRM-003	USGS	120.5 - 121.5	1700	35
BPR-DRM-004	USGS	150 - 152	1200	30
BPR-WHOI-004	WHOI	5 - 6	Modern (post-1950)	-
BPR-WHOI-008	WHOI	11 - 12	95	20
BPR-WHOI-009	WHOI	18 - 20	205	25
BPR-WHOI-012	WHOI	21 - 24	170	20
BPR-WHOI-026	WHOI	39 - 41	310	35
BPR-WHOI-022	WHOI	67 - 69	835	20

Table 4.2 - Summary of radiocarbon dating results. C14 Lab indicates where samples were processed and analyzed: U.S. Geological Survey Eastern Geology and Paleoclimate Science Center Radiocarbon Laboratory(USGS), or the Woods Hole Oceanographic Institute AMS Radiocarbon Facilities (WHOI).

sedimentation rates, this difference is minor, and helps support the varve chronology.

The average sedimentation rate from the ^{14}C age model is roughly 0.071cm/year, further supporting the varve chronology for the historic period. Based on the deepest radiocarbon age, this sedimentation rate seems fairly constant throughout the sediment record.

	Varve Counts	Radioisotopic Dating (Pb-210)	Radiocarbon Dating
Sedimentation Rate (cm/year)	0.0699	0.057	0.071

Table 4.3: Average Sedimentation Rates of the Basin Pond sediment record from various dating techniques (varve count chronology, radioisotopic dating, radiocarbon dating).

4.3 Non-destructive Analysis

4.3.1 Geotek Core Scanner Data

The Basin Pond sediment record is uniformly comprised of laminated, dark colored, organic-rich gyttja throughout the entirety of the record (Figure 4.5a). Geotek

core scanning produced magnetic susceptibility values ranging between 0.5 – 1.5 SI x 10^{-5} throughout most of the core, with the exception of the upper 15cm, where values increase to 2.5 – 3.0 SI x10^{-5}(Figure 4.5b). Similarily, bulk density was consistent throughout the sediment record, varying from 0.93gm/cc at the core top to 0.98gm/cc at the core base (Figure 4.5c). Spectral properties show more variability, with L* values and reflectance throughout the visible spectrum of light (wavelengths 360 – 740 μm) fluctuating from 15 – 35 and 2 – 8, respectively (Figure 4.5d).

4.3.2 Elemental XRF Scanning Data

The Itrax XRF core scanner at UMass – Amherst, outfitted with a 3kW Molybdenum tube, gives the ability to identify and measure elements ranging in molecular weight from aluminum to lead. Thus, a suite of 40 elements were identified and measured on the Basin Pond sediment record, including Si, Ar, K, Ca, Sc, Ti, V, Cr, Mn, Fe, Ni, Cu, Ge, Se, Br, Rb, Sr, Y, Zr, Pd, In, Sb, Cs, Ba, La, Ce, Pr, Nd, Pm, Sm, Gd, Tb, Yb, Lu, Hf, Ta, Re, Os, Ir, and Hg. XRF scans also produced x-ray radiographs, which show high-resolution variability in core density, as seen above when utilized in the varve count chronology (see Figure 4.3a).

Fluctuations seen in radiographic images and were compared with abundances of certain minerogenic elements (Fe, K, Si, Ti). Little correlation was found when comparing lamination grayscale values and abundances of iron and potassium (after normalizing to titanium) at the same sampling resolution (100 μm), with correlation coefficients of roughly 0.03 (figure 4.6a,b). However, slightly greater correlation exists between titanium and silicon (Si/Ti) counts, two additional elements used to track minerogenic, clastic, or detrital input, and the radiographic greyscale values (correlation

coefficients of 0.22-0.25) (figure 4.6c,d). These correlations are statistically significant ($p_{Ti:Rad} = 1.4417x10^{-218}$; $p_{Si/Ti:Rad} = 1.3431x10^{-92}$), which tells us that these particular minerogenic elements fluctuate at least somewhat with the annual laminations and sub-annual layers throughout the sediment record (figure 4.7). This indicates that the laminations of the Basin Pond sedimentary record, have a minor clastic component to them, and can potentially track minerogenic input into the lake. As seen in figure 4.7b, a highlighted interval (spanning 12 years) shows how the radiographic imagery closely tracks the varve chronology. Lower values, indicating a decrease in density, indicate lighter layers created during the bloom of microalgae during the growing season, whereas higher values (indicating an increase in density) are composed of darker, humous-rich layers of organic material deposited outside of the algal blooming period of the year.

4.4 Biogeochemical Data

Thirty discrete, 0.5cm samples from the Basin Pond sediment record were analyzed for several suites of biomarkers. These include long-chain hydrocarbons (*n*-alkanes), various algal lipids, and polycyclic aromatic hydrocarbons (PAHs).

4.4.1 *n*-alkanes

From the apolar fractions of each sample, a suite of *n*-alkanes were identified and quantified. In all samples, *n*-alkanes of chain lengths 21 through 33 (C_{21} - C_{33}, or alkanes with 21 carbon atoms to alkanes with 33 carbon atoms) were identified and peak areas from analysis on the GC-FID were measured. Areas were then converted to compound weight per sediment weight (μg compound per g of sediment extracted), and relative abundances of each *n*-alkane were then found.

4.4.2 Polycyclic Aromatic Hydrocarbons

17 PAH compounds were searched for on the GC-MS in all samples. 5 of the 17 PAH compounds could not be identified and were not present in most samples, including acenaphthene, fluorene, anthracene, indeno(1,2,3,cd) pyrene, and benzo[g,h,i]perylene. In most samples, the remaining 11 of the 17 PAH compounds searched for were identified. In particular, 4 PAH compounds were found in all samples: naphthalene, pyrene, retene, and chrysene. Mass spectra for each PAH compound can be seen in Appendix A.

4.4.3 Algal Lipids and *n*-alkanols

Various lipids eluting in the polar fractions of each sample were identified and quantified on the GC-MS and GC-FID, respectively. Compounds identified include: loliolide, isololiolide, cholesterol, cholestanol, C_{30} 1,13 *n*-alkyl diol, campesterol, campestanol, C_{29}-brassicasterol, C_{29}-brassicastanol, β-sitosterol, β-sitostanol, dinosterol, dinostanol, and arborinol. Similarily, straight-chained *n*-alkanols of various chain lengths were identified. In all samples, *n*-alkanols of chain length $C_{16} – C_{30}$ (those with 16-carbon chains through those with 30-carbon chains) were identified, excluding the C_{29} *n*-alkanol, which could not be identified in any sample.

4.5 Bulk Geochemical Data

Total bulk carbon and nitrogen values, as measured by the Elemental Analyzer (EA), range from 17 – 27% (carbon) and 1.5 – 2.5% (nitrogen) (Figure 4.8 a, b). Due to the lack of carbonate in the Basin Pond sediment record, as found in (Frost, 2005), no acidification step was taken in preparation of the samples for elemental analysis, and total carbon can and will be interpreted as Total Organic Carbon (TOC). C/N ratios for the samples vary between 10.5 and 13.5 (Figure 4.8c). Dry bulk density, measured on the same samples, show little variation, with a general decrease in values down-core. Dry

bulk density values range from 0.05 g/cm^3 to 0.20 g/cm^3 (Figure 4.8d).

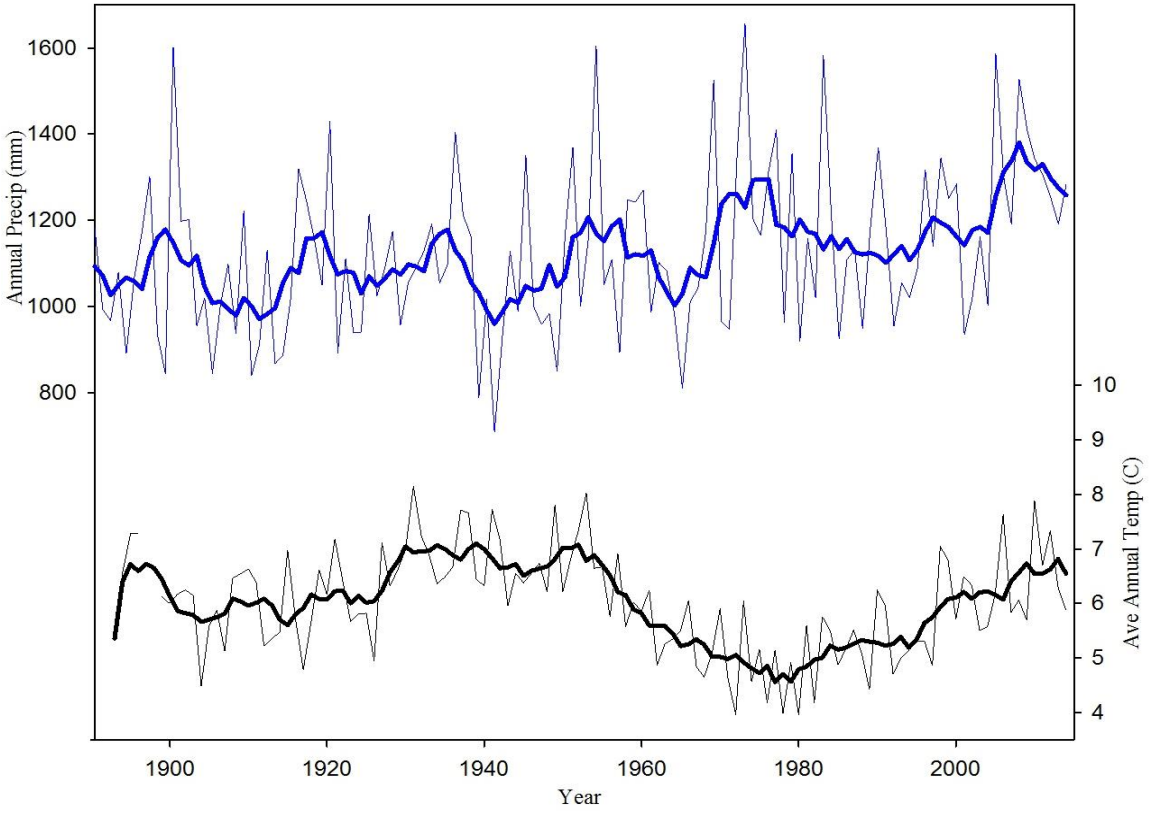

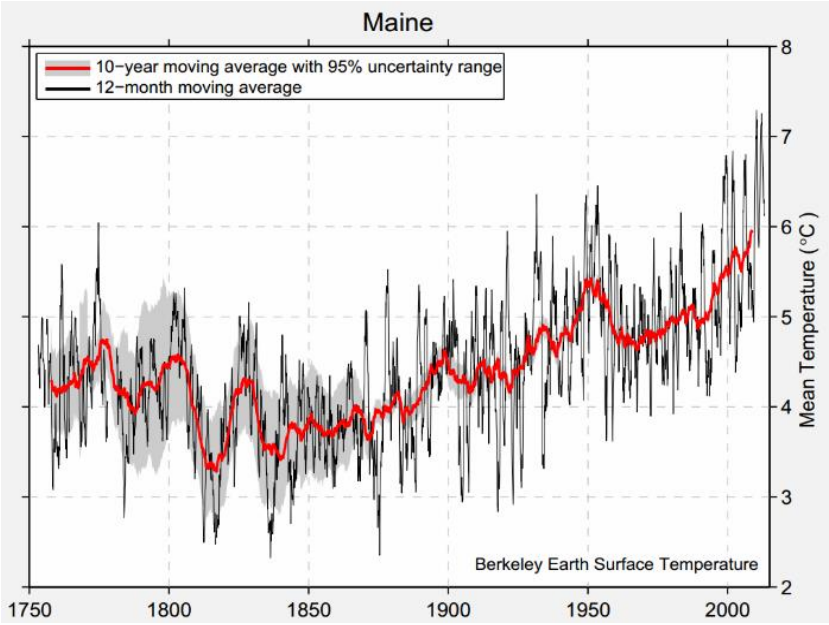

Top: Figure 4.1, showing annual precipitation totals (in mm) and average annual temperatures (in degrees C). Bold lines are seven-year moving averages.
Bottom: Figure 4.2, showing average temperature (and associated error) for the state of Maine, U.S.A, over the past 250 years. Data compiled by the Berkeley Earth Surface Temperature Project from 97 current stations and 74 former stations.

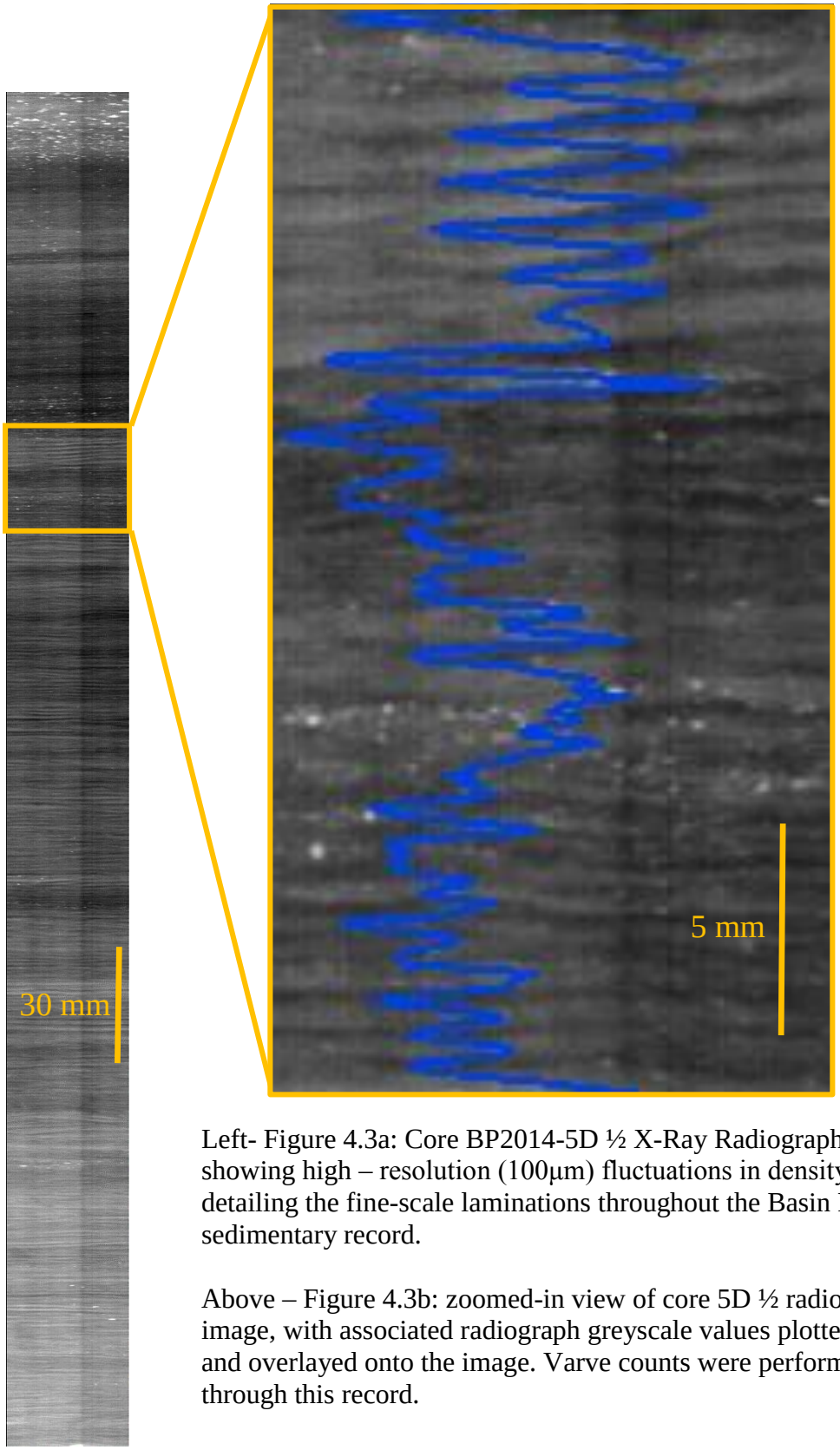

Left- Figure 4.3a: Core BP2014-5D ½ X-Ray Radiographic Image, showing high – resolution (100µm) fluctuations in density, detailing the fine-scale laminations throughout the Basin Pond sedimentary record.

Above – Figure 4.3b: zoomed-in view of core 5D ½ radiographic image, with associated radiograph greyscale values plotted in blue and overlayed onto the image. Varve counts were performed through this record.

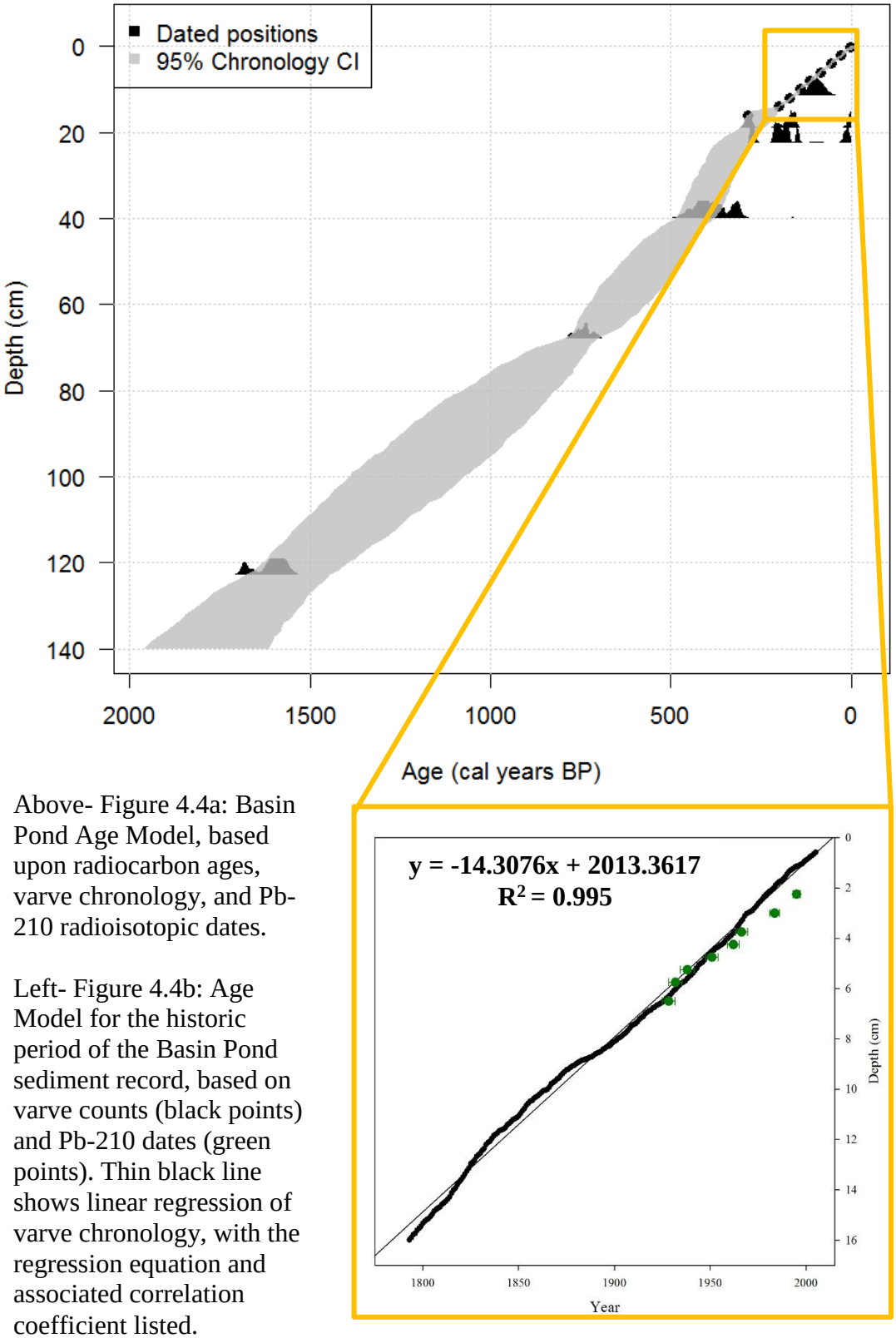

Above- Figure 4.4a: Basin Pond Age Model, based upon radiocarbon ages, varve chronology, and Pb-210 radioisotopic dates.

Left- Figure 4.4b: Age Model for the historic period of the Basin Pond sediment record, based on varve counts (black points) and Pb-210 dates (green points). Thin black line shows linear regression of varve chronology, with the regression equation and associated correlation coefficient listed.

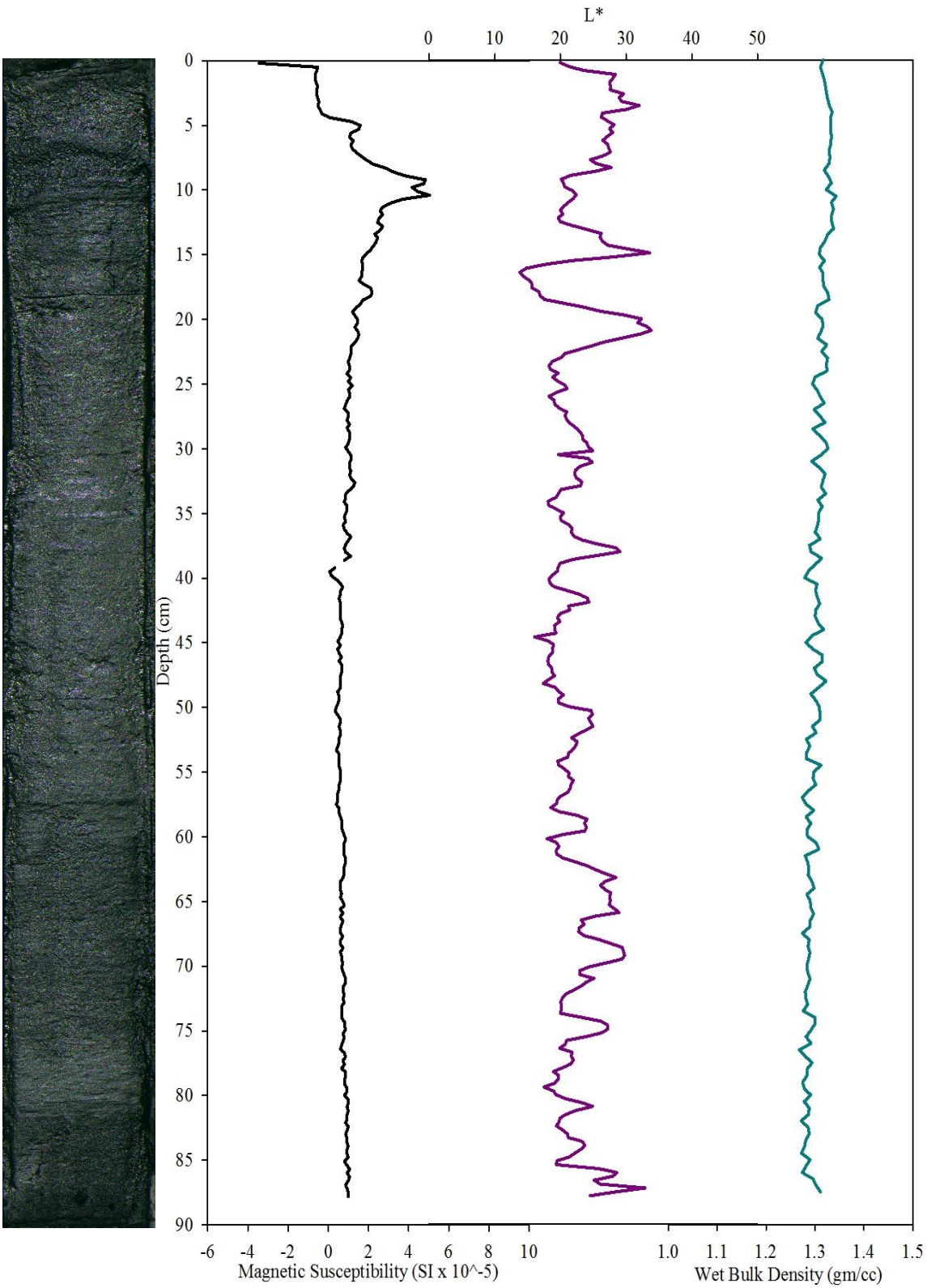

From Left to Right- Figures 4.5a-d: Image of the Basin Pond sediment core, bulk density values, magnetic susceptibility, and L* spectral values, as measured from the geotek core scanner.

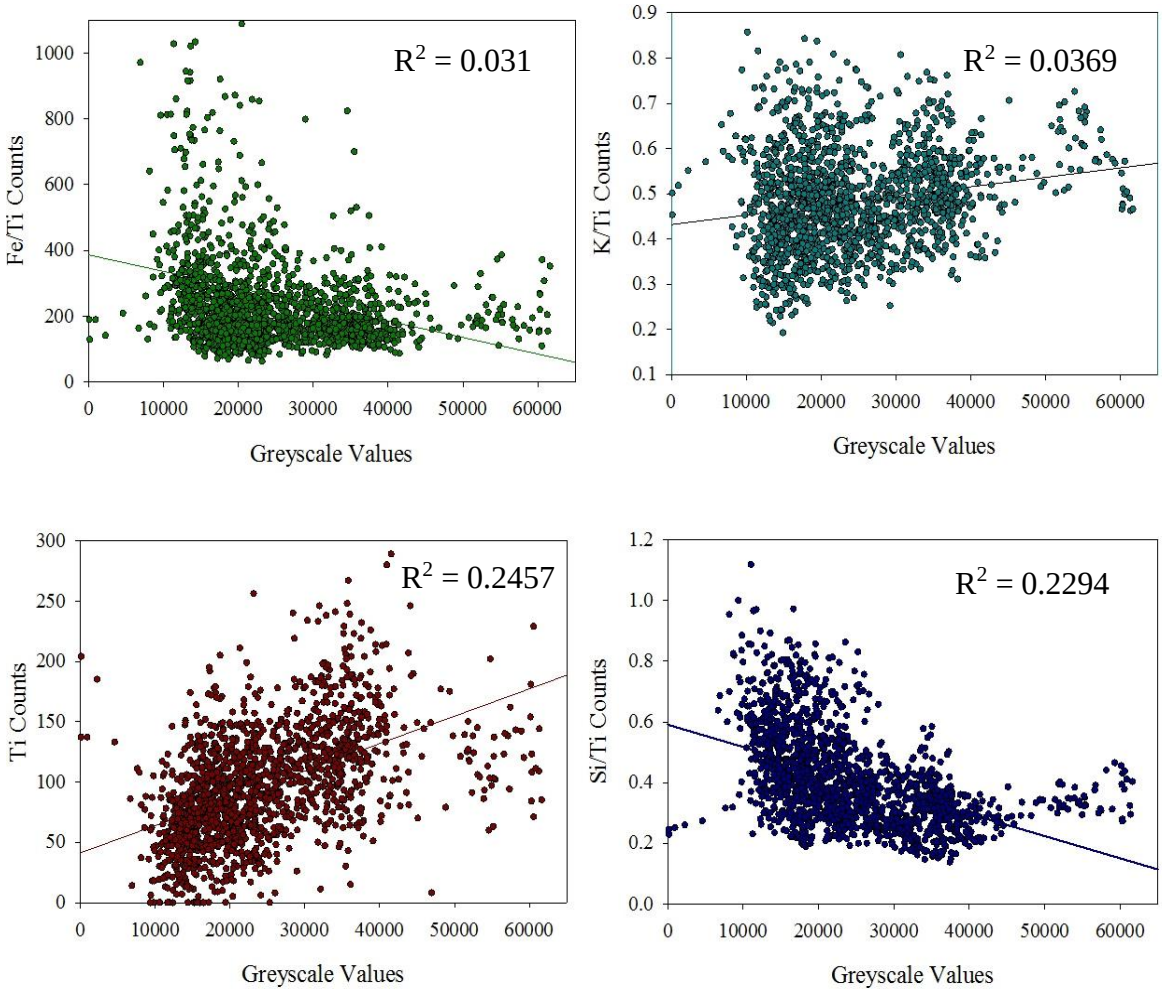

Figure 4.6: Correlation plots with linear regression analysis of X-Ray Radiographic Greyscale Values versus iron (top left, green), potassium (top right, light blue), titanium (bottom left, red), and silicon (bottom right, dark blue). All elemental data have been normalized to titanium. Correlation coefficients can be seen in the upper right corner of each plot. Note statistically significant ($p<0.00001$) correlation of Si/Ti and Ti with radiographic values, but little correlation is seen with Fe/Ti or K/Ti.

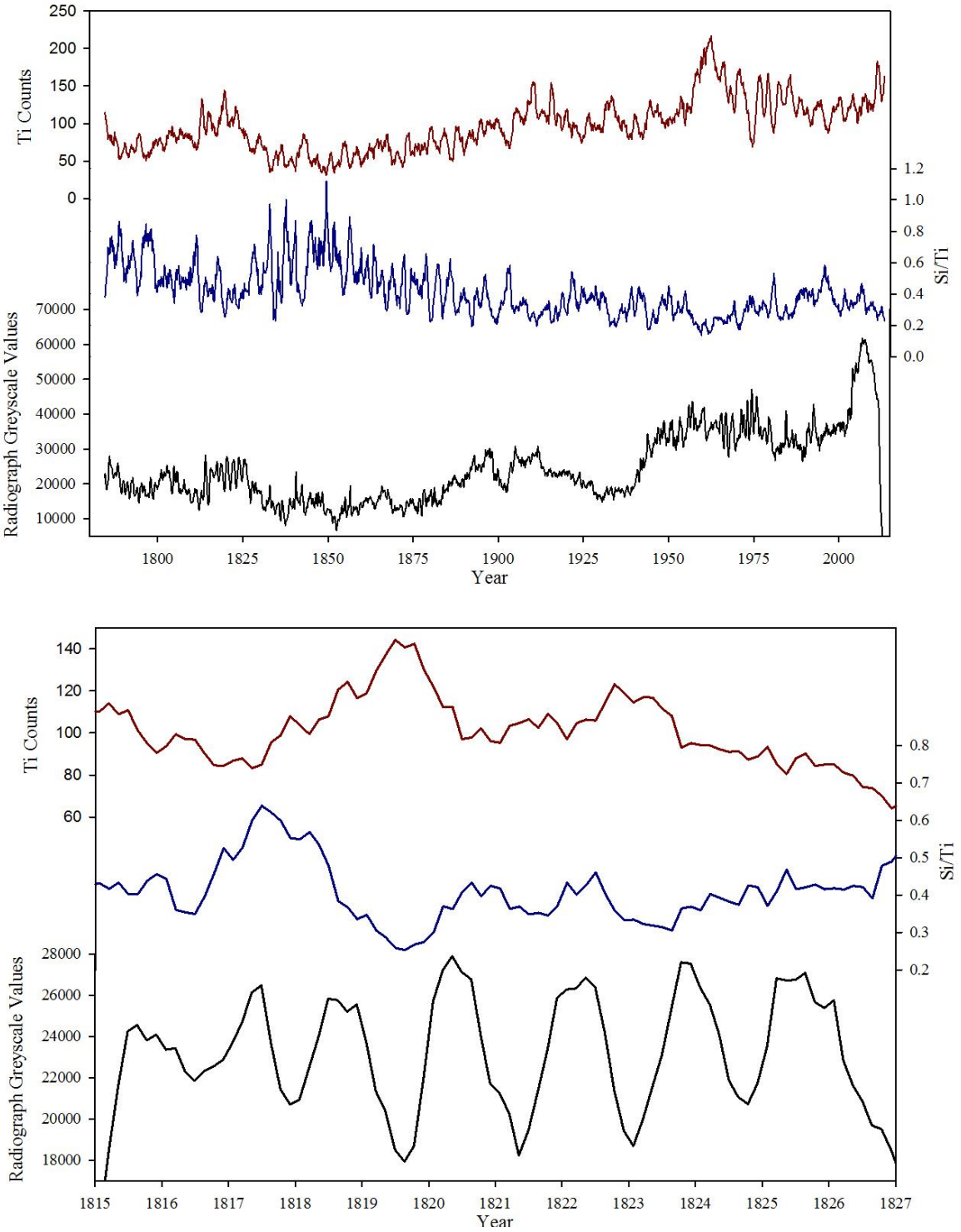

Figure 4.7a (top): Titanium abundance, Si/Ti abundances, and radiographic greyscale values plotted over the past ~230 years. Boxed-in section on top plot indicates the highlighted interval seen in figure 5.5.

Figure 4.7b (bottom): Highlighted interval from 1815 – 1827 seen in figure 5.4. This section was chosen based on distinguished laminations in the radiographic record.

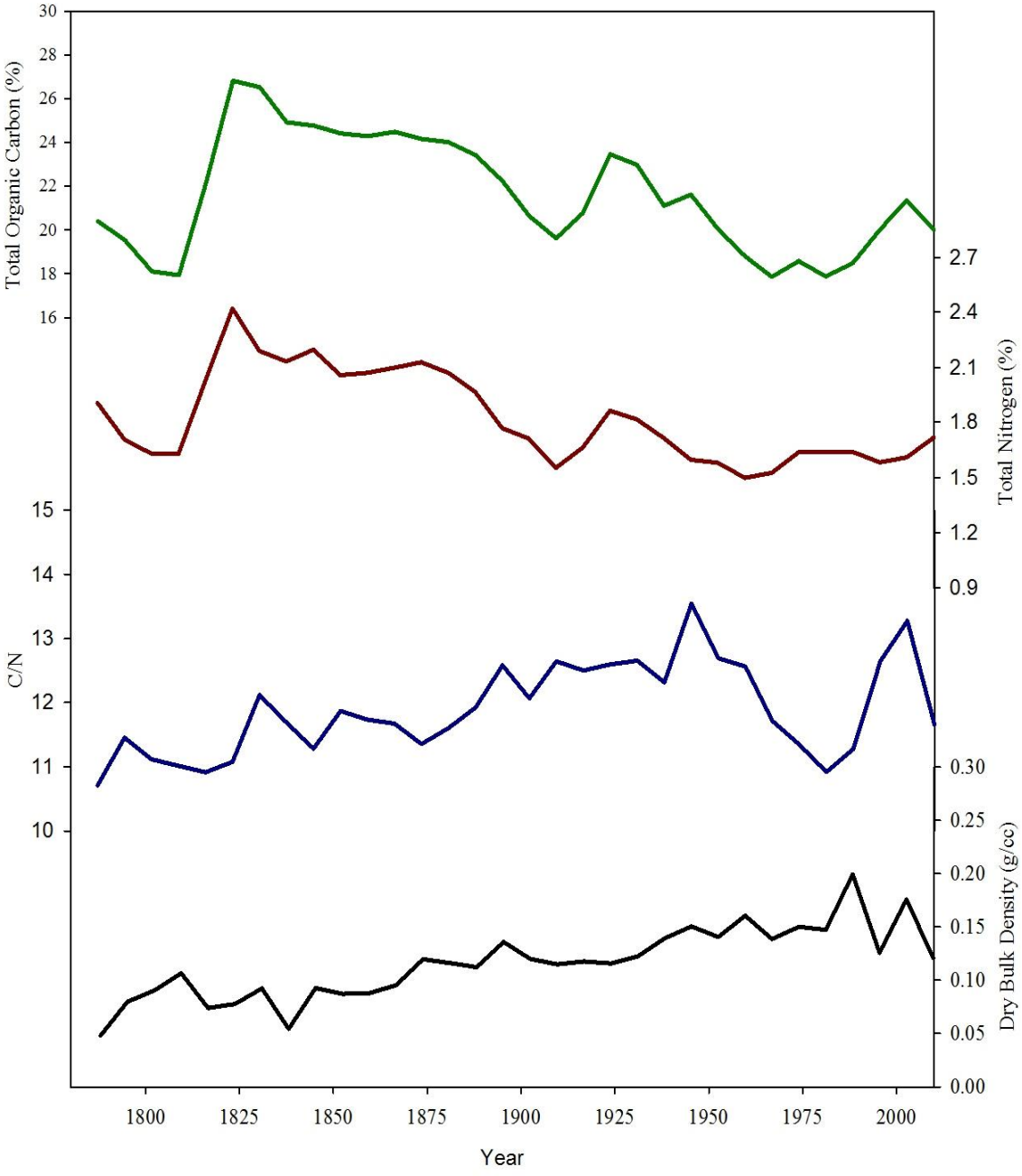

Figure 4.8: Bulk geochemical data from discrete samples of the Basin Pond sedimentary record, including a) total organic carbon content (TOC), b) total nitrogen content, c) the ratio of total carbon to total nitrogen (C/N), and d) dry bulk density, measured in grams per cubic centimeter.

CHAPTER 5

DISCUSSION

As stated in chapter 1, the goals of this thesis were to (1) determine how known extreme events are documented by instrumental measurements and historical records, (2) to identify how human activities and rapid environmental change in the catchment area are expressed in the sedimentary record, and (3) to distinguish and evaluate how climatic events are expressed in the physical and geochemical properties of a lacustrine sedimentary sequence. To address these questions, the following hypotheses have been tested:

(1) There has been human disturbance in the catchment area during the past 200 years and is seen in the sedimentary record of Basin Pond

(2) Extreme events (hurricanes, floods, droughts, and wildfires) can be identified in the Basin Pond sedimentary record throughout the historic period using a suite of sedimentary, organic geochemical, and inorganic geochemical analyses.

Answering these hypotheses require an in-depth multi-proxy analysis of the sedimentary record, and will comprise the bulk of the discussion in this chapter.

5.1 Human Disturbance and Catchment History

In order to accurately interpret how human activities have affected the paleoenvironmental signals recorded by organic matter in the Basin Pond sedimentary record, organic matter sources must first be identified and understood throughout the record. By a comparison of proxy records compiled through analyses performed, we see that the source of organic matter has varied over the historic period, giving insight into

Basin Pond's history.

5.1.1 Lake Primary Productivity Fluctuations from Lipid Biomarkers

In lacustrine environments, lipids found in the sediment record are dominantly sourced from microalgae organisms found within the lake (Castañeda and Schouten, 2011). Some of these lipid biomarkers can be very useful in studying lake sediments and can give valuable insight into catchment history, environmental change, and variability in productivity levels of certain types of algae throughout time.

Two such classes of compounds are sterols and stanols. Sterols and stanols are molecular compounds that are produced in all eukaryotic organisms and are utilized as membrane rigidfiers. Many sterols (and their saturated counterparts, stanols) can be indicative of certain groups of source organisms, in particular specific phytoplankton groups (Castañeda and Schouten, 2011; Volkman, 2003; Volkman et al., 1998). For example, dinosterol and dinostanol are found in dinoflagellates and are not produced in higher plants, and are therefore used as a biomarker for dinoflagellate species (Castañeda and Schouten, 2011; Volkman et al., 1998, 1999; Gillan et al 1983). The phytosterol class, including β-sitosterol/stanol and campesterol/stanol, has been linked to terrestrially-derived higher plant sources, along with arborinol (Fernholz and MacPhillamy, 1941; Segura et al., 2006; Volkman, 2003, 1986), but have also been found to be produced in certain algal species (Rampen et al., 2010). The compounds isololiolide and loliolide are known to be anoxic degradation products of diatoms, and have been used as a biomarker for diatom species (Castañeda and Schouten, 2011). Long-chain alkyl diols are produced by Eustagmatophyte algae, or yellow-green algae, and can be indicative of this algal class (Volkman et al., 1998).

In the case of Basin Pond, these lipid biomarkers help shed light on major changes in the lake productivity, as well as potentially the land-use changes and human disturbances in the catchment area throughout the historic period. Based on the mass accumulation rates of thesis lipid biomarkers, three distinct periods of activity can be seen: a slow decline in all lipids prior to ~1860 (i), a period of relatively flat lipid productivity from 1860 - 1920 (ii), and finally a large overall increase in all compounds throughout most of the 20th century, punctuated by an abrupt decline in the 1950's and 1960's (iii) (figure 5.1).

While absolute abundances and accumulation rates of individual lipids can be meaningful, relative abundances of algal lipids can also illustrate how the lake's ecosystem and productivity levels fluctuate over time. Due to their usefulness as biomarkers described above, and their abundance in the sedimentary record, a selection of these algal lipids was used to be representative biomarkers for certain algal classes. Dinosterol/stanol was chosen as a representation of dinoflagellates, C_{30} 1,13*n*-alkyl diol for eustagmatophyte algae, Isololiolide/loliolide for diatoms, and β-sitosterol/stanol for higher terrestrial plants (figure 5.2). By looking at the relative abundances of these lipids, again the most apparent change is a large overall increase in sitosterol/stanol and a similar decrease in dinoflagellate productivity throughout most of the 20th century, with the most rapid shift occurring post 1950 (figure 5.2). Interestingly, this occurs at roughly the same time period as the abrupt decline in the absolute abundances of all compounds seen in figure 5.1 during the 1950's and 1960's.

Decrease in Algal Productivity in the 1950's and 1960's

This abrupt decline could likely be a repercussion of the chemical treatment of the

lake using rotenone, which took place in 1955 (USGS, personal communication). Rotenone is a naturally occurring chemical with insecticidal, acaricidal and piscicidal properties, which exerts a toxic action by acting as a general inhibitor of cellular respiration. It has been used for fish eradications as part of water body management, and has been shown to have long-term effects (multi-year) on the biodiversity of a water body (Maslin, 1996). Rotenone's effects on the biodiversity of other aquatic organisms (specifically microalgae) and on lake productivity levels is unclear, but the Basin Pond record suggests that there were system-wide, long-term ecological effects on the aquatic biodiversity, resulting in abrupt declines in algal abundances.

20th Century Increase in Lipid Abundances

The 20th century overall increase in absolute lipid abundances could indicate a re-advancement of the forest around the catchment area in the mid-20th century to the current heavily-forested structure of the catchment area. If this were true, it would mean that the catchment area was influenced by human activity throughout the historical period up until the 1950's. In order to test this hypothesis, other sedimentological properties and data can be used to shed light on the deforestation of the catchment area. Magnetic susceptibility, which detects the presence of iron-bearing minerals per unit volume within sediments, can be used as a proxy for terrigenous inputs (Stein, 2004). Bulk density and minerogenic elemental abundances similarly can be used as proxies for clastic or allochthonous input, as clastic material is usually more dense and higher in minerogenic elements. However, at Basin Pond these proxies do not support this hypothesis, as magnetic susceptibility, bulk density, or minerogenic elemental abundances do not fluctuate substantially or indicate deforestation and increased runoff into the lake system

(figure 5.3).

It is important to note that this shift in algal abundances could be tracking a change in productivity in the lake that is not connected with large-scale catchment area land use changes (e.g. forest clearance or re-advancement). When looking at the relative abundance of sitosterol/stanol (lipids that have been considered "terrestrially" derived) and comparing it to other proxies of terrestrial organic matter input into the lake (long-chain *n*-alkane abundances), large discrepancies between the two are seen throughout the time period. This is indicating that at Basin Pond, these lipid compounds are *not* sourced from terrestrial plants, and that these lipids (such as sitosterol/stanol) are realistically tracking some other aquatic algal species produced *in situ* in Basin Pond.

To summarize, while it remains somewhat murky, human impact on Basin Pond and its catchment area seems to have been present, but minor. By looking at multiple lines of evidence from independently analyzed proxy records, an abrupt decrease in algal productivity in Basin Pond occurs in the 1950's and 1960's, and is likely a consequence of the chemical treatment of Basin Pond in 1955. The overall increase in algal lipid abundances throughout the remainder of the 20th century could be caused by other minor disturbances in the catchment area (i.e., construction of a home within the catchment area). One house is situated in the catchment area, and while this would be a minimal disturbance, it is reasonable to assume that at least minor catchment disturbance and lake contamination has occurred. It is common to see an increase in nutrient loading (and therefore an increase in certain algal species productivity) in lakes from increased human activities nearby, as increased nutrient loading can cause an increase in algal productivity. When comparing this with other proxies, it seems unlikely that human activity in the

catchment area had a large influence. C/N ratios, magnetic susceptibility, and elemental abundances during this time period do not exhibit a similar change (figure 5.3). Changes in these proxies would be expected if more catchment soil and terrestrial matter from deforestation or human disturbance in the watershed occurred (Kylander et al., 2011). If the catchment area was ever completely and continuously logged and harvested, a stronger signal of increased runoff would likely be evident in the sediment record. While there are large fluctuations in terrestrial long-chain *n*-alkane abundances, again there is no similar variation in inorganic terrestrial input. One possibility for this is that the catchment area was logged, but not fully, and was allowed to recover quickly afterwards. This would allow for drastic changes seen in long-chain *n*-alkane abundances without a corresponding signal in clastic input into the lake (partial clearance would aid in keeping more soil trapped by trees and other higher plants, as opposed to total clearance where more soil would be washed into the lake). Unfortunately, at this time no further information in historical documents could be found on the catchment area's history, but that would be a valuable task to undertake in future work on this lake.

5.2 Extreme Events in the Sedimentary Record

5.2.1 Paleo-storm Records at Basin Pond

In heavily-forested lake catchment areas such as at Basin Pond, well-developed soils and vegetation aid in limiting the availability and transport of minerogenic material into the lake. In these systems, decaying organic matter (both terrestrially and aquatically sourced) is transported into the lake sediment record and can form biogenic (organic) varves, reflecting the annual (or sub-annual) cycles of organic productivity at the lake (Zolitschka et al., 2015). In most biogenic-varved lakes, however, organic varves rarely

exist without some clastic components. It depends on the dominating component whether the sediment record of a lake is attributed to a more minerogenic (clastic-biogenic) or a more biogenic (biogenic-clastic) varve type.

It has previously been proposed that the Basin Pond sediment record is composed of biogenic varves due to the organic–rich nature of the sediments (Frost, 2005). The elemental abundances acquired from the XRF core scanner provide further evidence for this. If the Basin Pond varves were dominantly clastic in nature, elemental abundances indicating minerogenic or clastic input would correlate with the laminations seen in the radiographic images. Due to the potential of the laminations tracking minerogenic input from the catchment area into the lake, the data was compared to the storm and precipitation record from the past 150 years (figure 5.4). Extreme precipitation events (defined as events occurring from May to October, and greater than 4σ from the mean event in the MET records, or events producing greater than 3.61cm) were compiled and compared to elemental abundances of Fe and Ti, as well as varve thickness. Interestingly, the largest events (e.g. 16cm event on September 16, 1932 and 18.87cm event on June 14, 1998) are seen in the varve thickness record, with large peaks occurring in 1933 and 1999. Furthermore, peaks in the elemental abundances seem to occur at roughly similar times as these events (figure 5.4).

In conclusion, while there are large fluctuations in the varve characteristics and elemental data that do not correlate with individual precipitation events, the largest precipitation events in the record seem to be recorded by these proxy records. This shows that the Basin Pond laminations have potential to be used to reconstruct a storm history, as seen at other varved sites (i.e. Lower Mystic Lake, Boston, MA (Besonen, 2006;

Besonen et al., 2008)). However, more work is needed on better constraining these proxies and in applying them as a storm reconstruction. Furthermore, it should be noted that varve characteristics (such as varve counts and thickness) have only been performed in this study by one person up to this point, where common practice includes having three or more independent measurements being conducted for accurate results due to human error and bias during analysis. Having verification of the current varve data could help provide more conclusive evidence as to the relationship between these annual laminations and storm history.

5.3.2 Precipitation History and Hydrological Interpretations

Longer-term precipitation trends can also be seen in the varve thickness record (figure 5.5). When comparing the growing season total precipitation (May-October) to the varve thickness record, a relationship seems to exist, where the varve thickness record is slightly leading the precipitation record (figure 5.5). In reality, the varve thickness record should be equal to or slightly lagging the precipitation record, as sedimentation and preservation of varve layers occurs after precipitation events. In this case, the offset between records is minor (roughly 5 to 7 years) and can be explained by the error in the varve chronology.

Furthermore, results from biomarker analysis serve as an indicator of precipitation variability on longer time scales (multi-annual to decadal). Distributions of *n*-alkanes demonstrate a strong odd-over-even carbon number predominance, which is expected from past studies (figure 5.6). Generally, long-chain *n*-alkanes (C_{27}-C_{33}) are produced by terrestrial plants, whereas short-chain *n*-alkanes (C_{17}-C_{21}) are produced by aquatic algae, and mid-chains (C_{23}-C_{25}) by aquatic macrophytes. Therefore, the use of several proxies

such as the Average Chain Length (ACL) (average of C_{21}:C_{33}), percent aquatic (Paq) ((C_{21}+C_{23})/C_{21}:C_{33}) ratio, and the ratio of long-to-short chain *n*-alkanes can generally show trends relating to the sources of alkanes of particular chain length. However, caution must be exercised in using these proxies, as a handful of exceptions to the general chain-length distributions exist. Rhisozolenoid diatoms have been known to produce long-chain *n*-alkanes, while some aquatic macrophytes can produce C_{27} and C_{29} alkanes (Sun et al., 2013). At Basin Pond, due to the catchment area being dominated by C_3 forest (figure 5.7) with little variability, it is likely that the general conditions hold true, where terrestrial plants are producing long chain lengths and aquatic organisms are producing shorter chain lengths.

While at some sites these proxies capture temperature fluctuations, at Basin Pond these proxies capture the long-term trends in the precipitation regime (figure 5.8). The ACL is interpreted in this study as tracking input of terrestrial organic matter (allochthonous material) versus aquatic input (autochthonous production). Due to the fact that Basin Pond is a closed system, where input comes mainly from precipitation and groundwater discharge, fluctuations in ACL can be interpreted as loosely tracking precipitation changes. This is further supported by the Paq ratio, which is the abundance of mid-chain aquatically-derived *n*-alkanes over the distribution of all chain lengths, and is used to estimate moisture-dependent variations in lake catchment areas (Ficken et al., 2000; Sun et al., 2013; Zhou et al., 2010). The ratio of long-to-short (L:S) chain *n*-alkanes ((C_{31}+C_{33})/(C_{21}+C_{23})) gives further support, showing similar trends to both the ACL and Paq (R^2 = 0.91 and -0.96, respectively). At Basin Pond, the Paq and ACL are negatively correlated (R^2 = -0.936).

Interestingly, at Basin Pond the correlation between these proxies and precipitation is the opposite of what is expected. The biological function of *n*-alkanes in higher terrestrial plants is to maintain the moisture balance between the plant leaves and the environment. During hotter or more arid conditions, plants produce longer *n*-alkane chain lengths, as longer chain lengths have higher melting temperatures and are more rigid (Bush et al., 2013). Therefore, an increase in ACL and L:S values (indicating an increase in relative abundance of longer chain lengths to shorter chain lengths) can either be interpreted as an increase in aridity or an increase in temperature. However, at Basin Pond, we see the opposite relationship arise between the ACL and L:S proxies and growing season (April-September) precipitation, with higher values seeming to correlate well with increased precipitation. While the shorter-term cyclicity of the precipitation record may not be as well captured in these biomarker proxies, the long-term precipitation trends of the meteorological records are captured well by the proxy data, as seen in figure 5.8. This lack of short-term resolution is somewhat expected, as sampling resolution is likely too low to capture these pronounce cycles seen in the meteorological record. Unfortunately, none of the higher-resolution proxy records (XRF elemental scanning data) show any clear correlation with precipitation trends.

This surprising result is highlighting the possibility that *n*-alkane distributions and associated proxies seem to be dominated by a signal of the compound deposition rates as opposed to a signal of the biological function of these compounds. This theory is further supported when comparing the mass accumulation rates of the long-chain *n*-alkanes (MAR_{long}) to these proxies, as increases in MAR_{long}, ACL, and L:S values all correlate with increased precipitation. Furthermore, this brings light to the idea that the timescale

and resolution of studies involving *n*-alkane distributions is extremely important in how to interpret the proxies with respect to precipitation trends. In highly-resolved studies like the Basin Pond record, fluctuations in the production of *n*-alkane chain lengths in plants might be insignificant (or overshadowed) in the sediment record by the flux of compounds being washed into the lake from changes in precipitation. This would be an interesting hypothesis to test in other high-resolution studies, and could be an interesting development of our understanding of precipitation as a driver of varying chain lengths and the *n*-alkane proxies.

5.2.3 Wildfire Record

The northeastern U.S., while not typically a region that is viewed as being prone to wildfires, has experienced major forest fire disasters throughout the past 200 years. The most recent outbreak, taking place in October of 1947, saw hundreds of fires burn over 200,000 acres across southern Maine over a week, and became known as "The Week Maine Burned". A larger wildfire, known as the "Miramichi Fire", burned over 3 million acres of land in October of 1825 throughout Maine and New Brunswick, and remains one of the top 3 largest wildfires in North American history (Butler, 2014). These fires demonstrate that the northeastern U.S. is susceptible to wildfire catastrophes.

Pyrogenic polycyclic aromatic hydrocarbons (PAH) have been used in this study as organic biomarkers indicating regional fire activity. In particular, the PAH retene was investigated in detail, as it is produced from the diagenesis of abietic acid, which is prevalent in conifer resin (Ahad et al., 2015). Therefore, retene is found to be produced in abundance in coal tar from resinous woods or by the pyrolysis of conifer trees (Ramdahl, 1983). Due to the fact that retene can be produced through pyrolysis of conifer trees, it

has been utilized as an indicator of biomass in the Basin Pond region, as conifers (specifically hemlock) are an important part of the ecosystem in northern New England (Denis et al., 2012; Ramdahl, 1983). Furthermore, the retene/(retene+chrysene) ratio has been used in the past to distinguish the source of retene, as lower values (0.15 to 0.5) tend to indicate a fossil fuel source while higher values (>0.8) indicate a soft-wood combustion source (Denis et al., 2012; Kuo et al., 2011).

At Basin Pond, the retene/(retene + chrysene) ratio seems to track wildfire activity in the region extremely well, with clear peaks occurring in sediment samples roughly 5 to 12 years after the two large wildfires (figure 5.9). This ratio helps distinguish a wildfire signal from individual PAH abundances, which can show greater variability as seen in the MARs of both retene and chrysene (figure 5.9) For instance, while retene MAR records the 1947 and 1825 fires, there are multiple peaks throughout the record apart from these fires which make it difficult to distinguish the wildfire signal.

Through using PAH abundances and associated ratios, we now have the ability to capture distinct wildfire events on a regional scale in an area that traditionally demonstrates low frequencies in wildfire activity. The retene:chrysene ratio shows promise as a proxy for wildfire activity in the northeastern U.S. and as a way to reconstruct paleofire activity throughout the region.

Climatic Controls on Fire Activity

While there are multiple controlling factors that affect wildfire activity, frequency, and occurrence, climatic controls seem to be the most influential on short time scales. Environmental shifts, such as forest structure or ecosystem diversity changes, can have large effects on wildfire risk, but on centennial to millennial time scales. On annual

to interannual time scales, climate extremes (such as severe droughts) have large effects on fire occurrence.

Using the Fire of 1947 as an example in the historical period, the fire aligns with a short-term (sub-annual) intense drought that took place in the fall of 1947 (figure 5.10). Interestingly, the fire seems to be much more effected by seasonal precipitation totals (August-September-October) rather than annual precipitation totals, indicating that seasonal precipitation extremes have more of an effect on wildfire activity than longer-term precipitation trends, even on the annual timescale. Despite only having one example in the precipitation record to compare with the fire history of the region, this result is still significant, as the northeastern U.S. is prone to short, severe droughts on seasonal time scales.

5.3 Conclusions

The analysis of the sedimentary record from Basin Pond, Fayette, Maine, provides an intricate record of paleoenvironmental and paleoclimatic variability, as well as the role of human influence on the lake ecosystem and processes, throughout the historical period. The organic-rich characteristics of the sediment record makes the sediment an ideal target for biomarker analysis, as organic compounds that are in abundance throughout the record can be indicative of climatic fluctuations. Furthermore, due to the varved nature of the sediment record, Basin Pond provides a unique opportunity to study environmental change on a highly-resolved, accurate time scale, and allows for an opportunity to study shorter-term, rapid environmental and climatic extreme events.

Mixed results were seen in the application of multiple proxies to the sediment record. While some proxies seem to be tracking environmental change and human

disturbance in the catchment area, others seem to be tracking climatic change in the region, while others fail in tracking environmental or climatic change. While multiple sedimentary proxies (i.e. bulk density, magnetic susceptibility, elemental abundances) seem to fail to track any human disturbance in the catchment area, organic compounds (such as algal lipids) are tracking catchment area changes. Several proxies relating to the distribution of straight-chained *n*-alkane hydrocarbons correlate well with long-term (decadal to multidecadal) precipitation trends in the region. Perhaps more excitingly, polycyclic aromatic hydrocarbons were used to look at wildfire events in the northeastern U.S. It was found that the retene/ (retene + chrysene) ratio shows a strong correlation with known regional wildfire events, having both events in the historical period distinguishable in the proxy record. The use of the ret/ (ret+chr) ratio is a somewhat novel method to tracking wildfires in the Northeastern U.S, and provides promise to its utilization in future wildfire studies in this region.

In conclusion, the goals of this thesis were to (1) determine how known extreme events are documented by instrumental measurements and historical records, (2) to identify how human activities and rapid environmental change in the catchment area are expressed in the sedimentary record, and (3) to distinguish and evaluate how climatic events are expressed in the physical and geochemical properties of a lacustrine sedimentary sequence. To address these questions, the following hypotheses were tested and answered:

(1) *There has been human disturbance in the catchment area during the past 200 years and is seen in certain proxies of the sedimentary record of Basin Pond*: as seen through biomarker analysis, human disturbance on lake productivity

levels is evident throughout the 20th century, however changes in the lake catchment area appear to be minor, as other traditional sedimentary proxies and analysis (magnetic susceptibility, bulk density, elemental abundances) fail to provide any major fluctuations in the historical period.

(2) *Extreme events (hurricanes, floods, droughts, and wildfires) can be identified in the Basin Pond sedimentary record throughout the historic period*: Using a suite of sedimentary, organic geochemical, and inorganic geochemical analyses, major precipitation events can be seen in the sedimentary record, as well as longer-term precipitation trends and regional wildfire activity throughout the past 200 years.

5.4 Future Work

5.4.1 Extension of Paleoclimate Records into the Pre-historic Era

The first and most apparent direction of future work on the Basin Pond sediment record involves extending selected analyses into prehistoric times. Because of the robust correlation with known fire events in the historic era, studying the PAH distributions throughout the sedimentary record would provide useful information on regional wildfire activity and would allow for fire frequencies of the region to be determined. Furthermore, the extension of the precipitation proxy records could provide a useful tool in determining the relationship between wildfire activity and precipitation trends in the northeastern U.S. Furthermore, the Basin Pond sedimentary record potentially has a continuous, annually-resolved record since deglaciation, which makes it a valuable and unique site in the Northeastern U.S. for paleoclimatic and paleoenvironmental studies.

5.4.2 Comparison of PAH Fire Record and Other Fire Proxies

Comparing the PAH record from Basin Pond sediments with other, more traditional methods of paleofire reconstructions, would provide a useful constraint on each method and its usefulness as a proxy in this region. Traditionally, sedimentary charcoal counts or tree ring fire scars are used in looking at past fire activity at a site. However, these can be somewhat limited in usefulness, as they are both more spatially constrained than PAHs, which have much more aeolian characteristics and can travel in the atmosphere for greater distances or longer time periods than charcoal. A comparison of these proxies would help in determining which proxy is most useful at this site, and could even help in determining fire proximity to Basin Pond.

5.4.3 Age Model Fine-Tuning and Compound-Specific Radiocarbon Dating

Another interesting area of future work with the Basin Pond sedimentary record would include performing radiocarbon dating analysis on a suite of different organic compounds. Due to the highly organic nature of the sediment, organic compounds that can be used for compound specific radiocarbon analysis (including *n*-alkanes) are found in abundance throughout the record, and would be well suited for dating. Compound specific dating would aid in constraining the age model of the Basin Pond sedimentary record, and would shed light on the accuracy of the various dating methods (traditional macrofossil radiocarbon dating, radioisotopic dating, and varve counting) used in this study.

Additionally, comparing the age model found in this study with those of past studies (specifically Frost 2005) would allow for an independent accuracy check or confirmation of this age model. If the varve chronology found in this study does in fact

have an error of 5-7 years (as seen in figure 5.5), adjusting the age model would aid in better aligning other records of extreme events (e.g. PAH fire records).

5.4.4 Temperature Reconstructions from the Basin Pond Sedimentary Record

Lastly, creating a lacustrine temperature reconstruction from Basin Pond could be done. A class of organic compounds known as branched glycerol dialkyl glycerol tetraethers (brGDGTs) have been found in abundance throughout the Basin Pond sedimentary record. The distribution of brGDGTs in soils is highly correlated with mean annual temperature (Weijers et al., 2007) and comprises the methylation of branched tetraethers/ cyclization of branched tetraethers (MBT/CBT) temperature proxy (Weijers et al., 2007). brGDGTs were initially thought to be produced in soils and subsequently washed into lakes and deposited in the sediment record. Yet recent studies have revealed these compounds are also produced in situ within the water column of many lakes (Loomis et al., 2014; Buckles et al., 2014). This production may occur preferentially during summer or fall, i.e. peak productivity seasons, thus recording seasonal temperatures instead of mean annual temperatures. To develop a reliable record of the natural frequency of extreme cold and warm spells and of temperature reconstructions for a site, the timing and location of brGDGT production within a catchment must be assessed.

Currently at Basin Pond, a sediment trap study looking at the temporal distribution of organic matter throughout the water column is underway. With this study, we hope to determine whether or not GDGTs are being produced at certain times throughout the year by certain types of aquatic organisms or whether they are purely terrestrially-sourced. This will give the ability to understand what temperature these

membrane lipids are recording, and will aid in creating an accurate temperature reconstruction for the site, and provide a temperature calibration for mid-latitude lakes similar to Basin Pond.

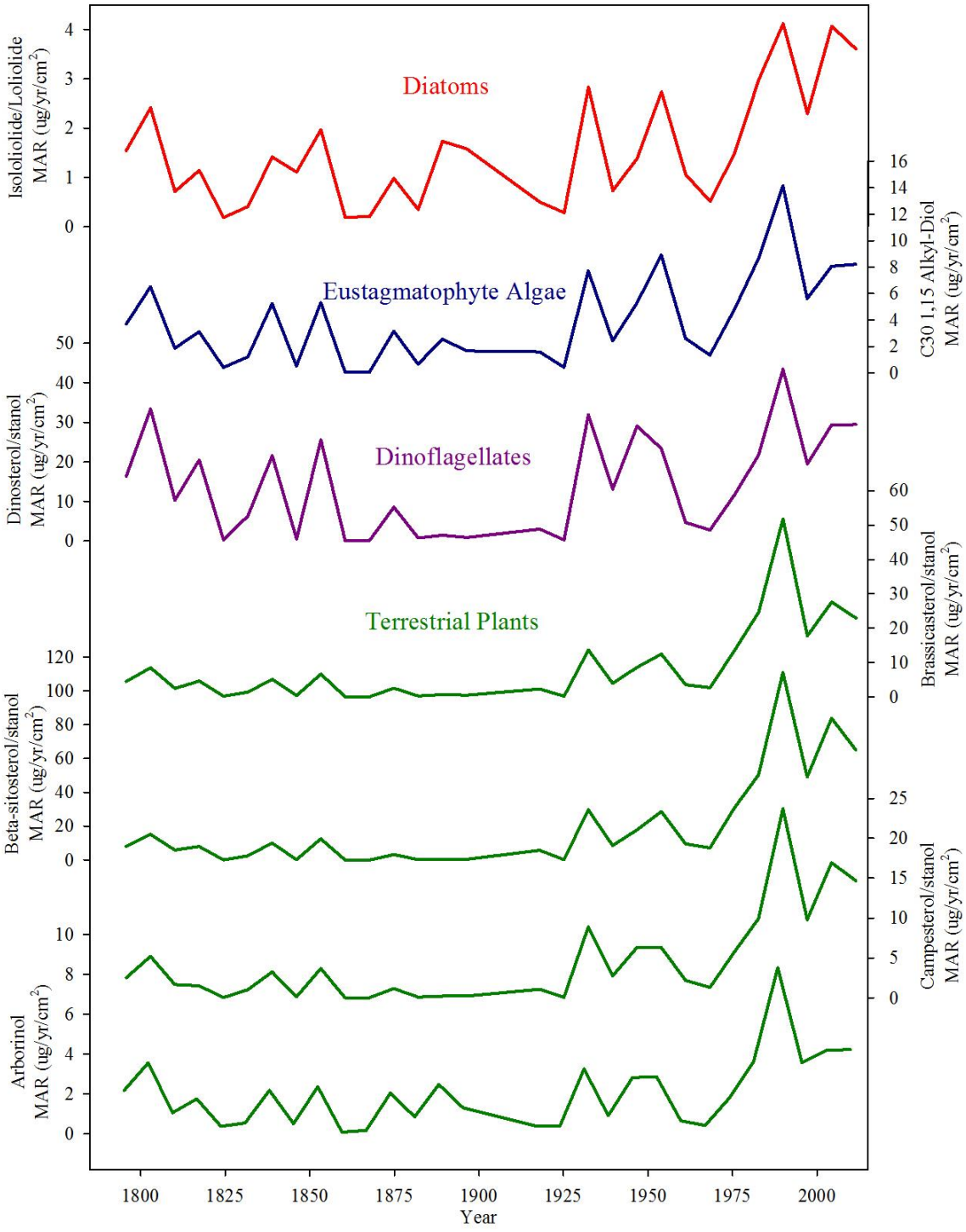

Figure 5.1: Mass Accumulation Rates (MAR), measured in μg/yr/cm^2, of all algal lipids found in Basin Pond sediment samples. From top to bottom: isololiolide and loliolide (red), a marker for diatom activity, C30 1,15 Alkyl-Diol (blue), a marker for yellow-green algae, dinosterol/stanol (purple), a marker for dinoflagellates, and brassicasterol/stanol, β-sitosterol/stanol, campesterol/stanol, and arborinol (green), markers traditionally used for higher terrestrial plants.

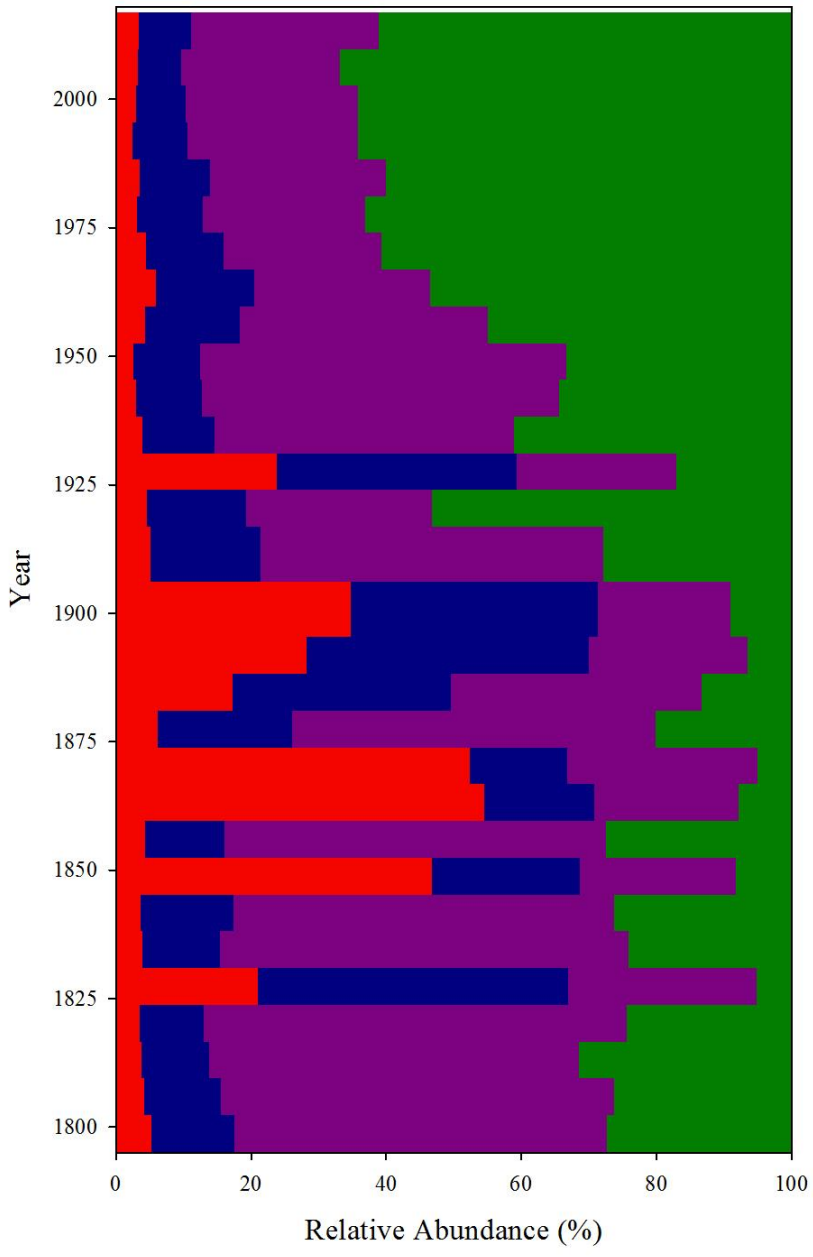

Figure 5.2: Relative abundances and distribution of selected algal lipids. Selected lipids can be seen in the key to the right. Note a substantial decrease in dinoflagellate activity (indicated by dinosterol/stanol abundances), and a similar increase in Beta-sitosterol/stanol abundances.

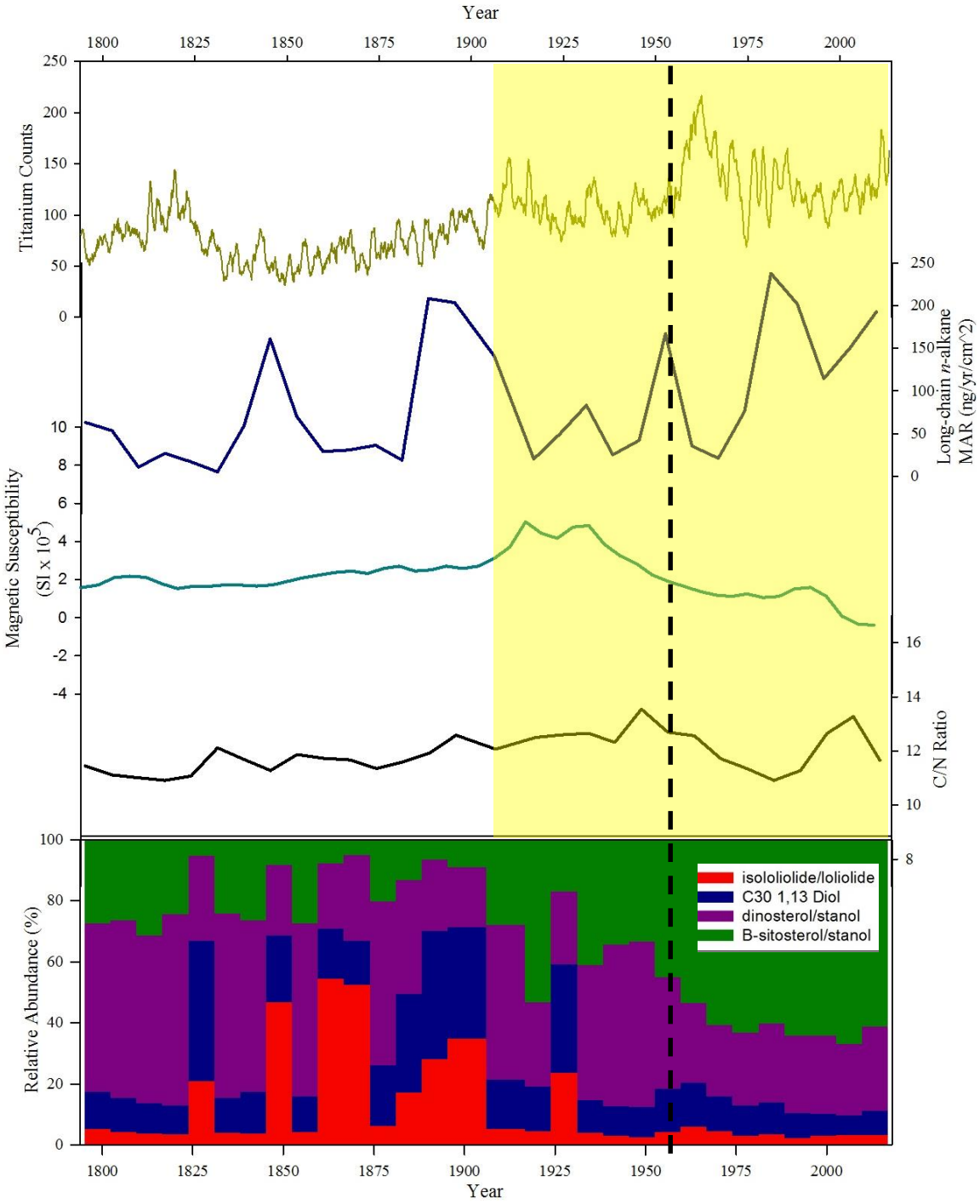

Figure 5.3: (top to bottom) Elemental Titanium Counts smoothed to 1mm resolution, mass accumulation rates (MAR) of the long-chain n-alkane abundances (C27+C29+C31+C33), measured in ug/g sediment), magnetic susceptibility measurements, bulk sediment total organic carbon to total nitrogen (C/N) ratio, and algal lipid relative abundances. Yellow highlighted area indicates the major shift in algal lipids distributions at Basin Pond, while the black dashed line indicates the chemical treatment of Basin Pond in July of 1955.

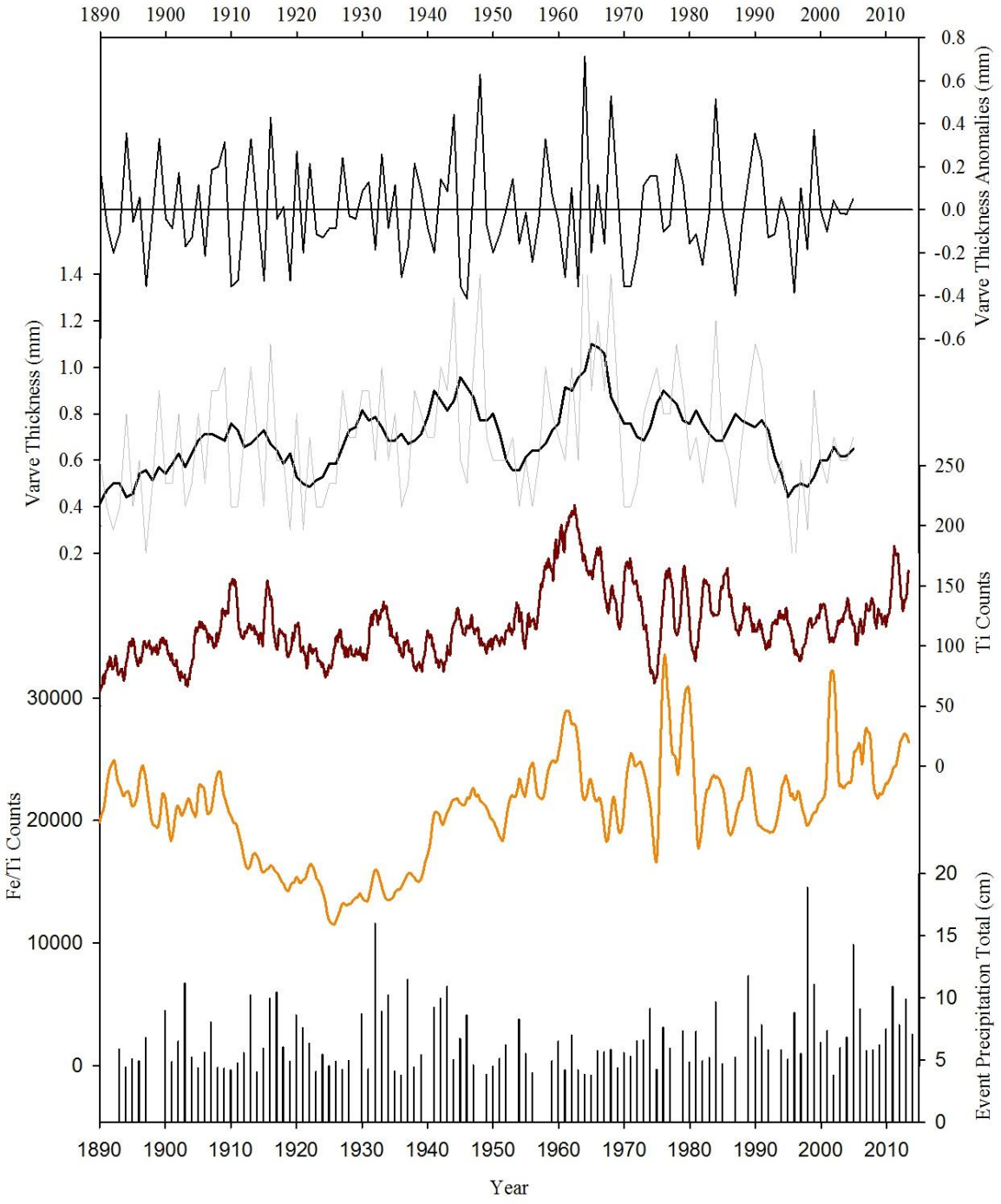

Figure 5.4: (top to bottom) Varve thickness anomalies (in mm), measured by subtracting varve thickness from the 7-year running average thickness. Titanium (dark red) and Fe/Ti (orange) abundances are also plotted. Extreme precipitation events (occurring from May – October) greater than 3.61cm in the Basin Pond region dating 130 years are plotted in the bottom bar graph. Note the highlighted (yellow) precipitation events occurring in 1932 and 1998, and the corresponding peaks in each of the proxy records shown.

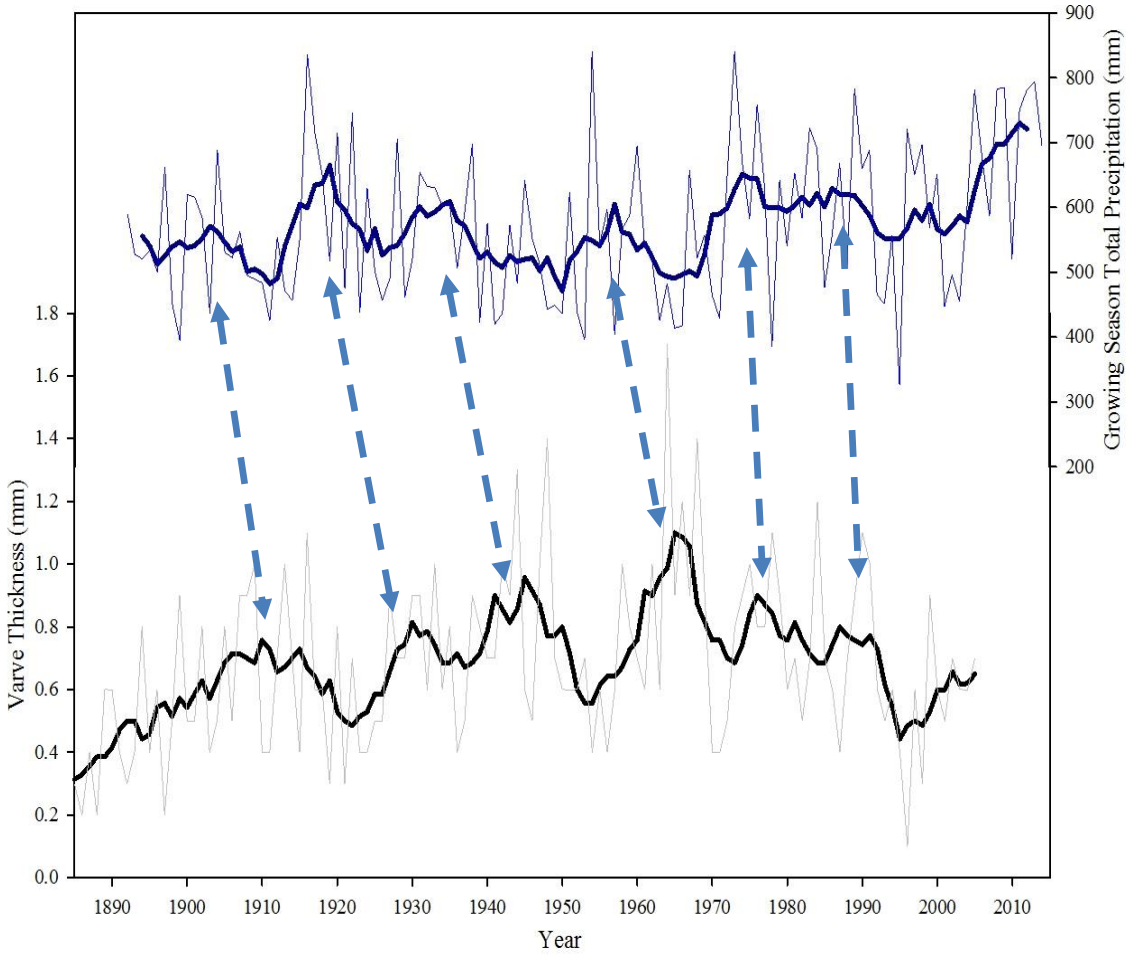

Figure 5.5: (top to bottom) Total Growing Season Precipitation record (in mm) and varve thickness measurements. Bolded lines indicate running averages (7-year running average). Arrows show potential areas of correlation between the two records, with the varve thickness record slightly leading the precipitation record. This slight discrepancy is likely caused by an error in the varve chronology by 5-7 years.

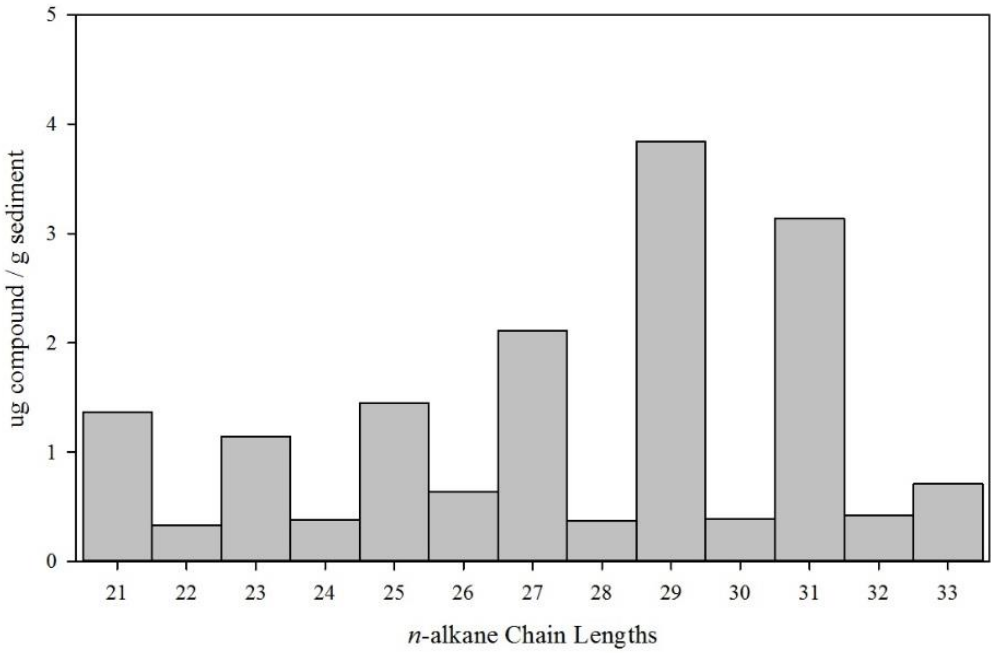

Figure 5.6 (above): *n* -alkane distribution throughout the Basin Pond sediment record. Histogram bars indicate mean values of each *n*-alkane (measured in μg/g sediment) throughout the record. Note a C29 > C31 > C27 pattern, a typical distribution in forested areas.

Figure 5.7 (above): Image of Basin Pond catchment area, showing C3 forest as the dominant vegetation type, and some aquatic vegetation.

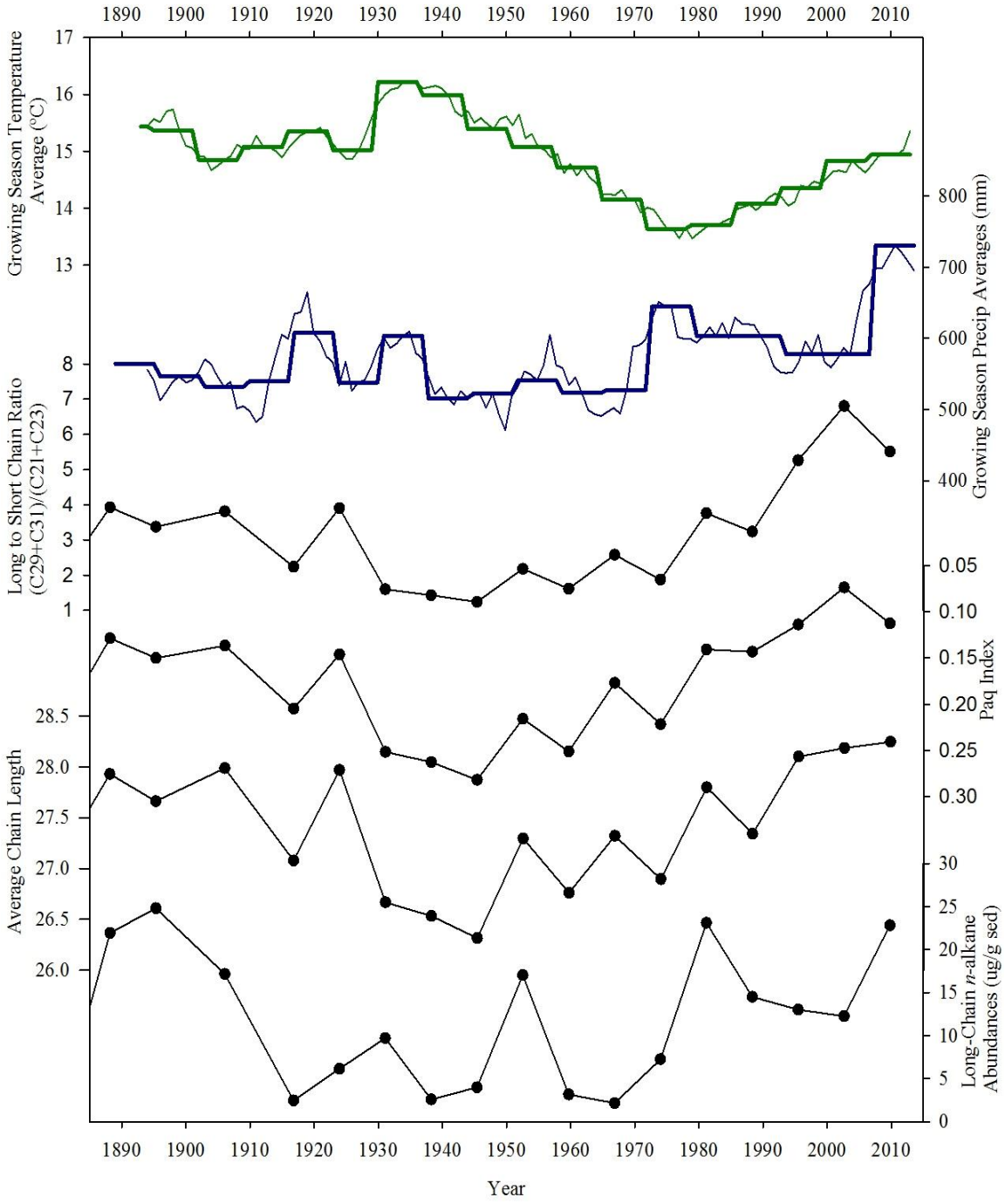

Figure 5.8: *n* - alkane proxies (from top to bottom, L:S chain ratio, Paq index, ACL, and long-chain abundances in µg compound per g sediment) compared to average growing season (April – September) precipitation (blue) and temperature (green) at Basin Pond. Bolded lines in the precipitation and temperature plots indicate the 7-yr averages, replicating the 7-year window of each sample used in biogeochemical analysis.

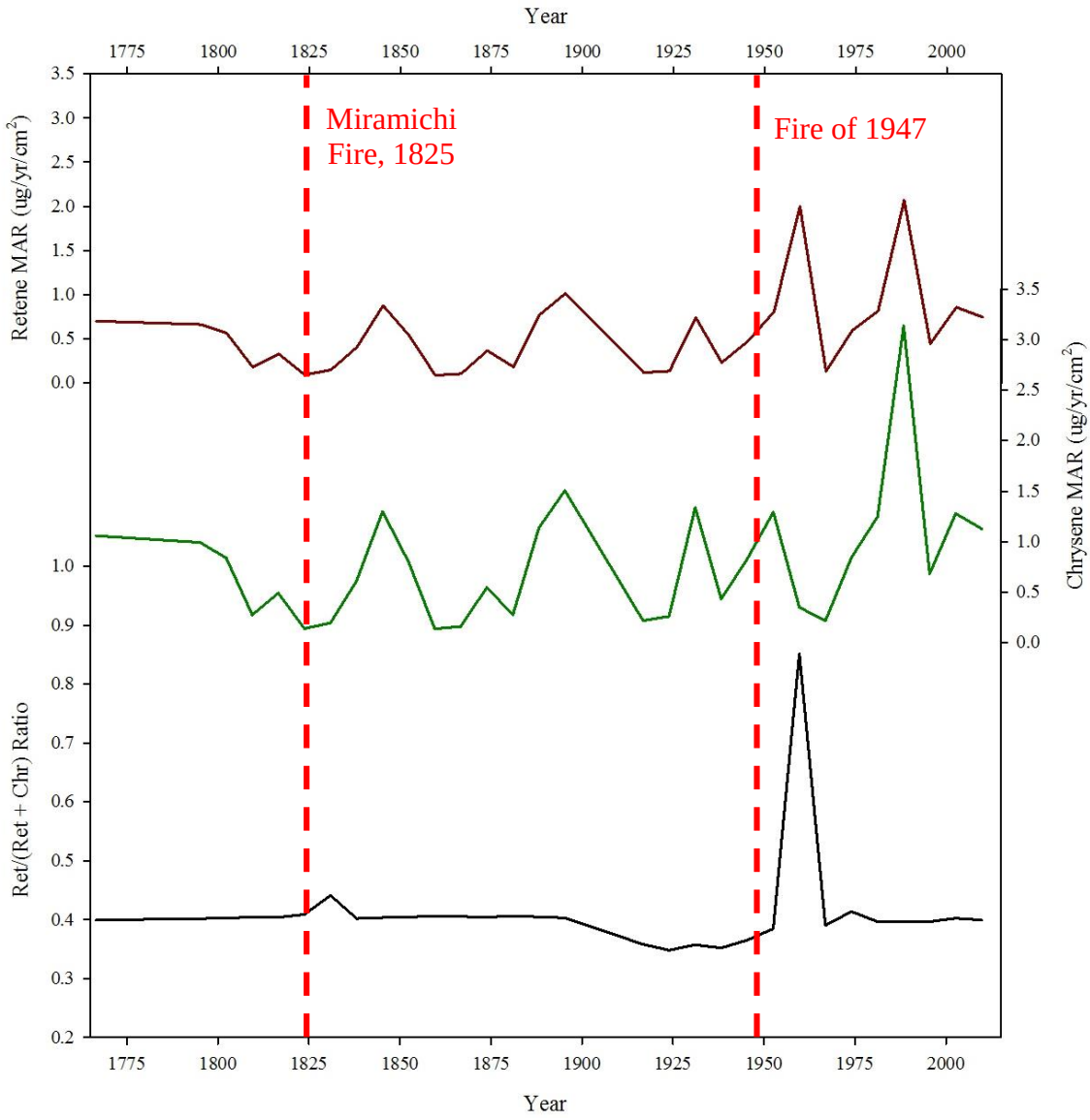

Figure 5.9: top to bottom: Mass Accumulation Rates (measured in µg/yr/cm^2) of the PAH retene (dark red) and chrysene (green), as well as the retene / (retene + chrysene) ratio (black). Vertical red lines indicate known wildfire events in the region, and are labeled at the top of the plot. Note a pronounced peak occurring following the 1947 fire, and a smaller, but still noticeable, peak occurring after the 1825 fire.

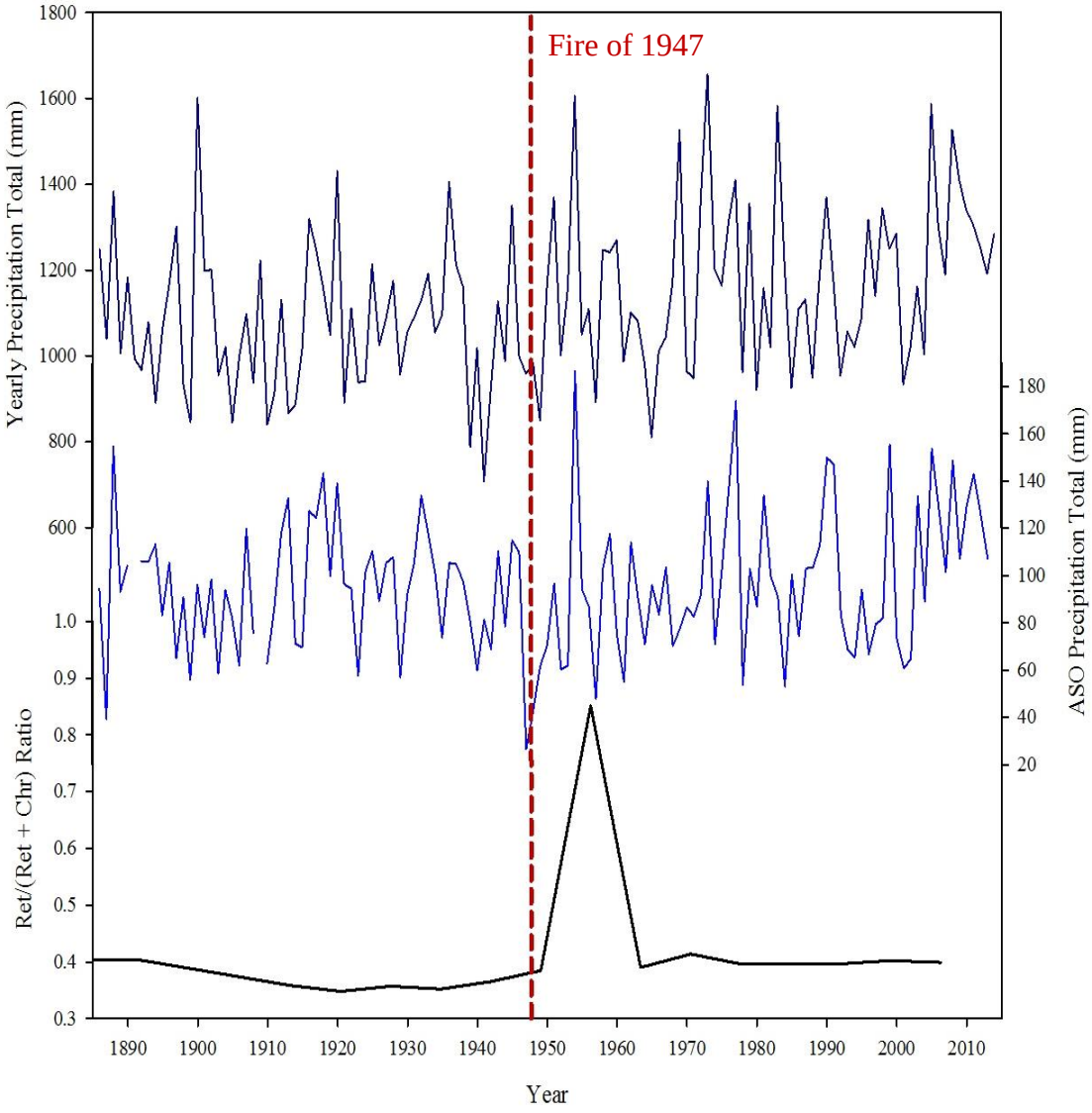

Figure 5.10: Comparison of precipitation records and the retene / (retene + chrysene) ratio from the Basin Pond sediment record (black). Top plot is the annual precipitation totals, while the middle plot is the August – September – October (ASO) seasonal precipitation totals. Vertical red line indicates the 1947 wildfire. Note that in the annual precipitation record, the short-term drought leading up to the 1947 fire is somewhat masked by precipitation throughout the year, whereas in the ASO precipitation record, the short-term drought is much more pronounced.

APPENDIX

SUPPLEMENTARY DATA TABLES AND MASS SPECTRA

A.1 NOAA Storm Track Information

Year	Name	Date of closest advisory	Closest Advisory Location	Cat	Wind Speed (kts)	Pressure (mb)	Range (mi) to BP	Precip Total (cm)
1869	Not Named	Sep 8, 1869 22z	(-71.1, 42.8)	H3	100	965	15	
1960	Donna	Sep 12, 1960 0z	(-71.2, 43.1)	H2	90	--	15	7.53
1869	Not Named	Oct 4, 1869 23z	(-70, 44)	H2	90	--	20	
1985	Gloria	Sept 27, 1985 12z	(-72.8, 41.9)	H2	85	951	50	4.68
1858	Not Named	Sep 16, 1858 18z	(-70, 45.5)	H1	70	979	30	
1961	Esther	Sep 26, 1961 06z	(-69.8, 44.7)	TS	35	999	15	5.485
1961	Unnamed	Sep 15, 1961 06z	(-70.1, 44.1)	TS	35	--	25	1.36
1908	Not Named	May 31, 1908, 0z	(-70.3, 43.8)	TS	35	--	15	6.07
1894	Not Named	Oct 10, 1894 18z	(-70.2, 44.8)	TS	55	--	20	3.73
1893	Not Named	Aug 29, 1893 18z	(-70.7, 44.3)	TS	55	--	20	3.02
1874	Not Named	Sep 30, 1874 06z	(-70, 44.3)	TS	60	980	15	
1960	Brenda	Jul 30, 1960 18z	(-71.1, 43.9)	TS	45	--	50	4.53
1949	Not Named	Aug 29, 1949 12z	(-71.9, 43.8)	TS	35	1000	50	1.47
1897	Not Named	Sep 24, 1897 13z	(-70.6, 43.3)	TS	45	--	50	1.02
1861	Not Named	Nov 3, 1861 12z	(-70, 44)	TS	50	1000	40	
2005	Cindy	July 9, 2005 18z	(-69.8, 44.9)	TD	30	1006	20	2.435
1933	Unnamed	Aug 25, 1933 18z	(-70.4, 44.5)	TD	30	--	5	6.465
1900	Not Named	Oct 14, 1900 18z	(-70.7, 44.1)	TD	30	--	20	2.13
1952	Able	Sep 2, 1952 12z	(-69.4, 44.4)	TD	25	--	40	3.67
1934	Unnamed	Sep 9, 1934 12z	(-70.3, 44.3)	ET	40	--	5	4.57
1899	Not Named	Nov 1, 1899 18z	(-68.9, 45.3)	ET	45	--	15	2.67
1896	Not Named	Sep 11, 1896 0z	(-70.1, 43.9)	ET	50	--	15	
2007	Barry	June 5, 2007 0z	(-69.5, 44.6)	ET	35	992	30	2.695
1979	David	Sep 6, 1979 18z	(-70, 45)	ET	40	992	40	3.61
1916	Not Named	May 17, 1916 18z	(-70.5, 45)	ET	50	990	40	10.23

A.2 Meteorological Station Data – Precipitation (measured in mm)

Year	Jan	Feb	Mar	Apr	May	Jun	Jul	Aug	Sep	Oct	Nov	Dec	Year
1885	-	-	-	-	-	-	-	-	-	105	105	74.4	-
1886	193	168	79.3	43.1	102	58.2	72.1	88.9	112	82.3	110	156	1265
1887	98.2	161	85.4	134	12.7	79.4	-	-	16.5	62.3	101	108	-
1888	131	-	137	44.1	76.9	-	-	92.7	218	153	129	62.7	-
1889	93.5	87.6	-	52.6	96.6	-	193	54	86.9	139	123	53.7	-
1890	-	90.4	184	47.7	176	118	98.3	129	80.4	104	57.3	93.6	1179
1891	160	86.6	139	46.9	55.5	77.4	-	-	-	53.9	45.5	142	-
1892	124	40.6	45.4	26.8	70.9	144	62.3	160	127	31.8	101	34.7	968
1893	61.2	115	75	72.4	172	70.7	40.6	95.5	76.6	145	76.1	79.1	1079
1894	41.8	-	56	47.9	131	81.4	48.8	66.4	146	127	75.3	70.1	891
1895	103	24.1	47.8	144	77.8	85.8	26.6	151	48.8	50.5	146	159	1064
1896	20.4	142	275	67.6	56	63.3	95.3	101	117	98.6	107	29.2	1173
1897	138	-	123	81	95.2	110	206	95	75.8	24.1	127	126	1202
1898	11.9	174	14	68.7	45.7	110	71.1	83.1	71.8	118	112	11.2	891
1899	65.4	66.1	147	23.4	50.2	61.3	129	48.6	82.8	36.3	66.1	68.9	845
1900	157	283	179	44.3	130	140	124	58.5	123	108	216	45	1607
1901	82.9	26.4	115	175	100	88.2	107	87.7	57.3	76.9	53.4	228	1198
1902	84.4	60.2	214	93.2	131	134	49	84.8	91.6	119	30.3	110	1201
1903	91.7	66.8	144	70.4	15	145	109	67.7	29.7	78.3	31.6	107	955
1904	89.6	18.4	79.5	162	145	26.2	126	116	113	53.2	46.4	44.9	1020
1905	96.2	18	35.9	53.9	67.5	91.5	103	78.8	136	31.5	65.7	66.8	845
1906	58.1	48.1	109	52.3	92.6	137	162	61.4	16.7	108	74.7	80.6	1001
1907	59.5	49.8	73.2	103	65.4	73.2	117	53.1	152	155	114	83.6	1098
1908	72.1	113	71.7	60.4	149	52.2	71.8	124	37.7	65.8	41.5	78.6	938
1909	146	161	99.5	100	-	48.3	52.1	-	-	-	-	-	-
1910	86.3	75.4	35.8	111	55	80.1	78.8	100	58.4	30.3	58.8	69.7	840
1911	49.8	52.5	141	26.1	30.4	120	68.2	99.1	81.5	78.2	86.6	77.8	911
1912	107	70.9	96.8	73.9	166	26.2	51.7	147	89.7	117	117	67.4	1131
1913	64.5	29.7	-	58.3	87.9	20	73.7	78.6	152	167	58.8	76.7	868
1914	55.6	46.1	135	125	41.1	67.8	68.1	112	43.6	57.9	80	54.9	887
1915	89.2	107	3.4	79.3	67.7	62.7	192	99	51.3	59	80	129	1019
1916	37.8	107	56.7	109	172	131	100	191	133	58.1	106	118	1320
1917	98.7	48.2	107	81	72.4	273	65	181	43	149	28.6	98.1	1245
1918	65.1	60.5	48.4	62.6	81.1	126	90.9	59.7	228	142	103	90.5	1158
1919	66	38.5	147	65.1	147	47.5	63.3	65.3	129	105	138	38	1050
1920	39.2	153	82.5	167	57.5	52.7	85	183	170	63.8	153	224	1430
1921	24.6	50.8	70.9	91.7	49	45.3	87.2	142	59.5	87.4	145	37.6	892
1922	56.1	72	92	91.8	133	218	52.7	132	119	32.3	35.3	78.2	1112
1923	142	31.7	58.1	189	49.3	56.6	57.8	42.2	42.7	88.4	69.2	111	939
1924	73.7	50.5	18	138	100	42.8	73.5	125	151	29	83.7	55.9	941
1925	75.8	104	156	18.1	54.6	129	137	34.3	129	168	130	79.5	1214
1926	76.4	68.5	68.4	79.5	42.1	100	65.6	90.5	79	98.6	184	72.1	1025
1927	51.1	98.7	27.5	27.4	172	67.2	72.1	110	41.4	165	118	141	1091

1928	104	47.5	73.5	105	162	101	82.1	120	137	66.2	56.1	120	1174
1929	91.3	56.7	105	148	123	65.5	33.7	68.4	23.4	78.9	72	89.2	955
1930	76.2	30.7	178	42.8	102	95.8	131	121	27.4	128	83.8	39.3	1056
1931	89.4	51.3	95.3	78.8	85.8	136	104	117	132	67.3	38	95.2	1091
1932	119	53.7	89.2	91.9	70.1	43.1	88.9	107	231	62.8	119	52	1129
1933	77.7	55.6	119	161	55.5	60.7	154	126	72.7	154	61.1	93.9	1192
1934	89.8	72.9	49.6	136	30.8	105	79.2	48.3	204	50.4	72.4	116	1055
1935	184	49.8	30.8	75.2	45.5	178	104	65.6	135	21.3	158	49.9	1097
1936	168	70	282	135	85.4	52.2	71	99.3	64	153	58.2	167	1405
1937	77.5	93.6	71.6	76	171	131	87	18.6	109	188	137	52.5	1213
1938	117	48.7	65.9	56	130	87.1	208	51.8	164	77.3	56.4	100	1162
1939	26.3	65.1	36.4	98.2	33.1	68.7	87.4	57.7	77.8	107	19.1	111	788
1940	49	50.6	97.2	138	78.9	120	71	69.6	98.4	12	154	80.8	1018
1941	39.7	53.5	34.6	15.5	61.6	31.8	141	109	61.2	74.4	27.9	58.4	708
1942	62.5	14.6	158	34.1	45	137	94.3	36	90	80.8	99.8	75.5	928
1943	17.2	58.4	57.8	78	51.2	159	120	123	42	166	225	30.8	1128
1944	44.5	93	90.9	74.1	23.1	102	128	26.5	129	80	131	66.3	989
1945	125	90.3	49.9	126	185	81.3	86.7	74.7	87.8	182	150	112	1350
1946	94.6	57.7	27.5	77.2	78.8	48.6	97.6	113	136	80.1	74.5	114	1000
1947	81	85.7	92.9	41.1	144	116	135	31.9	44.5	3.7	135	47.8	959
1948	58	26.7	70.6	62.4	195	71.3	62.3	38.5	13.2	76.5	203	106	984
1949	82.3	70.4	41.7	83	80.3	88.1	65.3	51.5	81.1	52.2	108	46.4	850
1950	143	58.5	148	79.8	35.1	125	52.6	104	38.9	68.3	170	138	1162
1951	67.1	110	147	186	75.7	48.5	124	91.3	98.3	100	182	139	1369
1952	91.6	139	81.7	67.7	142	101	16.4	31.2	81.1	69	35.4	146	1002
1953	106	61.4	286	126	77.3	49.8	57.2	44.4	40.9	101	112	96.3	1157
1954	97.8	127	108	97.5	133	126	87.7	166	231	162	129	139	1606
1955	30.2	135	99.8	63.3	114	152	50	132	32.2	119	93.5	30.6	1051
1956	117	77.7	113	99.6	80.6	74.3	143	95.5	104	61.5	76	68.2	1110
1957	49.1	30.1	46	52.2	77.9	92.9	89	48.3	44.5	50.8	154	158	892
1958	218	75.4	96.7	143	96	74.5	101	65.3	86.8	158	90.9	42.1	1247
1959	93.2	39.6	100	77.5	35.5	204	77.1	105	88.1	159	177	85.2	1243
1960	70.4	184	40.4	94.1	202	117	161	19.6	102	103	93.8	82.8	1270
1961	37.3	88.6	65.8	140	95.3	83.8	109	30.8	82.1	52.2	129	72.9	987
1962	79.4	56.8	59.9	120	66	45.6	96.8	84.5	105	153	123	112	1102
1963	73.9	62.7	85.7	55	89.7	29.1	70.5	124	56.9	91	287	57.7	1083
1964	102	21.4	107	70.6	46.9	100	120	112	32.5	68.3	105	94.8	981
1965	28.6	118	7.9	64.5	31.1	73.4	62.6	126	56.1	106	95.6	41.6	811
1966	92.3	61.7	108	26.8	62.5	106	74	60.2	88.5	102	161	69.4	1012
1967	42.8	65.8	17.7	81	103	137	91	132	114	65.1	85.5	108	1043
1968	68.6	39.4	133	114	73.3	116	67.1	31.9	120	58.8	183	169	1174
1969	97.8	181	81.3	61.7	76.3	100	124	94.6	100	37.9	178	393	1527
1970	24.1	178	0	88.6	66.9	105	72.1	68.6	63.9	127	71.5	99.3	965
1971	37.4	143	112	42.9	98.6	69.6	46.6	110	61.3	76.9	84	66.2	949
1972	33.3	159	130	111	59.7	152	146	87.9	90	98.3	121	170	1357
1973	81.8	70.3	63	147	146	164	114	164	106	150	85	366	1657
1974	68.2	64.8	111	120	153	122	96.3	90.2	90.4	32.5	117	139	1204

1975	82	47.3	122	64.9	52.1	139	110	90	126	91.5	125	114	1165
1976	68.8	93.5	81.9	73.4	148	71.1	212	186	69.8	157	57.6	95	1313
1977	98.6	80.5	147	104	30.1	163	22.1	133	179	210	100	144	1410
1978	222	47.5	95.3	93.5	78.2	100	39.3	59.3	15	87.9	52.6	72.2	963
1979	235	61.5	121	154	202	33.7	67.3	109	75.7	124	102	71.2	1356
1980	28.5	20.5	91.7	169	21.9	63.6	125	57.4	104	99.4	106	33.4	920
1981	13.4	109	23	75.9	76	130	133	90.6	148	163	85.3	110	1158
1982	103	56.3	84.8	89.1	25.4	131	61.2	131	146	22.6	125	46.6	1021
1983	126	75.8	147	171	176	55.3	120	144	57	72.2	263	176	1582
1984	46.7	109	141	145	197	191	64.2	65.6	27.6	66.5	77.1	84	1215
1985	27.2	101	78.7	53.1	58.7	87.3	48.6	118	112	71.5	120	50.2	926
1986	201	39.6	99.7	69.7	105	86.2	105	106	84.5	32.7	82.6	97.2	1109
1987	87.9	16.5	79.3	201	92.2	127	62.4	52.7	133	124	64.2	91.8	1132
1988	60.3	58.8	26.2	76.3	51.3	56.9	102	166	54.1	89.7	166	42	949
1989	35.8	54.2	69.9	98.6	252	163	14	144	113	81.3	120	38.4	1184
1990	115	53.1	45.7	84.1	151	131	70.1	106	117	227	97.9	171	1369
1991	62.2	22.1	142	91	117	82.3	60.6	227	110	104	89.5	69.5	1178
1992	85.9	70.8	141	50.2	9.9	142	82.4	103	77.6	68.8	90.1	32.5	954
1993	42.3	109	136	167	30.9	74.7	54.4	55.4	69.4	81.4	129	107	1056
1994	117	36.5	124	96.8	89.2	117	86.2	46.6	122	28	95.9	62.2	1022
1995	98.3	60.4	94.7	40.3	114	30.8	82.5	14.5	43.8	224	186	97.8	1087
1996	152	89.2	55.1	152	116	94.5	248	11	99.1	90.7	53.3	157	1318
1997	113	48.1	86.5	107	72.7	139	127	129	75.8	34	146	62.6	1141
1998	128	107	129	88.6	92	354	82.7	39.7	39.5	167	78.5	38.9	1344
1999	166	65.1	188	7.4	81.1	81.3	53	100	246	121	90.5	51	1250
2000	111	77.3	105	179	132	79.7	144	64	53.7	102	90.1	147	1285
2001	41.7	102	193	22.8	66.7	140	79.9	26.4	112	44.3	53.3	53.2	934
2002	78	85.4	97.4	126	107	90.7	69.5	18.2	84.9	91.2	108	62.9	1019
2003	33.9	49.6	84.3	39.1	73.8	51.9	102	63.8	125	212	129	198	1162
2004	12	45.7	33.9	131	109	60.5	91.6	148	58.4	61.2	132	122	1004
2005	55.4	86.6	90.1	225	184	151	65.7	86.4	69.6	305	158	111	1587
2006	105	58	29.4	48.3	123	210	137	77.8	82.1	225	126	81.2	1303
2007	60.2	41.9	82.1	201	58	60	107	106	55.3	144	164	112	1191
2008	71	151	99.6	133	30.4	152	124	178	165	103	196	124	1527
2009	48.1	87.5	58.3	99.4	107	238	162	137	41.2	144	150	138	1411
2010	106	112	166	91	47.2	106	41	97.1	139	154	132	152	1342
2011	51.5	79.8	127	160	116	97.9	68.2	182	127	120	96.8	79.6	1306
2012	79.3	28	53.4	92.5	157	261	52.2	94.9	124	157	16.1	138	1254
2013	24.3	80	53.6	44	142	170	144	177	117	26.6	117	96.1	1191
2014	91.8	95.8	123	79.8	129	120	229	119	19.3	-	-	-	-

A.3 Meteorological Station Data – Temperature (measured in degrees C)

Year	Jan	Feb	Mar	Apr	May	Jun	Jul	Aug	Sep	Oct	Nov	Dec
1893	-12	-9.1	-3.6	2.4	12	18	20	20	12	9.8	1.4	-7.6
1894	-8.5	-9.3	1.8	7.1	13	20	21	17	15	8.3	-2.1	-5.3
1895	-8.3	-8.2	-2.7	6.6	15	21	21	20	17	6	2.8	-4
1896	-11	-6.6	-2.5	7.3	14	18	23	21	15	7.7	2.2	-6.8
1897	-7.1	--	-2.1	7.2	13	16	22	19	13	--	--	--
1898	-3.4	1.1	4.7	12	17	20	20	15	9.4	2.1	-7	-8.3
1899	-8.9	-3.6	5.8	12	18	20	19	13	9.2	0.8	-3.5	-8.5
1900	-7.7	-5.5	5.4	9.3	18	20	19	15	11	2.1	-7.9	-8.9
1901	-9.3	-2.6	7.1	13	18	21	19	15	8.2	-1.5	-5.3	-8.5
1902	-5.7	2.7	6.8	12	15	18	17	15	7.9	2.8	-8.1	-8.4
1903	-6.5	3.2	6.4	13	15	19	16	15	8.4	0.4	-8	-13
1904	-11	-2.5	4.4	14	17	20	18	13	7.3	-1.7	-11	-11
1905	-10	-1.6	5.6	12	16	20	17	14	8.5	0.1	-4.5	-5.1
1906	-7.1	-4.9	4.5	11	16	20	20	14	8.8	1.2	-9.5	-11
1907	-11	-1.8	3.6	9.5	16	20	18	14	6	1.1	-2.8	-6
1908	-9.4	-1.9	4.1	13	18	21	18	16	10	1	-7.7	-8.5
1909	-7.3	-2.2	4.2	17	--	18	--	--	--	--	--	--
1910	-6.4	0.9	8.5	12	16	20	18	14	8.8	1.8	-8.1	-8.7
1911	-9.8	-4.2	3.9	16	17	22	19	14	8.1	0.9	-1.8	-14
1912	-8.2	-3.4	4.5	12	15	20	16	13	8.8	1.4	-3.6	-4.7
1913	-7.8	7.4	--	11	17	20	18	13	11	2.5	-3.6	-10
1914	-11	-1.9	3.6	13	16	19	18	15	9.8	-0.1	-7	-7.3
1915	-4.7	-1.1	7.4	12	17	19	19	16	8.8	1.9	-3.8	-7.8
1916	-8.1	-5.8	6.1	12	16	21	20	14	7.9	-0.3	-5.5	-9.6
1917	-9.9	-2.1	4.2	8.8	17	21	20	13	7	-0.3	-11	-13
1918	-11	-3.5	6.4	15	15	21	19	13	8.1	2.7	-5	-7.1
1919	-4.4	0.7	5.6	12	19	21	18	13	7.9	0.8	-8.7	-12
1920	-8.6	-1.2	4.4	12	17	19	21	15	12	-0.4	-4.6	-7.2
1921	-6.2	2.1	8.4	13	17	23	18	16	8.5	-0.2	-6.7	-10
1922	-8	0.6	6.6	14	18	20	19	15	7.5	1.9	-7.3	-10
1923	-11	-5.8	3.4	12	18	19	17	16	8.7	2.1	-0.9	-8.3
1924	-9.9	-0.1	4.9	11	16	20	19	14	9.5	2.2	-8	-12
1925	-3.9	0.4	6.5	11	17	20	18	14	4.6	0.7	-6.2	-9
1926	-8.4	-5.7	1.7	11	15	20	19	14	8	1.3	-7.9	-6.9
1927	-6.3	1.1	6.2	11	16	21	17	15	10	3.9	-3.7	-6.9
1928	-7.8	-2.9	4.1	11	16	21	21	13	9.3	1	-2.7	-8.3
1929	-6.9	-0.1	5.1	12	18	20	18	16	8.6	1.8	-6.6	-8.1

1930	-6.5	-1.4	5.1	13	20	20	18	16	9.1	3.2	-4.9	-7.7
1931	-5.4	1.5	7.2	13	18	22	19	16	11	5	-3.1	-2.5
1932	-6.7	-2.6	5.8	13	17	20	21	15	11	0.9	-3.2	-3.2
1933	-3.8	-2.2	5.4	14	19	20	20	16	8.7	-1.1	-8.9	-9
1934	-13	-2.1	6.7	14	18	21	18	18	7.6	3.4	-7	-11
1935	-8.3	-1.3	5.7	11	18	22	21	14	9.1	4.1	-6.9	-7.9
1936	-9.6	1.8	5.5	14	18	20	19	15	8.4	-0.6	-4.2	-3.3
1937	-3.8	-3.1	5.6	14	19	22	23	16	8.3	2.4	-6.2	-9
1938	-5.9	-1.3	7.7	12	19	21	21	14	11	2.8	-2.9	-8.2
1939	-7.2	-5	3.2	13	18	21	22	15	8.9	1.2	-4.6	-10
1940	-5.3	-2.6	4.3	13	17	21	19	15	7.7	2.4	-6.2	-7.8
1941	-4.3	-2.7	9.6	14	20	21	19	16	8.2	3.1	-2.4	-7.7
1942	-6.3	2.1	6.7	14	18	20	19	15	9	2	-7.4	-9.3
1943	-6.1	-2.7	3.4	13	18	21	19	14	8.9	2.1	-9.2	-6.8
1944	-7.5	-2.8	3.6	14	17	20	21	15	8.1	2.4	-6.3	-10
1945	-5.2	2.7	8.5	10	17	20	19	16	6.8	1.1	-9.1	-10
1946	-9.6	3.4	4.2	12	17	20	19	16	9.8	2.9	-4.9	-9
1947	-5.1	-0.2	4.5	11	16	22	21	15	12	0.3	-6.9	-10
1948	-9.8	-1.5	5.3	11	16	20	20	14	8	5.1	-3.4	-4.1
1949	-5.7	-0.4	7.2	13	19	22	22	14	11	0.3	-3.9	0
1950	-9	-3.9	3.6	13	18	19	18	12	8.9	4.2	-3.4	-6
1951	-4.9	-0	6.7	13	17	20	19	15	8.9	0.4	-6.6	-6.7
1952	-5.8	-0.6	6.3	11	19	23	20	15	7.3	2	-2.4	-4.9
1953	-5	0.6	6.9	14	18	20	18	15	9.5	4.4	-1.5	-9.5
1954	-3.1	-1	4.6	11	17	19	18	13	11	2.6	-4.2	-7.6
1955	-5.6	-2.9	6.5	14	18	22	20	14	8.6	1.6	-9.1	-4.6
1956	-5.3	-4.8	3.7	9.4	17	17	17	12	8.6	1.9	-4.5	-13
1957	-5.2	0.3	6.3	12	19	19	17	15	9	4.1	-2.2	-5
1958	-7.7	2	5.9	9.7	14	19	18	14	6.5	1.5	-12	-9.6
1959	-10	-3.5	5.5	14	15	21	20	15	7.9	0.9	-4	-8.2
1960	-4.7	-4.8	4.4	14	17	19	18	14	6.6	2.3	-8.6	-12
1961	-7.3	-2.1	4.5	11	16	19	18	18	9.4	2.9	-4.1	-10
1962	-13	-0.3	5.2	10	17	17	18	13	7	0.1	-6.5	-9.3
1963	-12	-2	4.5	11	18	21	17	12	10	2.9	-10	-7.8
1964	-7.3	-2	3.7	13	16	20	15	12	6.9	0.7	-6.8	-10
1965	-9	-1.1	3.6	13	17	18	19	14	6.6	-0.2	-5.4	-7.4
1966	-6.8	-0.8	3.8	11	17	19	18	12	8	2.5	-4.8	-7.4
1967	-12	-5.5	2.7	7.4	18	20	19	14	7.9	-0.4	-5.2	-13
1968	-11	-2.6	6.6	10	15	20	16	14	9	-0.7	-7.6	-10
1969	-7.4	-4.2	2.3	9.6	16	17	19	14	7.2	2.3	-5.3	-12

1970	-8.1	4.6	0	12	16	20	19	13	8.8	2.2	-10	-14
1971	-9.3	-3.5	3.1	10	16	18	18	14	10	-0.6	-7.3	-11
1972	-9.4	-5.8	2	11	16	19	17	13	4.9	-0.8	-8.5	-8.1
1973	-9.9	0.7	4.8	8.7	16	20	20	13	7.6	0.9	-2.9	-9.6
1974	-8	-4.3	3.9	8	15	18	18	13	3.6	1.4	-4.8	-8.8
1975	-8.4	-4.4	1.7	13	16	20	18	12	8.4	3	-9.2	-14
1976	-7.8	-4.4	5.2	9.8	18	17	18	12	6.2	-0	-10	-13
1977	-8.5	1	4.7	12	15	18	17	12	7.1	2.4	-7.4	-10
1978	-11	-4.3	2.5	12	15	18	17	11	6.4	-1.1	-7.9	-10
1979	-11	-1	4.1	11	15	19	16	12	6.1	2.2	-5.4	-8.7
1980	-11	-4.4	4.1	9.5	14	19	19	12	5.5	-0.7	-11	-14
1981	-3	-1.3	5.7	12	17	19	18	12	5.5	0.8	-4.6	-16
1982	-12	-3.7	2.4	11	14	18	16	13	6.8	1.9	-3.1	-8.7
1983	-6.2	0	4.8	9.7	16	19	18	15	6.7	1.3	-7.5	-12
1984	-3.9	-6.5	5.2	10	16	19	20	12	8.2	1.7	-4.6	-12
1985	-7.5	-2.2	4.5	11	14	20	18	13	7.9	0.7	-8.8	-8.6
1986	-8.4	-2.3	7.7	11	15	18	17	11	6.8	-1	-5.3	-9.9
1987	-8	-1.4	7	11	17	19	16	13	6.9	0.1	-3.5	-12
1988	-8.1	-3.4	4.9	12	16	20	19	12	5.6	2.1	-8.5	-9.5
1989	-8.7	-4.7	2.8	13	16	19	17	14	7.3	0	-14	-6.2
1990	-8.7	-1.1	4.8	10	16	19	19	13	8.9	2.5	-4.1	-11
1991	-6.1	-0.8	5.6	13	17	19	19	12	8.2	2.7	-6.4	-9.7
1992	-8	-4	3.3	11	16	17	17	13	5.5	-0.1	-4.8	-7.3
1993	-14	-4.2	4.9	12	16	19	19	13	4.9	0.6	-4.2	-15
1994	-12	-1.6	4	9.7	18	21	18	13	7.9	3	-3.5	-7
1995	-10	-1.3	2.6	11	17	20	19	11	9.6	-0.7	-8.1	-10
1996	-8.7	-3.5	4.7	10	16	18	18	14	6.7	-0.5	-1.9	-10
1997	-7.3	-5.1	3.3	8.5	16	19	17	13	6.8	0.7	-4.6	-7
1998	-3.5	-1.7	6	14	16	19	19	15	8.1	1.9	-1.5	-9.3
1999	-6	-0.8	5.3	13	19	20	18	16	5.8	3.3	-2.9	-8.8
2000	-6	1.2	4.9	11	16	17	18	13	7.7	2.5	-7.3	-9.4
2001	-9.2	-2.2	4.4	13	18	18	20	14	8.7	3.5	-1.3	-4.6
2002	-5.3	-1.4	5.5	10	16	19	20	15	5.7	0	-5	-12
2003	-9.5	-3.2	3.7	10	17	19	20	15	7.3	2.9	-4.8	-13
2004	-6.9	-0.5	5.6	12	15	18	19	14	7.7	1.7	-6.2	-10
2005	-6.2	-2.8	5.7	8.9	18	20	19	16	8.9	2.1	-5.3	-4.1
2006	-6.5	0.1	6.8	12	18	21	17	14	7.9	5.1	-0.6	-7.3
2007	-9.1	-2.1	3.7	12	17	18	18	15	11	0.5	-6.8	-6.6
2008	-7	-2.9	5.9	11	17	20	18	14	7.1	1.9	-5.7	-12
2009	-7	-1.4	7	11	15	18	19	13	5.9	4.1	-4.8	-5.6

2010	-2.9	2.8	8	13	16	22	19	15	8.2	2	-3.9	-8.7
2011	-8	-1.7	5.1	12	16	20	18	16	9.1	3.9	-3	-7
2012	-4.5	2.8	6.8	13	16	20	20	13	9.7	0.8	-3.3	-7.7
2013	-4.9	-0.3	5	12	17	21	18	14	9	0.2	-7.3	-10
2014	-8.8	-6.3	4.8	12	16	20	18	--	--	--	--	--

A.4 Polycyclic Aromatic Hydrocarbon Mass Spectra

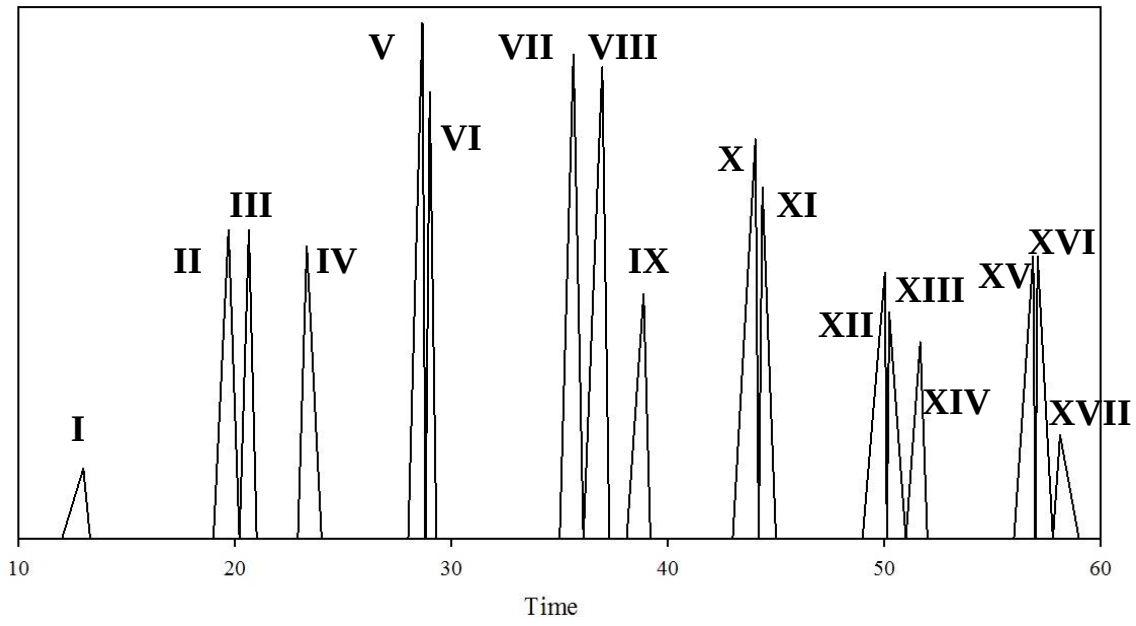

Retention Order	Compound	Major Ion	Retention Time (min)	Standard Used
I	naphthalene	128	12.989	Restek
II	acenaphthylene	152	19.617	Restek
III	acenaphthene	153	20.55	Restek
IV	fluorene	166	23.176	Restek
V	phenanthrene	178	28.465	Restek
VI	anthracene	178	28.731	Restek
VII	fluoranthene	202	35.414	Restek
VIII	pyrene	202	36.704	Restek
IX	retene	219	38.641	Chiron
X	benzo(a)anthracene	228	43.829	Restek
XI	chrysene	228	44.094	Restek
XII	benzo(b)fluoranthene	252	49.857	Restek
XIII	benzo(k)fluoranthene	252	50.012	Restek
XIV	benzo(a)pyrene	252	51.495	Restek
XV	indeno(1,2,3,cd)pyrene	276	56.754	Restek
XVII	dibenz(a,h)anthracene	278	56.831	Restek
XVI	benzo[g,h,i]perylene	276	57.97	Restek

I : Naphthalene

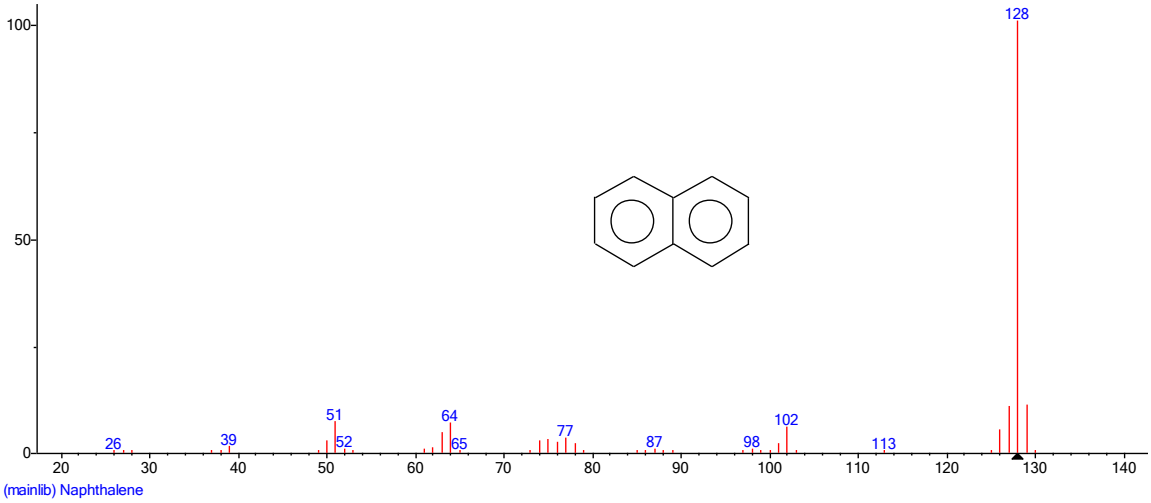

II : Acenaphthylene

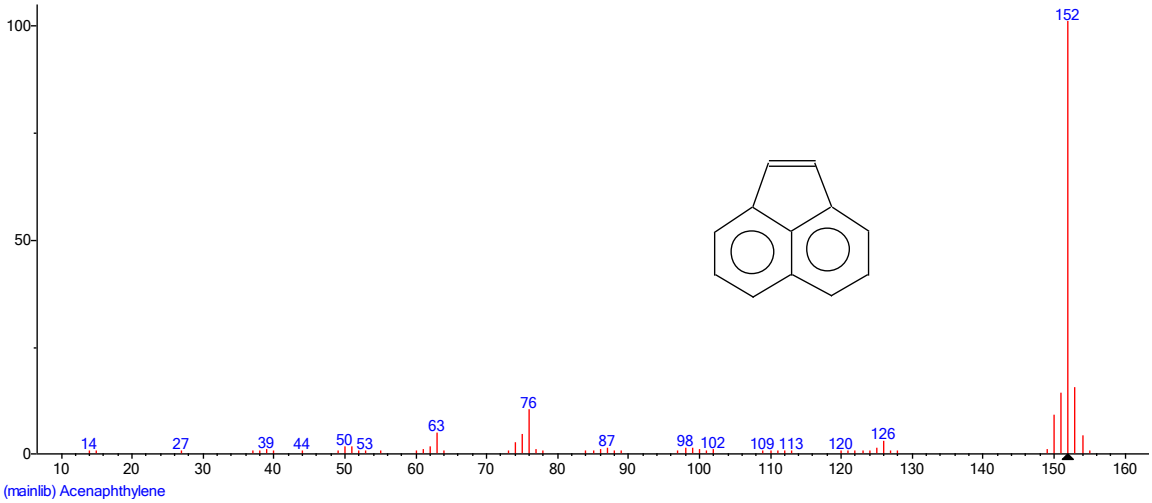

III : Acenaphthene

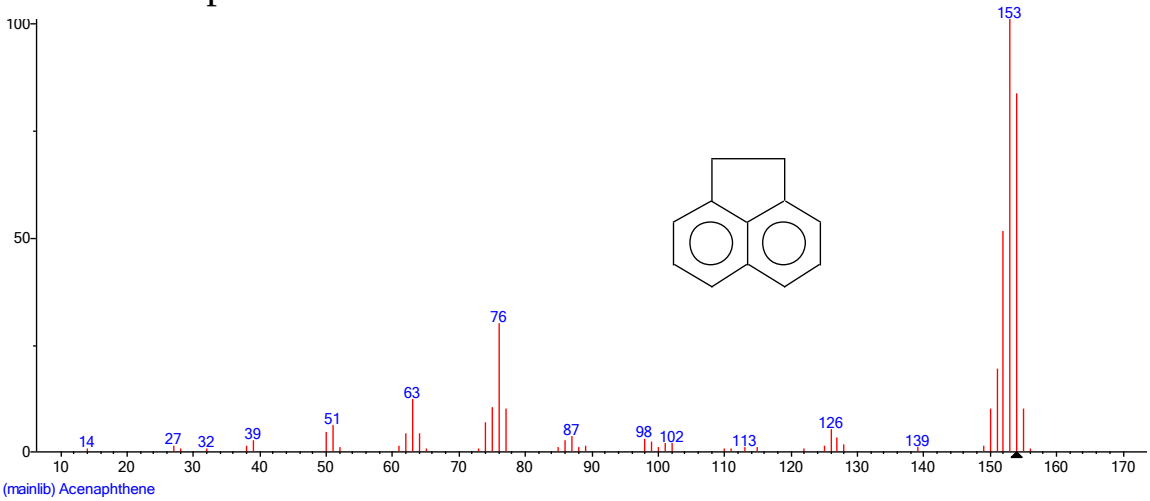

IV : Fluorene

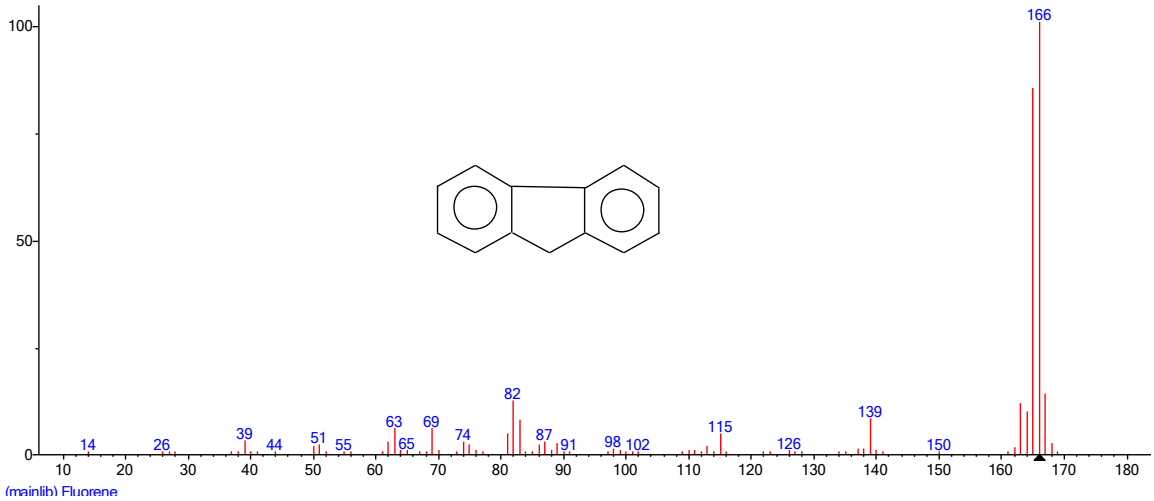

V : Phenanthrene

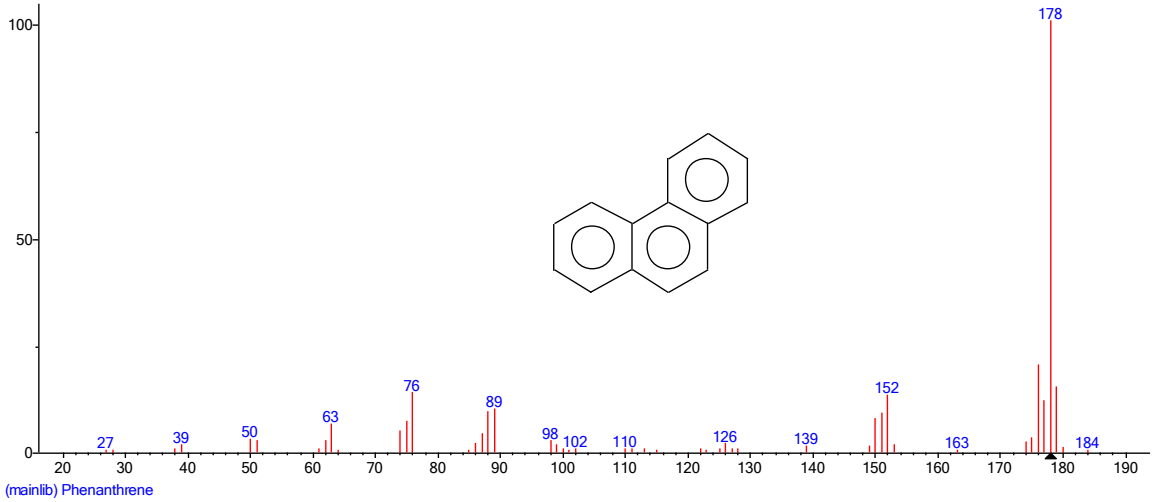

VI : Anthracene

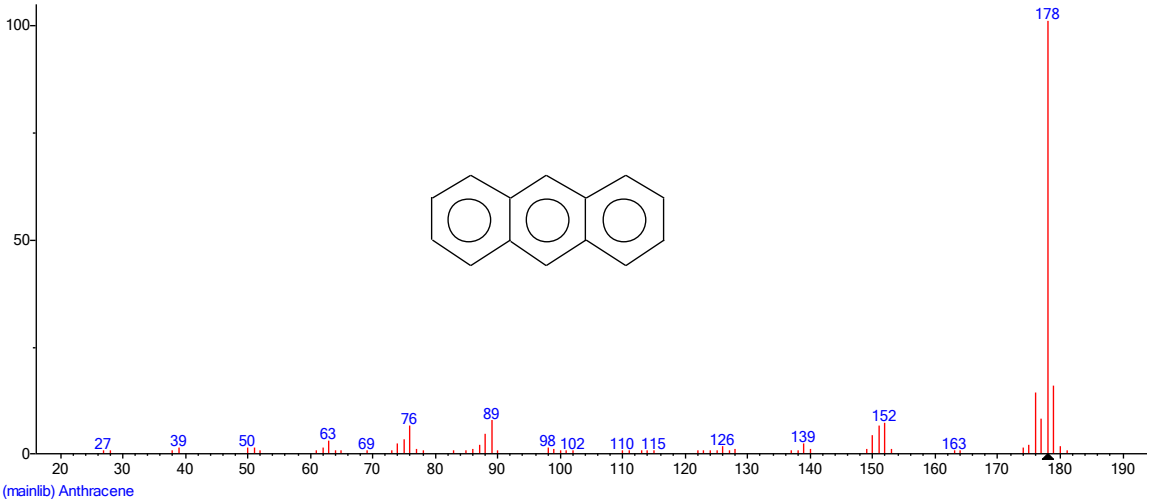

VII : Fluoranthene

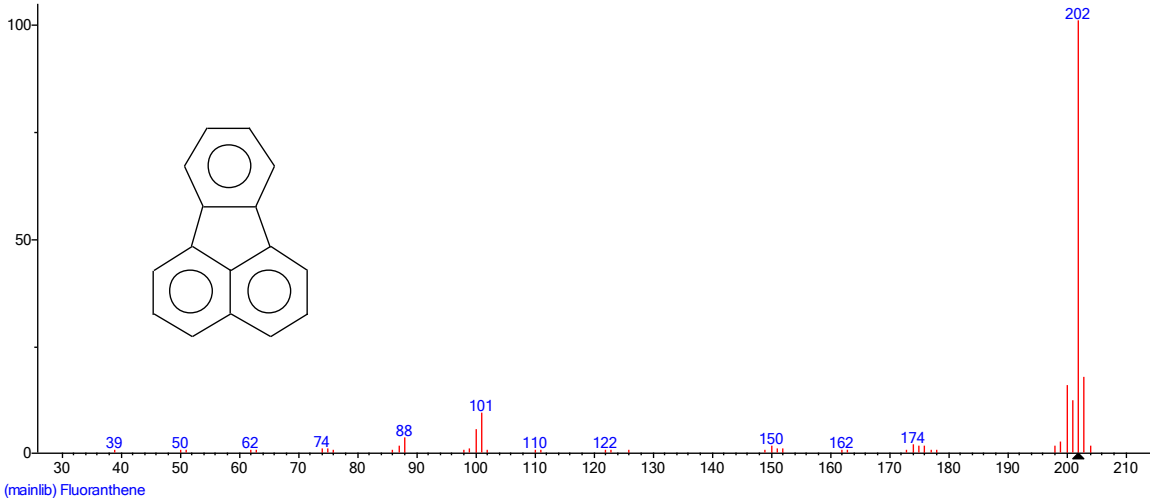

VIII : Pyrene

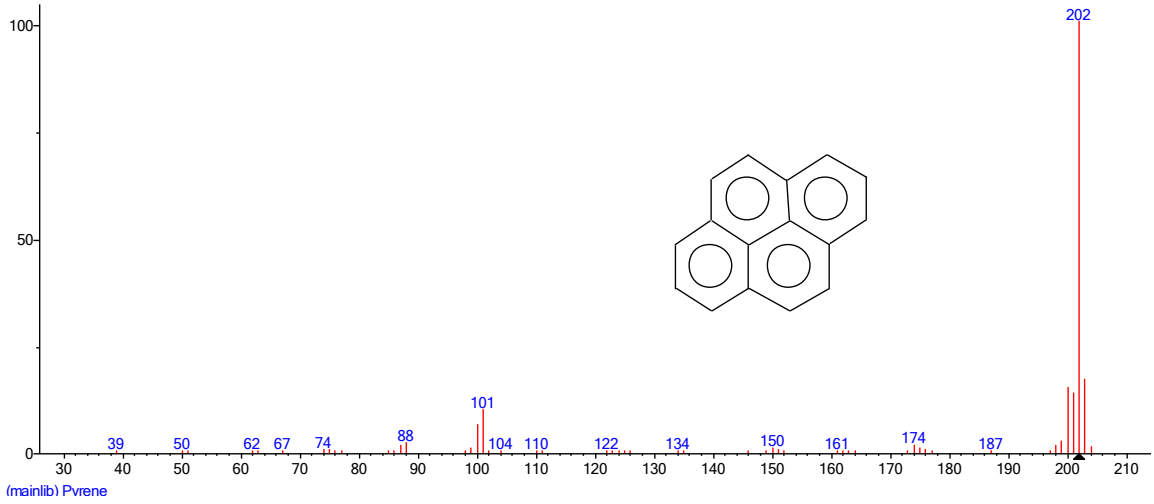

IX : Retene

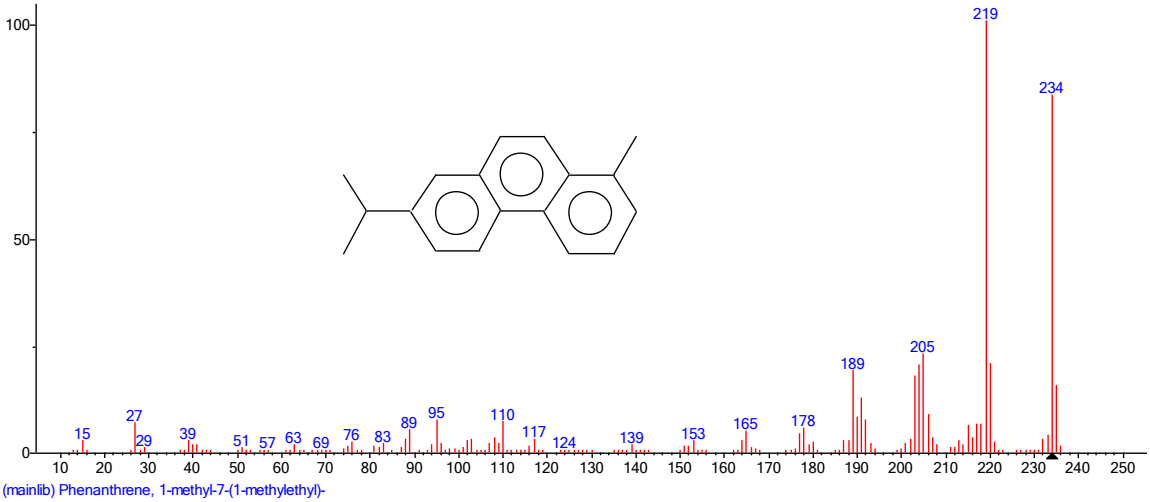

X : Benz[a]anthracene

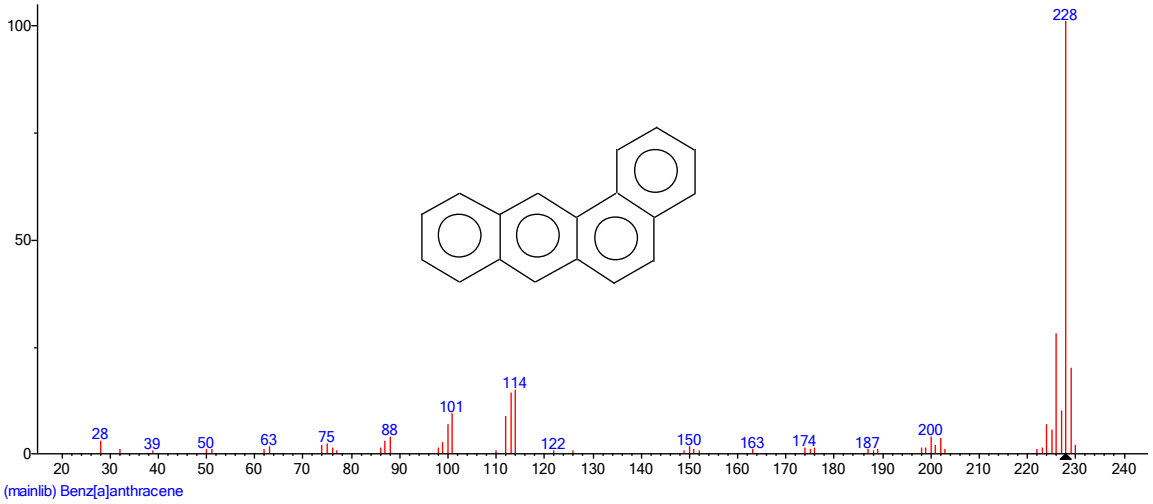

XI : Chrysene

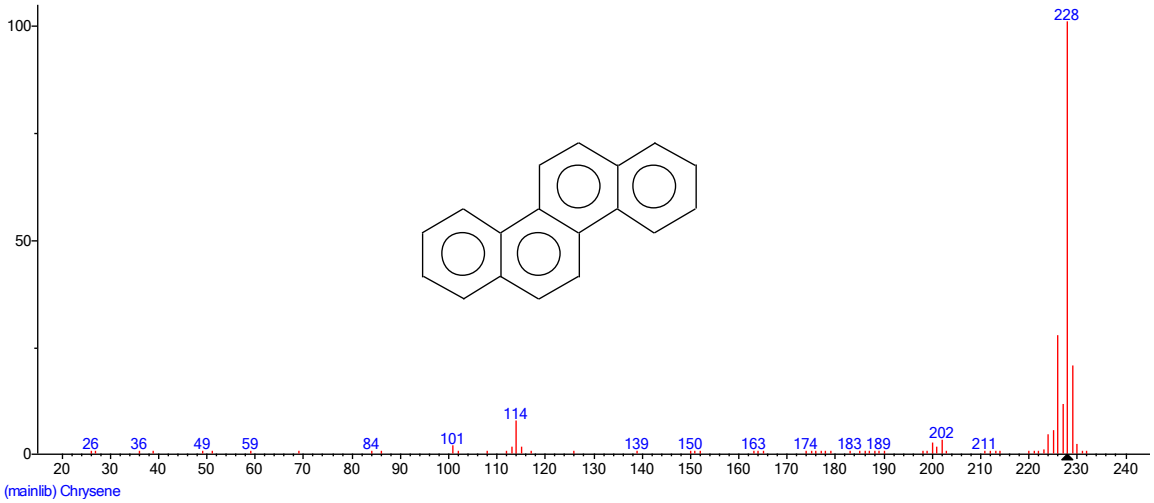

XII : Benzo[b]fluoranthene

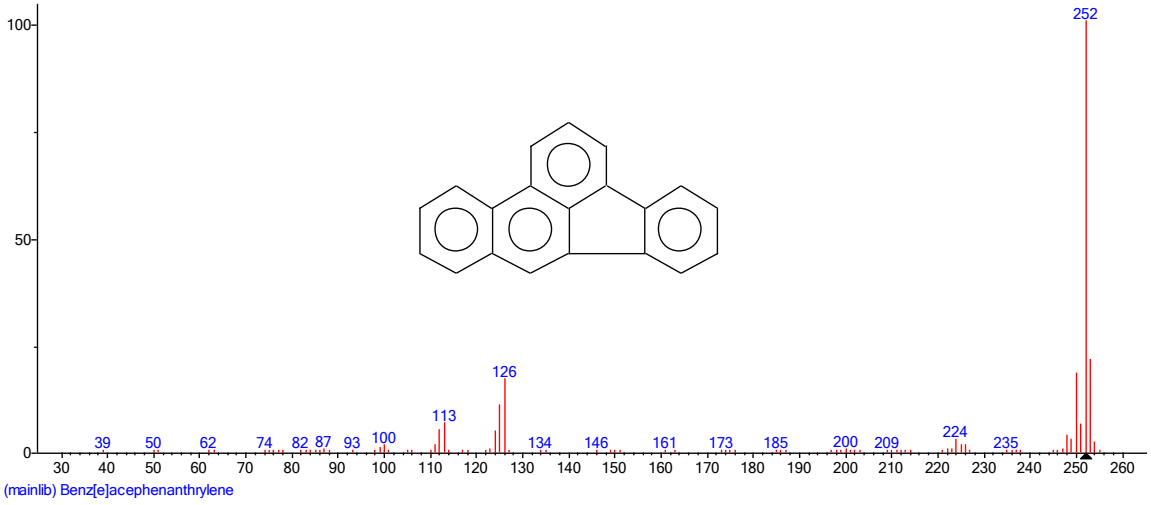

XIII : Benzo[k]fluoranthene

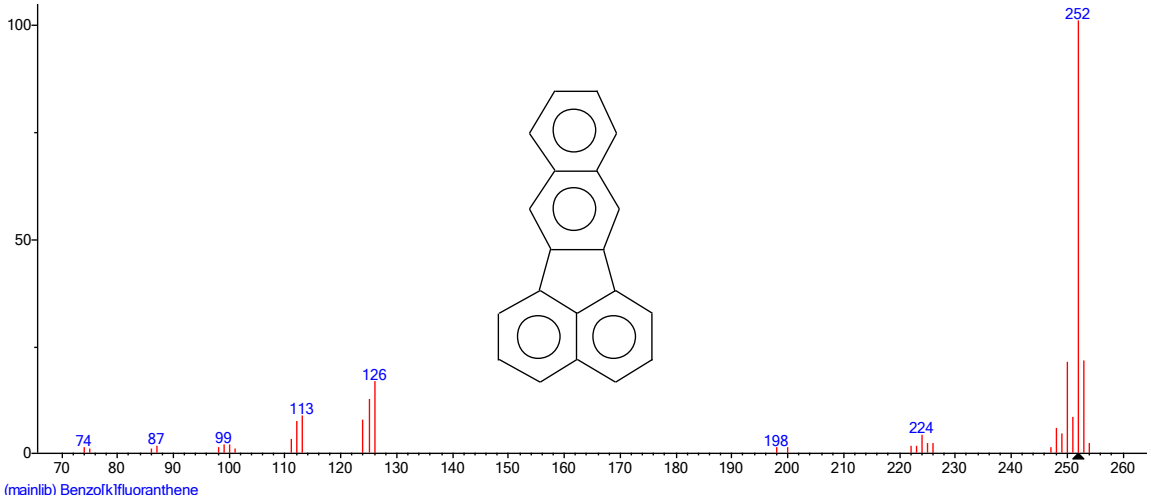

XIV : Benzo[a]pyrene

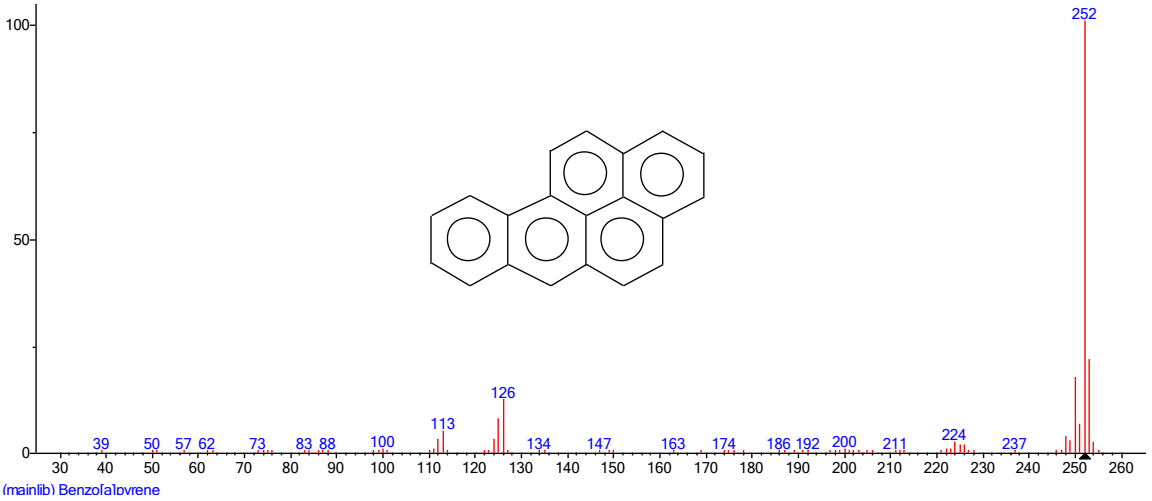

XV : Indeno[1,2,3,cd]pyrene

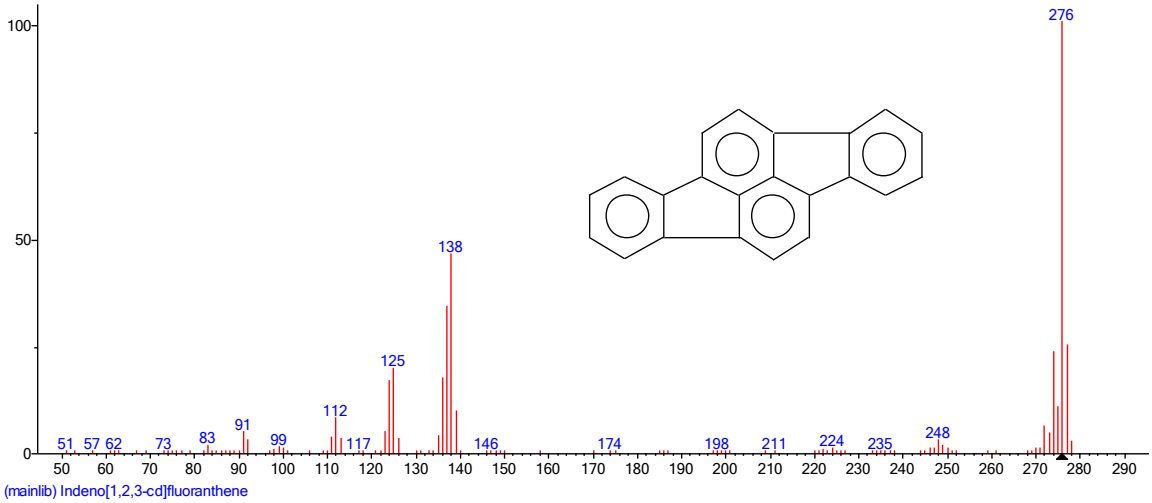

XVI : Dibenz[a,h]anthracene

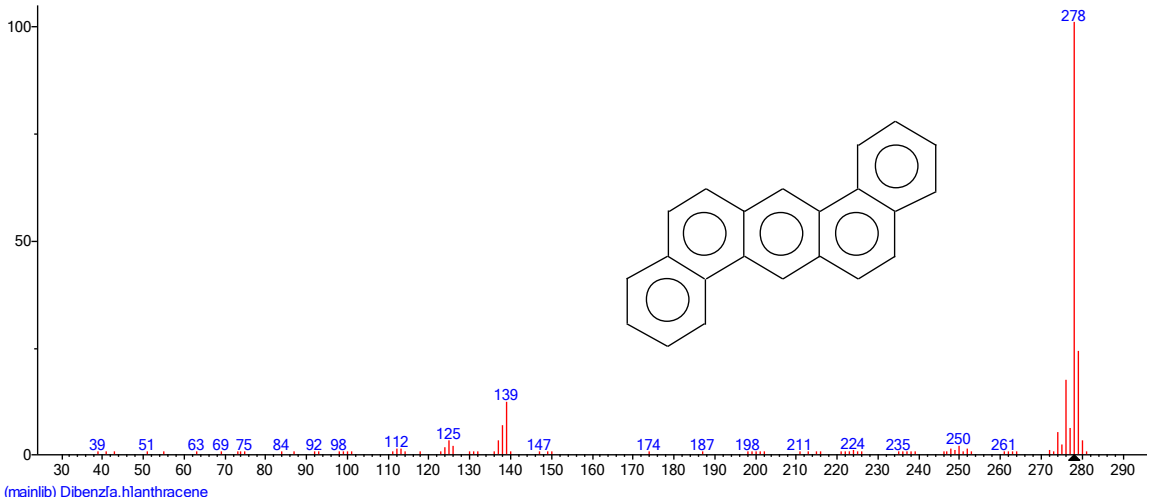

XVII : Benzo[g,h,i]perylene

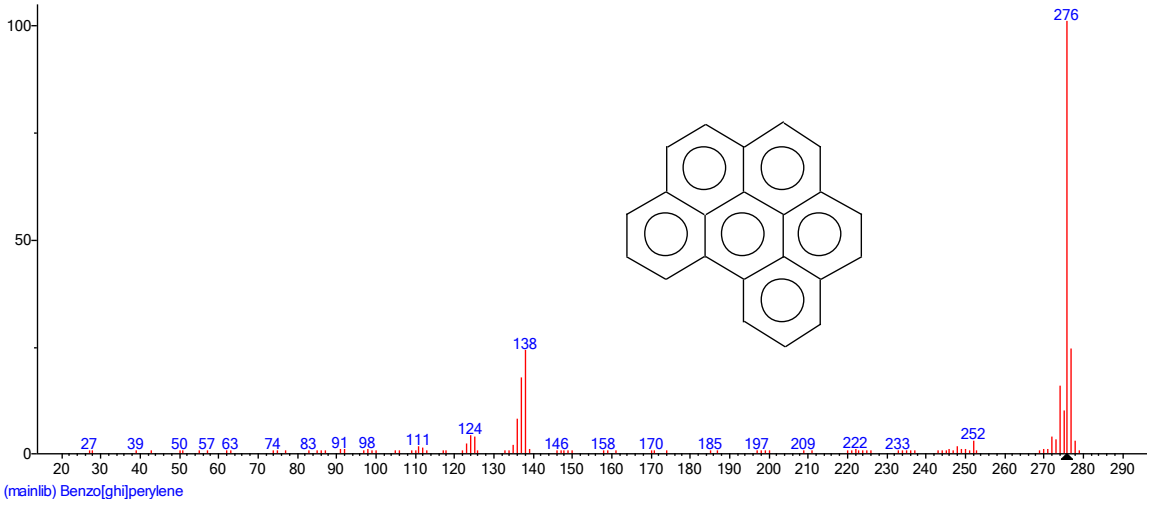

REFERENCES

Abrams, M.D., 1992. Fire and the Development of Oak Forests. BioScience 42, 346–353. doi:10.2307/1311781

Agel, L., Barlow, M., Qian, J.-H., Colby, F., Douglas, E., Eichler, T., 2014. Climatology of Daily Precipitation and Extreme Precipitation Events in Northeast US.

Ahad, J.M.E., Jautzy, J.J., Cumming, B.F., Das, B., Laird, K.R., Sanei, H., 2015. Sources of polycyclic aromatic hydrocarbons (PAHs) to northwestern Saskatchewan lakes east of the Athabasca oil sands. Organic Geochemistry 80, 35–45. doi:10.1016/j.orggeochem.2015.01.001

Aichner, B., Herzschuh, U., Wilkes, H., Vieth, A., Böhner, J., 2010. δD values of n-alkanes in Tibetan lake sediments and aquatic macrophytes–A surface sediment study and application to a 16ka record from Lake Koucha. Organic Geochemistry 41, 779–790.

Allison, T.D., Moeller, R.E., Davis, M.B., 1986. Pollen in Laminated Sediments Provides Evidence For a Mid-Holocene Forest Pathogen Outbreak. Ecology 67, 1101–1105. doi:10.2307/1939835

Anderson, R.S., Jacobson, G.L., Davis, R.B., Stuckenrath, R., 1992. Gould Pond, Maine: late-glacial transitions from marine to upland environments. Boreas 21, 359–371. doi:10.1111/j.1502-3885.1992.tb00040.x

Anderson, R.Y., Dean, W.E., 1988. Lacustrine varve formation through time. Palaeogeography, Palaeoclimatology, Palaeoecology 62, 215–235. doi:10.1016/0031-0182(88)90055-7

Andersson, M., Klug, M., Eggen, O.A., Ottesen, R.T., 2014. Polycyclic aromatic hydrocarbons (PAHs) in sediments from lake Lille Lungegårdsvannet in Bergen, western Norway; appraising pollution sources from the urban history. Science of The Total Environment 470–471, 1160–1172. doi:10.1016/j.scitotenv.2013.10.086

Antevs, E., 1922. The Recession of the Last Ice Sheet in New England. American Geographical Society.

Barlow, M., 2011. Influence of hurricane-related activity on North American extreme precipitation: Hurricanes And North American Extremes. Geophysical Research Letters 38, n/a–n/a. doi:10.1029/2010GL046258

Barton, A.M., White, A.S., Cogbill, C.V., 2012. The Changing Nature of the Maine Woods. UPNE.

Bechtel, A., Smittenberg, R.H., Bernasconi, S.M., Schubert, C.J., 2010. Distribution of branched and isoprenoid tetraether lipids in an oligotrophic and a eutrophic Swiss lake: Insights into sources and GDGT-based proxies. Organic Geochemistry 41, 822–832. doi:10.1016/j.orggeochem.2010.04.022

Bennett, M.M., Glasser, N.F., 2011. Glacial Geology: Ice Sheets and Landforms. John Wiley & Sons.

Berghuijs, W.R., Woods, R.A., Hrachowitz, M., 2014. A precipitation shift from snow towards rain leads to a decrease in streamflow. Nature Climate Change 4, 583–586. doi:10.1038/nclimate2246

Besonen, M., 2006. A 1,000 Year High-Resolution Hurricane History For The Boston Area Based On The Varved Sedimentary Record From The Lower Mystic Lake (Medford/Arlington, Ma) (Ph.D Dissertation). University of Massachusetts - Amherst.

Besonen, M.R., Bradley, R.S., Mudelsee, M., Abbott, M.B., Francus, P., 2008. A 1,000-year, annually-resolved record of hurricane activity from Boston, Massachusetts. Geophysical Research Letters 35. doi:10.1029/2008GL033950

Bianchi, T.S., Canuel, E.A., 2011. Chemical Biomarkers in Aquatic Ecosystems. Princeton University Press.

Birkholz, A., Smittenberg, R.H., Hajdas, I., Wacker, L., Bernasconi, S.M., 2013. Isolation and compound specific radiocarbon dating of terrigenous branched glycerol dialkyl glycerol tetraethers (brGDGTs). Organic Geochemistry 60, 9–19. doi:10.1016/j.orggeochem.2013.04.008

Bjorseth, A., Ramdahl, T., 1985. Polycyclic aromatic hydrocarbons.

Blaga, C.I., Reichart, G.-J., Heiri, O., Sinninghe Damsté, J.S., 2009. Tetraether membrane lipid distributions in water-column particulate matter and sediments: a study of 47 European lakes along a north–south transect. Journal of Paleolimnology 41, 523–540. doi:10.1007/s10933-008-9242-2

Boldt, K.V., Lane, P., Woodruff, J.D., Donnelly, J.P., 2010. Calibrating a sedimentary record of overwash from Southeastern New England using modeled historic hurricane surges. Marine Geology 275, 127–139. doi:10.1016/j.margeo.2010.05.002

Boose, E.R., Chamberlin, K.E., Foster, D.R., 2001. Landscape and regional impacts of hurricanes in New England. Ecological Monographs 71, 27–48.

Borns Jr., H.W., Doner, L.A., Dorion, C.C., Jacobson Jr., G.L., Kaplan, M.R., Kreutz, K.J., Lowell, T.V., Thompson, W.B., Weddle, T.K., 2004. The deglaciation of Maine, U.S.A., in: Gibbard, J.E. and P.L. (Ed.), Developments in Quaternary Sciences, Quaternary Glaciations-Extent and Chronology Part II: North America. Elsevier, pp. 89–109.

Boyle, J.F., 2002. Inorganic Geochemical Methods in Palaeolimnology, in: Last, W.M., Smol, J.P. (Eds.), Tracking Environmental Change Using Lake Sediments, Developments in Paleoenvironmental Research. Springer Netherlands, pp. 83–141.

Bradbury, J.P., Dean, W.E., 1993. Elk Lake, Minnesota: Evidence for Rapid Climate Change in the North-Central United States. Geological Society of America.

Bradbury, P., Cumming, B., Laird, K., 2002. A 1500-year record of climatic and environmental change in ElkLake, Minnesota III: measures of past primary productivity. Journal of Paleolimnology 27, 321–340.

Bradley, R.S. (Ed.), 2014. Paleoclimatology Reconstructing Climate of the Quaternary, in: Paleoclimatology (Third Edition). Academic Press, San Diego.

Bray, P.S., Brocks, J.J., George, S.C., 2014. 14C analysis of aliphatic hydrocarbon fractions from the hypersaline Lake Tyrrell, southeast Australia. Organic Geochemistry 73, 29–34. doi:10.1016/j.orggeochem.2014.05.005

Broccoli, A.J., Manabe, S., 1990. Can Existing Climate Models Be Used To Study Anthropogenic Changes In Tropical Cyclone Climate? Geophysical Research Letters 17, 1917–1920.

Brugam, R., 1978. Pollen indicators of land-use change in southern Connecticut. Quaternary Research 9, 349–362.

Brugam, R.B., 1978. Human Disturbance and the Historical Development of Linsley Pond. Ecology 59, 19. doi:10.2307/1936629

Bush, R.T., McInerney, F.A., 2013. Leaf wax n-alkane distributions in and across modern plants: Implications for paleoecology and chemotaxonomy. Geochimica et Cosmochimica Acta 117, 161–179. doi:10.1016/j.gca.2013.04.016

Butler, J., 2014. Wildfire loose: the week Maine burned. Down East Books.

Castañeda, I.S., Schefuß, E., Pätzold, J., Sinninghe Damsté, J.S., Weldeab, S., Schouten, S., 2010. Millennial-scale sea surface temperature changes in the eastern Mediterranean (Nile River Delta region) over the last 27,000 years. Paleoceanography 25. doi:10.1029/2009PA001740

Castañeda, I.S., Schouten, S., 2011. A review of molecular organic proxies for examining modern and ancient lacustrine environments. Quaternary Science Reviews 30, 2851–2891. doi:10.1016/j.quascirev.2011.07.009

Chibnall, A.C., Piper, S.H., Pollard, A., Williams, E.F., Sahai, P.N., 1934. The constitution of the primary alcohols, fatty acids and paraffins present in plant and insect waxes. Biochem J 28, 2189–2208.

Chivas, A.R., De Deckker, P., Cali, J.A., Chapman, A., Kiss, E., Shelley, G., Michael, J., 1993. Coupled Stable-Isotope and Trace-Element Measurements of Lacustrine Carbonates as Paleoclimatic Indicators. Climate change in continental isotopic records 113–121.

Clark, J.S., Royall, P.D., 1996. Local and Regional Sediment Charcoal Evidence for Fire Regimes in Presettlement North-Eastern North America. The Journal of Ecology 84, 365. doi:10.2307/2261199

Clark, J.S., Royall, P.D., 1995. Transformation of a northern hardwood forest by aboriginal (Iroquois) fire: charcoal evidence from Crawford Lake, Ontario, Canada. The Holocene 5, 1–9. doi:10.1177/095968369500500101

Clark, J.S., Royall, P.D., 1994. Pre-Industrial Particulate Emissions and Carbon Sequestration from Biomass Burning in North America. Biogeochemistry 24, 35–51.

Clark, J.S., Royall, P.D., Chumbley, C., 1996. The Role of Fire During Climate Change in an Eastern Deciduous Forest at Devil's Bathtub, New York. Ecology 77, 2148. doi:10.2307/2265709

Cohen, J., Screen, J.A., Furtado, J.C., Barlow, M., Whittleston, D., Coumou, D., Francis, J., Dethloff, K., Entekhabi, D., Overland, J., Jones, J., 2014. Recent Arctic amplification and extreme mid-latitude weather. Nature Geoscience 7, 627–637. doi:10.1038/ngeo2234

Cortright, E.M., 1968. SP-168: Exploring Space with a Camera.

Cranwell, P.A., Eglinton, G., Robinson, N., 1987. Lipids of aquatic organisms as potential contributors to lacustrine sediments—II. Organic Geochemistry 11, 513–527. doi:10.1016/0146-6380(87)90007-6

Croudace, I., Rothwell, G., 2010. Micro-XRF sediment core scanners: Important new tools for the environmental and earth sciences. SpectroscopyEurope 22, 6.

Damsté, J.S.S., Ossebaar, J., Abbas, B., Schouten, S., Verschuren, D., 2009. Fluxes and distribution of tetraether lipids in an equatorial African lake: Constraints on the application of the TEX86 palaeothermometer and BIT index in lacustrine settings. Geochimica et Cosmochimica Acta 73, 4232–4249. doi:10.1016/j.gca.2009.04.022

Darling, N., 1842. Notice of a hurricane that passed over New England in September, 1815. The American Journal of Science and Arts 42, 243–250.

Davis, M.B., 1969. Climatic Changes in Southern Connecticut Recorded by Pollen Deposition at Rogers Lake. Ecology 50, 409–422. doi:10.2307/1933891

Davis, M.B., Ford, M.S. (Jesse), 1982. Sediment focusing in Mirror Lake, New Hampshire1. Limnol. Oceanogr. 27, 137–150. doi:10.4319/lo.1982.27.1.0137

Davis, R.B., 1984. 137Cs and 210Pb dating of sediments from soft-water lakes in New England (U.S.A.) and Scandinavia, a failure of 137Cs dating. Chemical Geology 44, 151–185.

Davis, R.B., Jacobson Jr., G.L., 1985. Late glacial and early Holocene Landscapes in northern New England and adjacent areas of Canada. Quaternary Research 23, 341–368. doi:10.1016/0033-5894(85)90040-7

Dean, W., 2002. A 1500-year record of climatic and environmental change in ElkLake, Clearwater County, Minnesota II: geochemistry, mineralogy, and stableisotopes. Journal of Paleolimnology 27, 301–319.

Dean, W., Anderson, R., Bradbury, J.P., Anderson, D., 2002. A 1500-year record of climatic and environmental change in ElkLake, Minnesota I: Varve thickness and gray-scale density. Journal of Paleolimnology 27, 287–299.

Dean, W.E., 1997. Rates, timing, and cyclicity of Holocene eolian activity in north-central United States: Evidence from varved lake sediments. Geology 25, 331. doi:10.1130/0091-7613(1997)025<0331:RTACOH>2.3.CO;2

Denis, E.H., Toney, J.L., Tarozo, R., Scott Anderson, R., Roach, L.D., Huang, Y., 2012. Polycyclic aromatic hydrocarbons (PAHs) in lake sediments record historic fire events: Validation using HPLC-fluorescence detection. Organic Geochemistry 45, 7–17. doi:10.1016/j.orggeochem.2012.01.005

Dillon, J.T., Huang, Y., 2015. TEXPRESS v1.0: A MATLAB toolbox for efficient processing of GDGT LC–MS data. Organic Geochemistry 79, 44–48. doi:10.1016/j.orggeochem.2014.11.009

Doner, L., 1990. Communication of Basin Pond Data between Lisa Doner and John King, University of Rhode Island.

Donnelly, J.P., Butler, J., Roll, S., Wengren, M., Webb, T., 2004. A backbarrier overwash record of intense storms from Brigantine, New Jersey. Marine Geology 210, 107–121. doi:10.1016/j.margeo.2004.05.005

Donnelly, J.P., Roll, S., Wengren, M., Butler, J., Lederer, R., Webb, T., 2001a. Sedimentary evidence of intense hurricane strikes from New Jersey. Geology 29, 615. doi:10.1130/0091-7613(2001)029<0615:SEOIHS>2.0.CO;2

Donnelly, J.P., Smith Bryant, S., Butler, J., Dowling, J., Fan, L., Hausmann, N., Newby, P., Shuman, B., Stern, J., Westover, K., Webb III, T., 2001b. 700 yr sedimentary record of intense hurricane landfalls in southern New England. Geological Society of America Bulletin 113, 714–727. doi:10.1130/0016-7606(2001)113<0714:YSROIH>2.0.CO;2

Donnelly, J.P., Woodruff, J.D., 2007. Intense hurricane activity over the past 5,000 years controlled by El Niño and the West African monsoon. Nature 447, 465–468. doi:10.1038/nature05834

Eglinton, G., Hamilton, R.J., 1967. Leaf Epicuticular Waxes. Science 156, 1322–1335. doi:10.1126/science.156.3780.1322

Eglinton, G., Logan, G.A., Ambler, R.P., Boon, J.J., Perizonius, W.R.K., 1991. Molecular Preservation [and Discussion]. Philosophical Transactions of the Royal Society of London B: Biological Sciences 333, 315–328. doi:10.1098/rstb.1991.0081

Ellis, K.G., Mullins, H.T., Patterson, W.P., 2004. Deglacial to middle Holocene (16,600 to 6000 calendar years BP) climate change in the northeastern United States inferred from multi-proxy stable isotope data, Seneca Lake, New York. J Paleolimnol 31, 343–361. doi:10.1023/B:JOPL.0000021853.03476.95

Elsner, J.B., Jagger, T.H., Liu, K., 2008. Comparison of Hurricane Return Levels Using Historical and Geological Records. Journal of Applied Meteorology and Climatology 47, 368–374. doi:10.1175/2007JAMC1692.1

Ely, L.L., 1997. Response of extreme floods in the southwestern United States to climatic variations in the late Holocene. Geomorphology, Geomorphic responses to short-term climatic change 19, 175–201. doi:10.1016/S0169-555X(97)00014-7

Emanuel, K., 2005. Increasing destructiveness of tropical cyclones over the past 30 years. Nature 436, 686–688. doi:10.1038/nature03906

Emanuel, K.A., 1997. Climate variations and hurricane activity: Some theoretical issues, in: Hurricanes. Springer, pp. 55–65.

Emanuel, K.A., 1987. The dependence of hurricane intensity on climate. Nature 326, 483–485.

Fahey, T.J., Reiners, W.A., 1981. Fire in the Forests of Maine and New Hampshire. Bulletin of the Torrey Botanical Club 108, 362. doi:10.2307/2484716

Faison, E.K., Foster, D.R., Oswald, W.W., Hansen, B.C.S., Doughty, E., 2006. Early holocene openlands in southern new england. Ecology 87, 2537–2547. doi:10.1890/0012-9658(2006)87[2537:EHOISN]2.0.CO;2

Faure, G., Mensing, T.M., 2005. Isotopes: principles and applications. John Wiley & Sons Inc.

Fensterer, C., Scholz, D., Hoffmann, D., Spotl, C., Pajon, J.M., Mangini, A., 2012. Cuban stalagmite suggests relationship between Caribbean precipitation and the Atlantic Multidecadal Oscillation during the past 1.3 ka. The Holocene 22, 1405–1412. doi:10.1177/0959683612449759

Fernandez-Partagas, J., Diaz, H., 1996. Atlantic Hurricanes in the Second Half of the Nineteenth Century. Bulletin of the American Meteorological Society.

Fernández-Partagás, J.J., Diaz, H.F., Center, C.D., 1995. A Reconstruction of Historical Tropical Cyclone Frequency in the Atlantic from Documentary and Other Historical Sources, 1851 to 1880. Climate Diagnostics Center, Environmental Research Laboratories, NOAA.

Fernholz, E., MacPhillamy, H.B., 1941. Isolation of a New Phytosterol: Campesterol. J. Am. Chem. Soc. 63, 1155–1156. doi:10.1021/ja01849a079

Ficken, K.J., Li, B., Swain, D.L., Eglinton, G., 2000. An n-alkane proxy for the sedimentary input of submerged/floating freshwater aquatic macrophytes. Organic geochemistry 31, 745–749.

Fobes, C.B., 1948. Historic Forest Fires in Maine. Economic Geography 24, 269. doi:10.2307/141307

Foster, D.R., Hall, B., Barry, S., Clayden, S., Parshall, T., 2002. Cultural, environmental and historical controls of vegetation patterns and the modern conservation setting on the island of Martha's Vineyard, USA. Journal of Biogeography 29, 1381–1400. doi:10.1046/j.1365-2699.2002.00761.x

Foulds, S.A., Griffiths, H.M., Macklin, M.G., Brewer, P.A., 2014. Geomorphological records of extreme floods and their relationship to decadal-scale climate change. Geomorphology 216, 193–207. doi:10.1016/j.geomorph.2014.04.003

Frappier, A.B., Sahagian, D., Carpenter, S.J., González, L.A., Frappier, B.R., 2007. Stalagmite stable isotope record of recent tropical cyclone events. Geology 35, 111. doi:10.1130/G23145A.1

Fraver, S., White, A.S., Seymour, R.S., 2009. Natural disturbance in an old-growth landscape of northern Maine, USA. Journal of ecology 97, 289–298.

Freeman, K.H., Hayes, J.M., Trendel, J.-M., Albrecht, P., 1990. Evidence from carbon isotope measurements for diverse origins of sedimentary hydrocarbons. Nature 343, 254–256.

Fritz, S.C., Engstrom, D.R., Haskell, B.J., 1994. "Little Ice Age"aridity in the North American Great Plains: a high-resolution reconstruction of salinity fluctuations from Devils Lake, North Dakota, USA. The Holocene 4, 69–73.

Frost, D.S., 2005. Paleoclimate Reconstruction using Physical Sedimentology and Organic Matter Biogeochemistry if Varved Sediments, Basin Pond, Fayette, ME (Undergraduate Thesis). Bates College.

Fuller, J.L., Foster, D.R., McLachlan, J.S., Drake, N., 1998. Impact of Human Activity on Regional Forest Composition and Dynamics in Central New England. Ecosystems 1, 76–95. doi:10.1007/s100219900007

Gajewski, K., 1988. Late holocene climate changes in eastern North America estimated from pollen data. Quaternary Research 29, 255–262.

Gajewski, K., Swain, A.M., Peterson, G.M., 1987. Late Holocene Pollen Stratigraphy in Four Northeastern United States Lakes. Géographie physique et Quaternaire 41, 377. doi:10.7202/032693ar

Gierga, M., Schneider, M.P.W., Wiedemeier, D.B., Lang, S.Q., Smittenberg, R.H., Hajdas, I., Bernasconi, S.M., Schmidt, M.W.I., 2014. Purification of fire derived markers for μg scale isotope analysis (δ13C, Δ14C) using high performance liquid chromatography (HPLC). Organic Geochemistry 70, 1–9. doi:10.1016/j.orggeochem.2014.02.008

Giger, W., Schaffner, C., Wakeham, S.G., 1980. Aliphatic and olefinic hydrocarbons in recent sediments of Greifensee, Switzerland. Geochimica et Cosmochimica Acta 44, 119–129. doi:10.1016/0016-7037(80)90182-9

Gill, A.M., Bradstock, R.A., 1995. Extinction of biota by fires. Conserving biodiversity: threats and solutions 309–322.

Glaser, B., Zech, W., 2005. Reconstruction of climate and landscape changes in a high mountain lake catchment in the Gorkha Himal, Nepal during the Late Glacial and Holocene as deduced from radiocarbon and compound-specific stable isotope analysis of terrestrial, aquatic and microbial biomarkers. Organic Geochemistry 36, 1086–1098. doi:10.1016/j.orggeochem.2005.01.015

Glur, L., Wirth, S.B., Büntgen, U., Gilli, A., Haug, G.H., Schär, C., Beer, J., Anselmetti, F.S., 2013. Frequent floods in the European Alps coincide with cooler periods of the past 2500 years. Sci. Rep. 3. doi:10.1038/srep02770

Goldenberg, S., Landsea, C., Mestas-Nuñez, A., Gray, W., 2001. The Recent Increase in Atlantic Hurricane Activity: Causes and Implications. Science 293, 474–479. doi:10.1126/science.1060040

Gonzales, L.M., Grimm, E.C., 2009. Synchronization of late-glacial vegetation changes at Crystal Lake, Illinois, USA with the North Atlantic Event Stratigraphy. Quaternary Research 72, 234–245.

Graham, N.E., Hughes, M.K., Ammann, C.M., Cobb, K.M., Hoerling, M.P., Kennett, D.J., Kennett, J.P., Rein, B., Stott, L., Wigand, P.E., Xu, T., 2007. Tropical Pacific – mid-latitude teleconnections in medieval times. Climatic Change 83, 241–285. doi:10.1007/s10584-007-9239-2

Gray, W.M., 1990. Strong association between West African rainfall and US landfall of intense hurricanes. Science 249, 1251–1256.

Grimm, E.C., 2000. Global pollen database. IGBP PAGES/World Data Centre for Paleoclimatology, NOAA/NGDC Paleoclimatology Program, Boulder, CO, USA.

Grinsted, A., Moore, J.C., Jevrejeva, S., 2012. Homogeneous record of Atlantic hurricane surge threat since 1923. Proceedings of the National Academy of Sciences 109, 19601–19605. doi:10.1073/pnas.1209542109

Haase-Schramm, A., 2003. Sr/Ca ratios and oxygen isotopes from sclerosponges: Temperature history of the Caribbean mixed layer and thermocline during the Little Ice Age. Paleoceanography 18. doi:10.1029/2002PA000830

Hagen, A., 2010. A Reanalysis of the 1944-1953 Atlantic Hurricane Seasons- The First Decade of Aircraft Reconnaisance (Masters of Science). University of Miami, Coral Gables, Florida.

Hawbaker, T.J., Radeloff, V.C., Stewart, S.I., Hammer, R.B., Keuler, N.S., Clayton, M.K., 2013. Human and biophysical influences on fire occurrence in the United States. Ecological applications 23, 565–582.

Hetzinger, S., Pfeiffer, M., Dullo, W.-C., Keenlyside, N., Latif, M., Zinke, J., 2008. Caribbean coral tracks Atlantic Multidecadal Oscillation and past hurricane activity. Geology 36, 11. doi:10.1130/G24321A.1

Hetzinger, S., Pfeiffer, M., Dullo, W.-C., Ruprecht, E., Garbe-Schönberg, D., 2006. Sr/Ca and δ18O in a fast-growing Diploria strigosa coral: Evaluation of a new climate archive for the tropical Atlantic. Geochemistry, Geophysics, Geosystems 7.

Hites, R., 1980. Polycyclic aromatic hydrocarbons in an anoxic sediment core from the Pettaquamscutt River (Rhode Island, U.S.A.). Geochimica et cosmochimica acta 44, 873–878.

Hopmans, E.C., Weijers, J.W., Schefu\s s, E., Herfort, L., Damsté, J.S.S., Schouten, S., 2004. A novel proxy for terrestrial organic matter in sediments based on branched and isoprenoid tetraether lipids. Earth and Planetary Science Letters 224, 107–116.

Horton, R., Yohe, G., Easterling, W., Kates, R., Ruth, M., Sussman, E., Whelchel, A., Wolfe, D., Lipschultz, F., 2014. Ch. 16: Northeast. Climate Change Impacts in the United States: The Third National Climate Assessment. doi:10.7930/J0SF2T3P

Hou, W., Dong, H., Li, G., Yang, J., Coolen, M.J.L., Liu, X., Wang, S., Jiang, H., Wu, X., Xiao, H., Lian, B., Wan, Y., 2014. Identification of Photosynthetic Plankton Communities Using Sedimentary Ancient DNA and Their Response to late-Holocene Climate Change on the Tibetan Plateau. Scientific Reports 4, 6648. doi:10.1038/srep06648

Huang, Y., Shuman, B., Wang, Y., Webb, T., 2004. Hydrogen isotope ratios of individual lipids in lake sediments as novel tracers of climatic and environmental change: a surface sediment test. Journal of Paleolimnology 31, 363–375.

Huang, Y., Street-Perrott, F.A., Perrott, R.A., Metzger, P., Eglinton, G., 1999. Glacial–interglacial environmental changes inferred from molecular and compound-specific δ13C analyses of sediments from Sacred Lake, Mt. Kenya. Geochimica et Cosmochimica Acta 63, 1383–1404. doi:10.1016/S0016-7037(99)00074-5

Hubeny, J.B., 2006. Late Holocene climate variability as preserved in high-resolution estuarine and lacustrine sediment archives. University of Rhode Island.

Hubeny, J.B., King, J.W., Cantwell, M., 2009. Anthropogenic influences on estuarine sedimentation and ecology: examples from the varved sediments of the Pettaquamscutt River Estuary, Rhode Island. Journal of Paleolimnology 41, 297–314. doi:10.1007/s10933-008-9226-2

Hunter, M., 1993. Natural Fire Regimes as Spatial Models for Managing Boreal Forests. Biological Conservation 65, 115–120.

IPCC, 2012. Managing the Risks of Extreme Events and Disasters to Advance Climate Change Adaptation. A Special Report of Working Groups 1 and 2 of the Intergovernmental Panel on Climate Change., in: Field, C.B., Barros, V., Stocker, T.F., Qin, D., Dokken, D.J., Ebi, K.L., Mastrandrea, M.D., Mach, K.J., Plattner, G.-K., Allen, S.K., Tignor, M., Midgley, P.. (Eds.), IPCC. Cambridge University Press, Cambridge, UK and New York, NY, p. 582.

Ito, E., 2002. Application Of Stable Isotope Techniquesto Inorganic And Biogenic Carbonates, in: Last, W.M., Smol, J.P. (Eds.), Tracking Environmental Change Using Lake Sediments, Developments in Paleoenvironmental Research. Springer Netherlands, pp. 351–371.

Jarvinen, B.R., Neumann, C.J., Davis, M.A.S., 1984. A tropical cyclone data tape for the North Atlantic Basin, 1886–1983: Contents, limitations. and uses. Tech. Memo. NWS NHC 22, National Oceanic and Atmospheric Administration.

Jautzy, J., Ahad, J.M.E., Gobeil, C., Savard, M.M., 2013. Century-Long Source Apportionment of PAHs in Athabasca Oil Sands Region Lakes Using Diagnostic Ratios and Compound-Specific Carbon Isotope Signatures. Environ. Sci. Technol. 47, 6155–6163. doi:10.1021/es400642e

Kennard, O., Riva di Sanseverino, L., Vorbrűggen, H., Djerassi, C., 1965. The complete structure of the triterpene arborinol. Tetrahedron Letters 6, 3433–3438. doi:10.1016/S0040-4039(01)89324-2

Kim, J.-H., van der Meer, J., Schouten, S., Helmke, P., Willmott, V., Sangiorgi, F., Koç, N., Hopmans, E.C., Damsté, J.S.S., 2010. New indices and calibrations derived from the distribution of crenarchaeal isoprenoid tetraether lipids: Implications for past sea surface temperature reconstructions. Geochimica et Cosmochimica Acta 74, 4639–4654. doi:10.1016/j.gca.2010.05.027

Kirby, M.E., Mullins, H.T., Patterson, W.P., Burnett, A.W., 2002. Late glacial–Holocene atmospheric circulation and precipitation in the northeast United States inferred from modern calibrated stable oxygen and carbon isotopes. Geological Society of America Bulletin 114, 1326–1340. doi:10.1130/0016-7606(2002)114<1326:LGHACA>2.0.CO;2

Kirby, M.E., Mullins, H.T., Patterson, W.P., Burnett, A.W., 2001. Lacustrine isotopic evidence for multidecadal natural climate variability related to the circumpolar vortex over the northeast United States during the past millennium. Geology 29, 807–810. doi:10.1130/0091-7613(2001)029<0807:LIEFMN>2.0.CO;2

Kirby, M., Patterson, W., Mullins, H., Burnett, A., 2002. Post-Younger Dryas climate interval linked to circumpolar vortex variability: isotopic evidence from Fayetteville Green Lake, New York. Climate Dynamics 19, 321–330. doi:10.1007/s00382-002-0227-y

Kirchgeorg, T., Schüpbach, S., Kehrwald, N., McWethy, D.B., Barbante, C., 2014. Method for the determination of specific molecular markers of biomass burning in lake sediments. Organic Geochemistry 71, 1–6. doi:10.1016/j.orggeochem.2014.02.014

Knox, J.C., 2000. Sensitivity of modern and Holocene floods to climate change. Quaternary Science Reviews 19, 439–457. doi:10.1016/S0277-3791(99)00074-8

Knox, J.C., 1993. Large increases in flood magnitude in response to modest changes in climate. Nature 361, 430–432. doi:10.1038/361430a0

Knutson, T.R., 1998. Simulated Increase of Hurricane Intensities in a CO2-Warmed Climate. Science 279, 1018–1021. doi:10.1126/science.279.5353.1018

Kunkel, K.E., 2013. Regional climate trends and scenarios for the US National Climate Assessment. US Department of Commerce, National Oceanic and Atmospheric Administration, National Environmental Satellite, Data, and Information Service.

Kuo, L.-J., Louchouarn, P., Herbert, B.E., Brandenberger, J.M., Wade, T.L., Crecelius, E., 2011. Combustion-derived substances in deep basins of Puget Sound: historical inputs from fossil fuel and biomass combustion. Environmental Pollution 159, 983–990.

Kurek, J., Cwynar, L.C., Ager, T.A., Abbott, M.B., Edwards, M.E., 2009a. Late Quaternary paleoclimate of western Alaska inferred from fossil chironomids and its relation to vegetation histories. Quaternary Science Reviews 28, 799–811. doi:10.1016/j.quascirev.2008.12.001

Kurek, J., Cwynar, L.C., Vermaire, J.C., 2009b. A late Quaternary paleotemperature record from Hanging Lake, northern Yukon Territory, eastern Beringia. Quaternary Research 72, 246–257. doi:10.1016/j.yqres.2009.04.007

Kylander, M., Ampel, L., Wohlfarth, B., Veres, D., 2011. High-resolution X-ray fluorescence core scanning analysis of Les Echets (France) sedimentary sequence: new insights from chemical proxies. Journal of Quaternary Science 26, 109–117. doi:10.1002/jqs.1438

Lamoureux, S.F., Bollmann, J., 2005. Image Acquisition, in: Francus, P. (Ed.), Image Analysis, Sediments and Paleoenvironments, Developments in Paleoenvironmental Research. Springer Netherlands, pp. 11–34.

Landsea, C., 2007. Counting Atlantic tropical cyclones back to 1900. Eos, Transactions American Geophysical Union 88, 197–202.

Landsea, C., Franklin, J., Beven, J., 2012. The revised Atlantic hurricane database (HURDAT2). National Hurricane Center.

Lane, P., Donnelly, J.P., Woodruff, J.D., Hawkes, A.D., 2011. A decadally-resolved paleohurricane record archived in the late Holocene sediments of a Florida sinkhole. Marine Geology 287, 14–30. doi:10.1016/j.margeo.2011.07.001

Last, W.M., Smol, J.P., Birks, H.J.B., 2001. Tracking Environmental Change Using Lake Sediments: Volume 2: Physical and Geochemical Methods. Springer Science & Business Media.

Leopold, E.B., 1956. Two Late-Glacial Deposits In Southern Connecticut. Proc Natl Acad Sci U S A 42, 863–867.

Lesieur, D., Gauthier, S., Bergeron, Y., 2002. Fire frequency and vegetation dynamics for the south-central boreal forest of Quebec, Canada. Canadian Journal of Forest Research 32, 1996–2009. doi:10.1139/x02-113

Lichtfouse, É., Derenne, S., Mariotti, A., Largeau, C., 1994. Possible algal origin of long chain odd n-alkanes in immature sediments as revealed by distributions and carbon isotope ratios. Organic Geochemistry 22, 1023–1027. doi:10.1016/0146-6380(94)90035-3

Liu, K., Fearn, M.L., 2000. Reconstruction of Prehistoric Landfall Frequencies of Catastrophic Hurricanes in Northwestern Florida from Lake Sediment Records. Quaternary Research 54, 238–245. doi:10.1006/qres.2000.2166

Liu, K., Lu, H., Shen, C., 2009. Some fundamental misconceptions about paleotempestology. Quaternary Research 71, 253–254. doi:10.1016/j.yqres.2008.11.001

Liu, K., Lu, H., Shen, C., 2008. A 1200-year proxy record of hurricanes and fires from the Gulf of Mexico coast: Testing the hypothesis of hurricane–fire interactions. Quaternary Research 69, 29–41. doi:10.1016/j.yqres.2007.10.011

Lorimer, C.G., 1977. The Presettlement Forest and Natural Disturbance Cycle of Northeastern Maine. Ecology 58, 139. doi:10.2307/1935115

Ludlum, D.M., 1963. Early American Hurricanes, 1492-1870. Amer Meteorological Society.

Ludlum, S.D., 1976. Laminated sediments in holomictic Berkshire lakes1. Limnol. Oceanogr. 21, 743–746. doi:10.4319/lo.1976.21.5.0743

Madsen, A.T., Duller, G.A.T., Donnelly, J.P., Roberts, H.M., Wintle, A.G., 2009. A chronology of hurricane landfalls at Little Sippewissett Marsh, Massachusetts, USA, using optical dating. Geomorphology 109, 36–45. doi:10.1016/j.geomorph.2008.08.023

Mann, M., Emanuel, K., 2006. Atlantic Hurricane Trends Linked to Climate Change. EOS 87, 233–244.

Maslin, P., 1996. Long Term Effect of Rotenone Treatment on the Fish Community of Big Chico Creek, California [WWW Document]. URL http://www.sgreen.us/pmaslin/rsrch/rotenone/Intro.html (accessed 5.20.15).

McAndrews, J.H., Boyko-Diakonow, M., 1989. Pollen analysis of varved sediment at Crawford Lake, Ontario: evidence of Indian and European farming. Quaternary Geology of Canada and Greenland, RJ Fulton, ed. Geological Survey of Canada, Ottawa, Ontario 528–530.

Medina-Elizalde, M.A., Polanco-Martinez, J., Lases-Hernandez, F., Bradley, R., Burns, S., 2014. Testing the "tropical storm hypothesis" of Yucatan Peninsula climate variability during the Maya Terminal Classic Period.

Meyers, P.A., 1997. Organic geochemical proxies of paleoceanographic, paleolimnologic, and paleoclimatic processes. Organic Geochemistry 27, 213–250. doi:10.1016/S0146-6380(97)00049-1

Miller, D.L., Mora, C.I., Grissino-Mayer, H.D., Mock, C.J., Uhle, M.E., Sharp, Z., 2006. Tree-ring isotope records of tropical cyclone activity. Proceedings of the National Academy of Sciences 103, 14294–14297.

Miller, S.A., Collettini, C., Chiaraluce, L., Cocco, M., Barchi, M., Kaus, B.J.P., 2004. Aftershocks driven by a high-pressure CO2 source at depth. Nature 427, 724–727. doi:10.1038/nature02251

Mügler, I., Sachse, D., Werner, M., Xu, B., Wu, G., Yao, T., Gleixner, G., 2008. Effect of lake evaporation on δD values of lacustrine n-alkanes: A comparison of Nam Co (Tibetan Plateau) and Holzmaar (Germany). Organic Geochemistry 39, 711–729. doi:10.1016/j.orggeochem.2008.02.008

Munoz, S.E., Gajewski, K., Peros, M.C., 2010. Synchronous environmental and cultural change in the prehistory of the northeastern United States. Proceedings of the National Academy of Sciences 107, 22008–22013.

Murnane, R.J., Liu, K., 2004. Hurricanes and typhoons: past, present, and future. Columbia University Press.

Musa Bandowe, B.A., Srinivasan, P., Seelge, M., Sirocko, F., Wilcke, W., 2014. A 2600-year record of past polycyclic aromatic hydrocarbons (PAHs) deposition at Holzmaar (Eifel, Germany). Palaeogeography, Palaeoclimatology, Palaeoecology 401, 111–121. doi:10.1016/j.palaeo.2014.02.021

National Oceanic and Atmospheric Administration (NOAA), 2014a. Historical Hurricane Tracks [WWW Document]. URL http://coast.noaa.gov/hurricanes (accessed 10.20.14).

National Oceanic and Atmospheric Administration (NOAA), 2014b. National Climatic Data Center [WWW Document]. URL www.ncdc.noaa.gov (accessed 10.17.14).

Ndiaye, M., 2012. A Semi Automated Method for Laminated Sediments Analysis. International Journal of Geosciences 03, 206–210. doi:10.4236/ijg.2012.31023

Nelson, J.A., Licht, K., Yansa, C., Filippelli, G., 2009. Climate-related cyclic deposition of carbonate and organic matter in Holocene lacustrine sediment, Lower Michigan, USA. J Paleolimnol 44, 1–13. doi:10.1007/s10933-009-9381-0

Nelson, R.E., Clark, C.K., Littlefield, E.F., Krumdieck, N.W., 2010. Palynology of Three Bog Cores Shows Complex European Impact on the Forests of Central Maine. Northeastern Naturalist 17, 63–76. doi:10.1656/045.017.0105

Neupane, R.P., Yao, J., White, J.D., 2014. Estimating the effects of climate change on the intensification of monsoonal-driven stream discharge in a Himalayan watershed. Hydrol. Process. 28, 6236–6250. doi:10.1002/hyp.10115

Newby, P.E., Shuman, B.N., Donnelly, J.P., Karnauskas, K.B., Marsicek, J., 2014. Centennial-to-millennial hydrologic trends and variability along the North Atlantic Coast, USA, during the Holocene. Geophysical Research Letters 41, 4300–4307. doi:10.1002/2014GL060183

Nichols, J.E., Huang, Y., 2012. Hydroclimate of the northeastern United States is highly sensitive to solar forcing: NORTHEAST US SENSITIVE TO SOLAR FORCING. Geophysical Research Letters 39, n/a–n/a. doi:10.1029/2011GL050720

Noren, A.J., Bierman, P.R., Steig, E.J., Lini, A., Southon, J., 2002. Millennial-scale storminess variability in the northeastern United States during the Holocene epoch. Nature 419, 821–824. doi:10.1038/nature01132

Nott, J., 2004. Palaeotempestology: the study of prehistoric tropical cyclones—a review and implications for hazard assessment. Environment International 30, 433–447. doi:10.1016/j.envint.2003.09.010

Nowaczyk, N.R., 2002. Logging of Magnetic Susceptibility, in: Last, W.M., Smol, J.P. (Eds.), Tracking Environmental Change Using Lake Sediments, Developments in Paleoenvironmental Research. Springer Netherlands, pp. 155–170.

O'Sullivan, P.E., 1983. Annually-laminated lake sediments and the study of Quaternary environmental changes — a review. Quaternary Science Reviews 1, 245–313. doi:10.1016/0277-3791(83)90008-2

Oswald, W., Faison, E.K., Foster, D.R., Doughty, E.D., Hall, B.R., Hansen, B.C.S., 2007. Post-glacial changes in spatial patterns of vegetation across southern New England. Journal of Biogeography 34, 900–913. doi:10.1111/j.1365-2699.2006.01650.x

Otvos, E.G., 2009. Discussion of "A 1200-year proxy record of hurricanes and fires from the Gulf of Mexico coast…" (Liu et al., 2008). Quaternary Research 71, 251–252. doi:10.1016/j.yqres.2008.11.002

Paasche, Ø., Støren, E.W., 2014. How Does Climate Impact Floods? Closing the Knowledge Gap. Eos, Transactions American Geophysical Union 95, 253–254.

Page, D.S., Boehm, P.D., Douglas, G.S., Bence, A.E., Burns, W.A., Mankiewicz, P.J., 1999. Pyrogenic polycyclic aromatic hydrocarbons in sediments record past human activity: a case study in Prince William Sound, Alaska. Marine Pollution Bulletin 38, 247–260.

Parris, A.S., Bierman, P.R., Noren, A.J., Prins, M.A., Lini, A., 2009. Holocene paleostorms identified by particle size signatures in lake sediments from the northeastern United States. J Paleolimnol 43, 29–49. doi:10.1007/s10933-009-9311-1

Parshall, T., Foster, D.R., 2002. Fire on the New England landscape: regional and temporal variation, cultural and environmental controls. Journal of Biogeography 29, 1305–1317. doi:10.1046/j.1365-2699.2002.00758.x

Parshall, T., Foster, D.R., Faison, E., MacDonald, D., Hansen, B.C.S., 2003. Long-term history of vegetation and fire in pitch pine–oak forests on cape cod, massachusetts. Ecology 84, 736–748. doi:10.1890/0012-9658(2003)084[0736:LTHOVA]2.0.CO;2

Pautler, B.G., Reichart, G.-J., Sanborn, P.T., Simpson, M.J., Weijers, J.W.H., 2014. Comparison of soil derived tetraether membrane lipid distributions and plant-wax δD compositions for reconstruction of Canadian Arctic temperatures. Palaeogeography, Palaeoclimatology, Palaeoecology 404, 78–88. doi:10.1016/j.palaeo.2014.03.038

Pederson, D.C., Peteet, D.M., Kurdyla, D., Guilderson, T., 2005. Medieval Warming, Little Ice Age, and European impact on the environment during the last millennium in the lower Hudson Valley, New York, USA. Quaternary Research 63, 238–249. doi:10.1016/j.yqres.2005.01.001

Pederson, N., Bell, A.R., Cook, E.R., Lall, U., Devineni, N., Seager, R., Eggleston, K., Vranes, K.P., 2012. Is an Epic Pluvial Masking the Water Insecurity of the Greater New York City Region?*,+. J. Climate 26, 1339–1354. doi:10.1175/JCLI-D-11-00723.1

Peltzer, E.T., Gagosian, R.B., 1989. Organic geochemistry of aerosols over the Pacific Ocean. Chemical oceanography 10, 281–338.

Perkins, J.S., 1985. Lake Watershed Responses to the Hemlock Decline (4800 years BP) at Basin Pond, Fayette, Maine (Masters of Science Thesis Proposal). University of Maine.

Peterse, F., van der Meer, J., Schouten, S., Weijers, J.W.H., Fierer, N., Jackson, R.B., Kim, J.-H., Sinninghe Damsté, J.S., 2012. Revised calibration of the MBT–CBT paleotemperature proxy based on branched tetraether membrane lipids in surface soils. Geochimica et Cosmochimica Acta 96, 215–229. doi:10.1016/j.gca.2012.08.011

Peters, K.E., Walters, C.C., Moldowan, J.M., 2004. The Biomarker Guide: Volume 1, Biomarkers and Isotopes in the Environment and Human History. Cambridge University Press.

Powers, L.A., 2005. Large temperature variability in the southern African tropics since the Last Glacial Maximum. Geophysical Research Letters 32. doi:10.1029/2004GL022014

Powers, L.A., Johnson, T.C., Werne, J.P., Castañeda, I.S., Hopmans, E.C., Sinninghe Damsté, J.S., Schouten, S., 2011. Organic geochemical records of environmental variability in Lake Malawi during the last 700 years, Part I: The TEX86 temperature record. Palaeogeography, Palaeoclimatology, Palaeoecology 303, 133–139. doi:10.1016/j.palaeo.2010.09.006

Ramdahl, T., 1983. Retene—a molecular marker of wood combustion in ambient air. Nature 306, 580–582. doi:10.1038/306580a0

Reams, G.A., Van Deusen, P.C., 1996. Detection of a hurricane signal in bald cypress tree-ring chronologies. Tree Rings, Environment, and Humanity 265–271.

Ridge, J.C., Balco, G., Bayless, R.L., Beck, C.C., Carter, L.B., Dean, J.L., Voytek, E.B., Wei, J.H., 2012. The new North American Varve Chronology: A precise record of southeastern Laurentide Ice Sheet deglaciation and climate, 18.2-12.5 kyr BP, and correlations with Greenland ice core records. Am J Sci 312, 685–722. doi:10.2475/07.2012.01

Rommerskirchen, F., Eglinton, G., Dupont, L., Güntner, U., Wenzel, C., Rullkötter, J., 2003. A north to south transect of Holocene southeast Atlantic continental margin sediments: Relationship between aerosol transport and compound-specific δ13C land plant biomarker and pollen records. Geochemistry, Geophysics, Geosystems 4.

Rosén, P., Vogel, H., Cunningham, L., Hahn, A., Hausmann, S., Pienitz, R., Zolitschka, B., Wagner, B., Persson, P., 2011. Universally Applicable Model for the Quantitative Determination of Lake Sediment Composition Using Fourier Transform Infrared Spectroscopy. Environmental Science & Technology 45, 8858–8865. doi:10.1021/es200203z

Rosén, P., Vogel, H., Cunningham, L., Reuss, N., Conley, D.J., Persson, P., 2010. Fourier transform infrared spectroscopy, a new method for rapid determination of total organic and inorganic carbon and biogenic silica concentration in lake sediments. Journal of Paleolimnology 43, 247–259. doi:10.1007/s10933-009-9329-4

Rothwell, R.G., Rack, F.R., 2006. New techniques in sediment core analysis: an introduction. Geological Society, London, Special Publications 267, 1–29. doi:10.1144/GSL.SP.2006.267.01.01

Sachse, D., Billault, I., Bowen, G.J., Chikaraishi, Y., Dawson, T.E., Feakins, S.J., Freeman, K.H., Magill, C.R., McInerney, F.A., van der Meer, M.T.J., Polissar, P., Robins, R.J., Sachs, J.P., Schmidt, H.-L., Sessions, A.L., White, J.W.C., West, J.B., Kahmen, A., 2012. Molecular Paleohydrology: Interpreting the Hydrogen-Isotopic Composition of Lipid Biomarkers from Photosynthesizing Organisms. Annual Review of Earth and Planetary Sciences 40, 221–249. doi:10.1146/annurev-earth-042711-105535

Sachse, D., Radke, J., Gleixner, G., 2006. δD values of individual n-alkanes from terrestrial plants along a climatic gradient – Implications for the sedimentary biomarker record. Organic Geochemistry 37, 469–483. doi:10.1016/j.orggeochem.2005.12.003

Sachse, D., Sachs, J.P., 2008. Inverse relationship between D/H fractionation in cyanobacterial lipids and salinity in Christmas Island saline ponds. Geochimica et Cosmochimica Acta 72, 793–806. doi:10.1016/j.gca.2007.11.022

Schefuß, E., Ratmeyer, V., Stuut, J.-B.W., Jansen, J.H.F., Sinninghe Damsté, J.S., 2003. Carbon isotope analyses of n-alkanes in dust from the lower atmosphere over the central eastern Atlantic. Geochimica et Cosmochimica Acta 67, 1757–1767. doi:10.1016/S0016-7037(02)01414-X

Schillereff, D.N., Chiverrell, R.C., Macdonald, N., Hooke, J.M., 2014. Flood stratigraphies in lake sediments: A review. Earth-Science Reviews 135, 17–37. doi:10.1016/j.earscirev.2014.03.011

Schön, J.H., Kloc, C., Bucher, E., Batlogg, B., 2000. Efficient organic photovoltaic diodes based on doped pentacene. Nature 403, 408–410.

Schouten, S., Hopmans, E.C., Rosell-Melé, A., Pearson, A., Adam, P., Bauersachs, T., Bard, E., Bernasconi, S.M., Bianchi, T.S., Brocks, J.J., Carlson, L.T., Castañeda, I.S., Derenne, S., Selver, A.D., Dutta, K., Eglinton, T., Fosse, C., Galy, V., Grice, K., Hinrichs, K.-U., Huang, Y., Huguet, A., Huguet, C., Hurley, S., Ingalls, A., Jia, G., Keely, B., Knappy, C., Kondo, M., Krishnan, S., Lincoln, S., Lipp, J., Mangelsdorf, K., Martínez-García, A., Ménot, G., Mets, A., Mollenhauer, G., Ohkouchi, N., Ossebaar, J., Pagani, M., Pancost, R.D., Pearson, E.J., Peterse, F., Reichart, G.-J., Schaeffer, P., Schmitt, G., Schwark, L., Shah, S.R., Smith, R.W., Smittenberg, R.H., Summons, R.E., Takano, Y., Talbot, H.M., Taylor, K.W.R., Tarozo, R., Uchida, M., van Dongen, B.E., Van Mooy, B.A.S., Wang, J., Warren, C., Weijers, J.W.H., Werne, J.P., Woltering, M., Xie, S., Yamamoto, M., Yang, H., Zhang, C.L., Zhang, Y., Zhao, M., Damsté, J.S.S., 2013a. An interlaboratory study of TEX86 and BIT analysis of sediments, extracts, and standard mixtures. Geochem. Geophys. Geosyst. 14, 5263–5285. doi:10.1002/2013GC004904

Schouten, S., Hopmans, E.C., Schefu\s s, E., Damste, J.S.S., 2002. Distributional variations in marine crenarchaeotal membrane lipids: a new tool for reconstructing ancient sea water temperatures? Earth and Planetary Science Letters 204, 265–274.

Schouten, S., Hopmans, E.C., Sinninghe Damsté, J.S., 2013b. The organic geochemistry of glycerol dialkyl glycerol tetraether lipids: A review. Organic Geochemistry 54, 19–61. doi:10.1016/j.orggeochem.2012.09.006

Schouten, S., Huguet, C., Hopmans, E.C., Kienhuis, M.V.M., Sinninghe Damsté, J.S., 2007. Analytical Methodology for TEX $_{86}$ Paleothermometry by High-Performance Liquid Chromatography/Atmospheric Pressure Chemical Ionization-Mass Spectrometry. Analytical Chemistry 79, 2940–2944. doi:10.1021/ac062339v

Schouten, S., van der Meer, M.T.J., Hopmans, E.C., Rijpstra, W.I.C., Reysenbach, A.-L., Ward, D.M., Sinninghe Damste, J.S., 2007. Archaeal and Bacterial Glycerol Dialkyl Glycerol Tetraether Lipids in Hot Springs of Yellowstone National Park. Applied and Environmental Microbiology 73, 6181–6191. doi:10.1128/AEM.00630-07

Scileppi, E., Donnelly, J.P., 2007. Sedimentary evidence of hurricane strikes in western Long Island, New York: Hurricane Strikes In New York. Geochemistry, Geophysics, Geosystems 8, n/a–n/a. doi:10.1029/2006GC001463

Segura, R., Javierre, C., Lizarraga, M.A., Ros, E., 2006. Other relevant components of nuts: phytosterols, folate and minerals. British Journal of Nutrition 96, S36–S44. doi:10.1017/BJN20061862

Shanahan, T.M., Overpeck, J.T., Hubeny, J.B., King, J., Hu, F.S., Hughen, K., Miller, G., Black, J., 2008. Scanning micro-X-ray fluorescence elemental mapping: A new tool for the study of laminated sediment records: XRF MAPPING OF LAMINATED SEDIMENTS. Geochemistry, Geophysics, Geosystems 9, n/a–n/a. doi:10.1029/2007GC001800

Shuman, B., 2003. Controls on loss-on-ignition variation in cores from two shallow lakes in the northeastern United States. Journal of Paleolimnology 30, 371–385.

Shuman, B., Bravo, J., Kaye, J., Lynch, J.A., Newby, P., Webb III, T., 2001. Late Quaternary Water-Level Variations and Vegetation History at Crooked Pond, Southeastern Massachusetts. Quaternary Research 56, 401–410. doi:10.1006/qres.2001.2273

Shuman, B., Donnelly, J.P., 2006. The influence of seasonal precipitation and temperature regimes on lake levels in the northeastern United States during the Holocene. Quaternary Research 65, 44–56. doi:10.1016/j.yqres.2005.09.001

Shuman, B., Henderson, A.K., Plank, C., Stefanova, I., Ziegler, S.S., 2009. Woodland-to-forest transition during prolonged drought in Minnesota after ca. AD 1300. Ecology 90, 2792–2807. doi:10.1890/08-0985.1

Sinninghe Damsté, J.S., Ossebaar, J., Schouten, S., Verschuren, D., 2012. Distribution of tetraether lipids in the 25-ka sedimentary record of Lake Challa: extracting reliable TEX86 and MBT/CBT palaeotemperatures from an equatorial African lake. Quaternary Science Reviews 50, 43–54. doi:10.1016/j.quascirev.2012.07.001

Sluijs, A., Schouten, S., Pagani, M., Woltering, M., Brinkhuis, H., Damsté, J.S.S., Dickens, G.R., Huber, M., Reichart, G.-J., Stein, R., Matthiessen, J., Lourens, L.J., Pedentchouk, N., Backman, J., Moran, K., the Expedition 302 Scientists, 2006. Subtropical Arctic Ocean temperatures during the Palaeocene/Eocene thermal maximum. Nature 441, 610–613. doi:10.1038/nature04668

Soclo, H.H., Garrigues, P., Ewald, M., 2000. Origin of Polycyclic Aromatic Hydrocarbons (PAHs) in Coastal Marine Sediments: Case Studies in Cotonou (Benin) and Aquitaine (France) Areas. Marine Pollution Bulletin 40, 387–396. doi:10.1016/S0025-326X(99)00200-3

Song, X., Li, J., Xu, S., Ying, R., Ma, J., Liao, C., Liu, D., Yu, J., Chen, L., 2012. Determination of 16 polycyclic aromatic hydrocarbons in seawater using molecularly imprinted solid-phase extraction coupled with gas chromatography-mass spectrometry. Talanta 99, 75–82. doi:10.1016/j.talanta.2012.04.065

Soukup, M.A., 1975. The limnology of a eutrophic, hardwater New England Lake, with major emphasis on the biogeochemistry of dissolved silica. (PhD Thesis). University of Massachusetts - Amherst, Amherst, MA.

Spear, R.W., Davis, M.B., Shane, L.C.K., 1994. Late Quaternary History of Low- and Mid-Elevation Vegetation in the White Mountains of New Hampshire. Ecological Monographs 64, 85–109. doi:10.2307/2937056

Stahle, D.W., Cook, E.R., Cleaveland, M.K., Therrell, M.D., Meko, D.M., Grissino-Mayer, H.D., Watson, E., Luckman, B.H., 2000. Tree-ring data document 16th century megadrought over North America. Eos, Transactions American Geophysical Union 81, 121–125.

Steinman, B.A., Mann, M.E., Miller, S.K., 2015. Atlantic and Pacific multidecadal oscillations and Northern Hemisphere temperatures. Science 347, 988–991. doi:10.1126/science.1257856

Stein, R., Dittmers, K., Fahl, K., Kraus, M., Matthiessen, J., Niessen, F., Pirrung, M., Polyakova, Y., Schoster, F., Steinke, T., Fütterer, D.K., 2004. Arctic (palaeo) river discharge and environmental change: evidence from the Holocene Kara Sea sedimentary record. Quaternary Science Reviews, Quaternary Environments of the Eurasian North (QUEEN) 23, 1485–1511. doi:10.1016/j.quascirev.2003.12.004

Stone, B.D., Borns, H.W., 1986. Pleistocene glacial and interglacial stratigraphy of New England, Long Island, and adjacent Georges Bank and Gulf of Maine. Quaternary science reviews 5, 39–52.

St-Onge, G., Long, B.F., 2009. CAT-scan analysis of sedimentary sequences: An ultrahigh-resolution paleoclimatic tool. Engineering Geology, Applications of X-ray Computed Tomography in Engineering Geology 103, 127–133. doi:10.1016/j.enggeo.2008.06.016

Støren, E.N., Kolstad, E.W., Paasche, Ø., 2012. Linking past flood frequencies in Norway to regional atmospheric circulation anomalies. Journal of Quaternary Science 27, 71–80.

Støren, E.N., Paasche, Ø., 2014. Scandinavian floods: From past observations to future trends. Global and Planetary Change 113, 34–43. doi:10.1016/j.gloplacha.2013.12.002

Sun, Q., Xie, M., Shi, L., Zhang, Z., Lin, Y., Shang, W., Wang, K., Li, W., Liu, J., Chu, G., 2013. Alkanes, compound-specific carbon isotope measures and climate variation during the last millennium from varved sediments of Lake Xiaolongwan, northeast China. J Paleolimnol 50, 331–344. doi:10.1007/s10933-013-9728-4

Swain, A.M., 1973. A history of fire and vegetation in northeastern Minnesota as recorded in lake sediments. Quaternary Research, The Ecological Role of Fire in Natural Conifer Forests of Western and Northern America 3, 383–396. doi:10.1016/0033-5894(73)90004-5

Tennant, R.K., Jones, R.T., Brock, F., Cook, C., Turney, C.S.M., Love, J., Lee, R., 2013. A new flow cytometry method enabling rapid purification of fossil pollen from terrestrial sediments for AMS radiocarbon dating. J. Quaternary Sci. 28, 229–236. doi:10.1002/jqs.2606

Thorson, R.M., Webb, R.S., 1991. Postglacial history of a cedar swamp in southeastern Connecticut. Journal of Paleolimnology 6, 17–35.

Tierney, J.E., Mayes, M.T., Meyer, N., Johnson, C., Swarzenski, P.W., Cohen, A.S., Russell, J.M., 2010. Late-twentieth-century warming in Lake Tanganyika unprecedented since AD 500. Nature Geoscience 3, 422–425. doi:10.1038/ngeo865

Uchikawa, J., Popp, B.N., Schoonmaker, J.E., Xu, L., 2008. Direct application of compound-specific radiocarbon analysis of leaf waxes to establish lacustrine sediment chronology. Journal of Paleolimnology 39, 43–60. doi:10.1007/s10933-007-9094-1

United States Geological Survey (USGS), 1996. Basin Pond Survey and Bathymetic Mapping, Fayette, ME [WWW Document].

Valero-Garcés, B.L., Laird, K.R., Fritz, S.C., Kelts, K., Ito, E., Grimm, E.C., 1997. Holocene Climate in the Northern Great Plains Inferred from Sediment Stratigraphy, Stable Isotopes, Carbonate Geochemistry, Diatoms, and Pollen at Moon Lake, North Dakota. Quaternary Research 48, 359–369. doi:10.1006/qres.1997.1930

Verschuren, D., Laird, K.R., Cumming, B.F., 2000. Rainfall and drought in equatorial east Africa during the past 1,100 years. Nature 403, 410–414. doi:10.1038/35000179

Vogel, H., Rosén, P., Wagner, B., Melles, M., Persson, P., 2008. Fourier transform infrared spectroscopy, a new cost-effective tool for quantitative analysis of biogeochemical properties in long sediment records. Journal of Paleolimnology 40, 689–702. doi:10.1007/s10933-008-9193-7

Volkman, J., 2003. Sterols in microorganisms. Appl Microbiol Biotechnol 60, 495–506. doi:10.1007/s00253-002-1172-8

Volkman, J.K., 1986. A review of sterol markers for marine and terrigenous organic matter. Organic Geochemistry 9, 83–99. doi:10.1016/0146-6380(86)90089-6

Volkman, J.K., Barrett, S.M., Blackburn, S.I., Mansour, M.P., Sikes, E.L., Gelin, F., 1998. Microalgal biomarkers: A review of recent research developments. Organic Geochemistry 29, 1163–1179. doi:10.1016/S0146-6380(98)00062-X

Wakeham, S.G., Schaffner, C., Giger, W., 1980. Polycyclic aromatic hydrocarbons in Recent lake sediments—I. Compounds having anthropogenic origins. Geochimica et Cosmochimica Acta 44, 403–413. doi:10.1016/0016-7037(80)90040-X

Webster, P.J., 2005. Changes in Tropical Cyclone Number, Duration, and Intensity in a Warming Environment. Science 309, 1844–1846. doi:10.1126/science.1116448

Weddle, T.K., Retelle, M.J., 2001. Deglacial History and Relative Sea-level Changes, Northern New England and Adjacent Canada. Geological Society of America.

Weijers, J.W.H., Schouten, S., Spaargaren, O.C., Sinninghe Damsté, J.S., 2006. Occurrence and distribution of tetraether membrane lipids in soils: Implications for the use of the TEX86 proxy and the BIT index. Organic Geochemistry 37, 1680–1693. doi:10.1016/j.orggeochem.2006.07.018

Wellner, R.W., Dwyer, T.R., 1996. Late Pleistocene-Holocene lake-level fluctuations and paleoclimates at Canandaigua Lake, New York. Special Papers-Geological Society Of America 65–76.

Werf, G.R. van der, Randerson, J.T., Collatz, G.J., Giglio, L., Kasibhatla, P.S., Arellano, A.F., Olsen, S.C., Kasischke, E.S., 2004. Continental-Scale Partitioning of Fire Emissions During the 1997 to 2001 El Niño/La Niña Period. Science 303, 73–76. doi:10.1126/science.1090753

Wetzel, A., 1983. Biogenic structures in modern slope to deep-sea sediments in the sulu sea basin (Philippines). Palaeogeography, Palaeoclimatology, Palaeoecology 42, 285–304. doi:10.1016/0031-0182(83)90027-5

Whitehead, D.R., 1979. Late-glacial and postglacial vegetational history of the Berkshires, western Massachusetts. Quaternary Research 12, 333–357. doi:10.1016/0033-5894(79)90033-4

Whitlock, C., Anderson, R.S., 2003. Fire history reconstructions based on sediment records from lakes and wetlands, in: Fire and Climatic Change in Temperate Ecosystems of the Western Americas. Springer, pp. 3–31.

Whitlock, C., Larsen, C., 2001. Charcoal as a Fire Proxy, in: Smol, J.P., Birks, H.J.B., Last, W.M., Bradley, R.S., Alverson, K. (Eds.), Tracking Environmental Change Using Lake Sediments, Developments in Paleoenvironmental Research. Springer Netherlands, pp. 75–97.

Wilcke, W., 2000. SYNOPSIS Polycyclic Aromatic Hydrocarbons (PAHs) in Soil — a Review. Z. Pflanzenernähr. Bodenk. 163, 229–248. doi:10.1002/1522-2624(200006)163:3<229::AID-JPLN229>3.0.CO;2-6

Winkler, M.G., 1985. A 12,000-year history of vegetation and climate for Cape Cod, Massachusetts. Quaternary Research 23, 301–312. doi:10.1016/0033-5894(85)90037-7

Winkler, M.G., Sanford, P.R., 1995. Coastal Massachusetts pond development: edaphic, climatic, and sea level impacts since deglaciation. Journal of Paleolimnology 14, 311–336.

Wirth, S.B., Glur, L., Gilli, A., Anselmetti, F.S., 2013. Holocene flood frequency across the Central Alps – solar forcing and evidence for variations in North Atlantic atmospheric circulation. Quaternary Science Reviews 80, 112–128. doi:10.1016/j.quascirev.2013.09.002

Woltering, M., Johnson, T.C., Werne, J.P., Schouten, S., Sinninghe Damsté, J.S., 2011. Late Pleistocene temperature history of Southeast Africa: A TEX86 temperature record from Lake Malawi. Palaeogeography, Palaeoclimatology, Palaeoecology 303, 93–102. doi:10.1016/j.palaeo.2010.02.013

Woodruff, J.D., Sriver, R.L., Lund, D.C., 2012. Tropical cyclone activity and western North Atlantic stratification over the last millennium: a comparative review with viable connections. Journal of Quaternary Science 27, 337–343. doi:10.1002/jqs.1551

Wuchter, C., Schouten, S., Wakeham, S.G., Sinninghe Damsté, J.S., 2006. Archaeal tetraether membrane lipid fluxes in the northeastern Pacific and the Arabian Sea: Implications for TEX $_{86}$ paleothermometry: TEX $_{86}$ PALEOTHERMOMETRY. Paleoceanography 21, n/a–n/a. doi:10.1029/2006PA001279

Xia, J., Haskell, B.J., Engstrom, D.R., Ito, E., 1997. Holocene climate reconstructions from tandem trace-element and stable-isotope composition of ostracodes from Coldwater Lake, North Dakota, USA. Journal of Paleolimnology 17, 85–100.

Yamamoto, S., Kawamura, K., Seki, O., Meyers, P.A., Zheng, Y., Zhou, W., 2010. Environmental influences over the last 16 ka on compound-specific δ13C variations of leaf wax n-alkanes in the Hani peat deposit from northeast China. Chemical Geology 277, 261–268. doi:10.1016/j.chemgeo.2010.08.009

Yan, B., Abrajano, T.A., Bopp, R.F., Chaky, D.A., Benedict, L.A., Chillrud, S.N., 2005. Molecular tracers of saturated and polycyclic aromatic hydrocarbon inputs into Central Park Lake, New York City. Environmental science & technology 39, 7012–7019.

Yang, C.-R., Lin, T.-C., Chang, F.-H., 2007. Particle size distribution and PAH concentrations of incense smoke in a combustion chamber. Environmental Pollution 145, 606–615. doi:10.1016/j.envpol.2005.10.036

Yunker, M.B., Backus, S.M., Graf Pannatier, E., Jeffries, D.S., Macdonald, R.W., 2002. Sources and Significance of Alkane and PAH Hydrocarbons in Canadian Arctic Rivers. Estuarine, Coastal and Shelf Science 55, 1–31. doi:10.1006/ecss.2001.0880

Yunker, M.B., Macdonald, R.W., 2003. Petroleum biomarker sources in suspended particulate matter and sediments from the Fraser River Basin and Strait of Georgia, Canada. Organic Geochemistry 34, 1525–1541. doi:10.1016/S0146-6380(03)00157-8

Yunker, M.B., Macdonald, R.W., 1995. Composition and Origins of Polycyclic Aromatic Hydrocarbons in the Mackenzie River and on the Beaufort Sea Shelf. Arctic 48, 118–129.

Yunker, M.B., Macdonald, R.W., Goyette, D., Paton, D.W., Fowler, B.R., Sullivan, D., Boyd, J., 1999. Natural and anthropogenic inputs of hydrocarbons to the Strait of Georgia. Science of the Total Environment 225, 181–209.

Yunker, M.B., Macdonald, R.W., Snowdon, L.R., Fowler, B.R., 2011. Alkane and PAH biomarkers as tracers of terrigenous organic carbon in Arctic Ocean sediments. Organic Geochemistry. doi:10.1016/j.orggeochem.2011.06.007

Yunker, M.B., Macdonald, R.W., Vingarzan, R., Mitchell, R.H., Goyette, D., Sylvestre, S., 2002. PAHs in the Fraser River basin: a critical appraisal of PAH ratios as indicators of PAH source and composition. Organic Geochemistry 33, 489–515. doi:10.1016/S0146-6380(02)00002-5

Zhang, Z., Zhao, M., Eglinton, G., Lu, H., Huang, C.-Y., 2006. Leaf wax lipids as paleovegetational and paleoenvironmental proxies for the Chinese Loess Plateau over the last 170 kyr. Quaternary Science Reviews 25, 575–594. doi:10.1016/j.quascirev.2005.03.009

Zhou, W., Zheng, Y., Meyers, P.A., Jull, A.J.T., Xie, S., 2010. Postglacial climate-change record in biomarker lipid compositions of the Hani peat sequence, Northeastern China. Earth and Planetary Science Letters 294, 37–46. doi:10.1016/j.epsl.2010.02.035

Zolitschka, B., Francus, P., Ojala, A.E.K., Schimmelmann, A., 2015. Varves in lake sediments – a review. Quaternary Science Reviews 117, 1–41. doi:10.1016/j.quascirev.2015.03.019

Zolitschka, B., Pike, J., von Gunten, L., Kiefer, T., 2014. Annual Recorders of the Past. Past Global Changes 22, 1–56.